VOLUME 3

Well-to-Tank Energy Use and Greenhouse Gas Emissions of Transportation Fuels

– North American Analysis –

General Motors Corporation

Argonne National Laboratory

BP

ExxonMobil

and

Shell

June 2001

Contents

Contents (Cont.)

Figures

Figures (Cont.)

Figures (Cont.)

Tables

Tables (Cont.)

Tables (Cont.)

Tables (Cont.)

Tables (Cont.)

Notation

Acronyms and Abbreviations

AMI	American Methanol Institute
ANL	Argonne National Laboratory
API	American Petroleum Institute
ATR	autothermal reforming
CAAA	Clean Air Act Amendments
CACD	California conventional diesel
CALSD	California low-sulfur diesel
CARB	California Air Resources Board
CARBOB	California reformulated blendstock for oxygenate blending
CARFG1	California Phase 1 reformulated gasoline
CARFG2	California Phase 2 reformulated gasoline
CARFG3	California Phase 3 reformulated gasoline
CC	combined-cycle
CG	conventional gasoline
CH_4	methane
CNG	compressed natural gas
CO	carbon monoxide
CO_2	carbon dioxide
CTR	Center for Transportation Research
DGS	distillers' grains and solubles
EC-D	emission control diesel
EPA	U.S. Environmental Protection Agency
EtOH	ethanol
EV	electric vehicles
FCD	federal conventional diesel
FCV	fuel-cell vehicle
FG	flared gas
FLSD	federal low-sulfur diesel
FRFG1	federal Phase 1 reformulated gasoline
FRFG2	federal Phase 2 reformulated gasoline
FT	Fischer-Tropsch
FTD	Fischer-Tropsch diesel
GAPC	Global Alternative Propulsion Center
GBS	gasoline blendstock
$G.H_2$	gaseous hydrogen
GHG	greenhouse gas
GM	General Motors Corporation
GREET	Greenhouse gases, Regulated Emissions, and Energy use in Transportation
GWP	global warming potential
HEV	hybrid electric vehicle
IPCC	Intergovernmental Panel on Climate Change
$L.H_2$	liquid hydrogen

LNG	liquefied natural gas
LP	linear programming
LPG	liquefied petroleum gas
LS	low-sulfur
MeOH	methanol
MTBE	methyl tertiary butyl ether
NA	North American
NG	natural gas
NNA	non-North-American
NPC	National Petroleum Council
N_2O	nitrous oxide
NO_x	nitrogen oxides
NRC	National Research Council
P20	20% probability
P50	50% probability
P80	80% probability
PADD	Petroleum Administration Defense District
PM_{10}	particulate matter with diameter of 10 μm or less
POX	partial oxidation
PSA	pressure swing adsorption
RFG	reformulated gasoline
RVP	Reid vapor pressure
S	sulfur
SMR	steam-methane reforming
SO_x	sulfur oxides
U.S. DOC	U.S. Department of Commerce
U.S. DOT	U.S. Department of Transportation
EPA	U.S. Environmental Protection Agency
VOC	volatile organic compounds
WTT	well-to-tank

Units of Measure

bbl	barrel(s)	kW	kilowatt(s)
Btu	British thermal unit(s)	mi	mile(s)
ºC	degree(s) Celsius	min	minute(s)
ºF	degree(s) Farenheit	mmBtu	million (10^6) Btu
g	gram(s)	ppm	part(s) per million
gal	gallon(s)	psi	pound(s) per square inch
J	joule(s)	yr	year(s)
K	Kelvin	μm	micrometer(s)
kg	kilogram(s)		

1 Introduction

Various fuels are being proposed for use in fuel-cell vehicles (FCVs) and hybrid electric vehicles (HEVs). Some of these fuels will be able to power advanced internal combustion engine technologies as well. These fuels are made through different fuel production pathways, resulting in different energy efficiencies and emissions from feedstock recovery to vehicle operation. To fully analyze energy and emission impacts of vehicle/fuel systems, a full fuel-cycle analysis — from energy feedstock recovery (wells) to fuel use by vehicle (wheels) — needs to be conducted for fuel/vehicle systems. Figure 1 shows the well-to-tank stages included in Argonne's study.

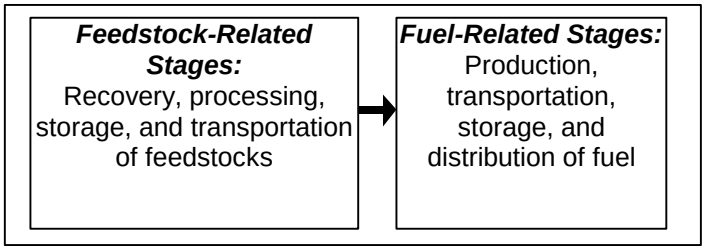

Figure 1 Well-to-Tank Stages Covered in Argonne's Study

The Global Alternative Propulsion Center (GAPC) of General Motors Corporation (GM) commissioned the Center for Transportation Research (CTR) of Argonne National Laboratory (ANL) to conduct a study to evaluate energy and emission impacts of producing different transportation fuels from wells to fuels available in vehicle tanks (well-to-tank [WTT] analysis). Three energy companies — BP, ExxonMobil, and Shell —participated in the study by providing input and reviewing Argonne's results. This report presents methodologies, assumptions, and results of Argonne's study.

2 The GREET Model

In 1995, ANL began to develop a spreadsheet-based model for estimating the full fuel-cycle energy and emission impacts of alternative transportation fuels and advanced vehicle technologies. The intent was to provide an analytical tool to allow researchers to readily analyze various parametric assumptions that affect fuel-cycle energy use and emissions associated with fuels and vehicle technologies. The model, called GREET (Greenhouse gases, Regulated Emissions, and Energy use in Transportation), calculates fuel-cycle energy use in British thermal units per mile (Btu/mi) and emissions in grams per mile (g/mi) for various transportation fuels and vehicle technologies. For energy use, GREET includes total energy use (all energy sources), fossil energy use (petroleum, natural gas, and coal), and petroleum use (each energy item is a part of the preceding energy item). For emissions, the model includes three major greenhouse gases (GHGs) (carbon dioxide [CO_2], methane [CH_4], and nitrous oxide [N_2O]) and five criteria pollutants (volatile organic compounds [VOCs], carbon monoxide [CO], nitrogen oxides [NO_x], particulate matter with diameters of 10 μm or less [PM_{10}], and sulfur oxides [SO_x]).

In the GREET model, the three GHGs are combined together with their global warming potentials (GWPs) to calculate CO_2-equivalent GHG emissions. The default GWPs in GREET — 1 for CO_2, 21 for CH_4, and 310 for N_2O — are recommended by the Intergovernmental Panel on Climate Change (IPCC) for the 100-year time horizon. On the other hand, emissions of the five criteria pollutants are further separated into total and urban emissions. Total emissions are emissions occurring everywhere. Urban emissions are those occurring within urban areas. The separation is conducted on the basis of information on facility locations and is intended to provide an approximation of population exposure of air pollution caused by the criteria pollutants.

For the GAPC project, Argonne estimated energy use for the three energy items and CO_2-equivalent GHG emissions for the three GHGs. Because of data quality and time and resource constraints, emissions of criteria pollutants were not included in this study.

Development and use of the GREET model are documented in Wang (1999a and 1999b) and in Wang and Huang (1999). The current version of the model that is available to the general public is GREET1.5a, which was completed in January 2000. The model is in the public domain, and any party can use it free of charge. GREET1.5a and associated reports prepared by Argonne are posted on Argonne's transportation Web site at www.transportation.anl.gov/ttrdc/greet.

Figure 2 is a simplified diagram showing calculation logic for energy use and emissions associated with activities from wells to tanks. For a given stage, energy use by fuel type is estimated by using energy efficiency and fuel type shares. We then calculate emissions by using energy use by fuel type, emission factors by fuel type, and combustion technology shares. Finally, urban emissions are estimated from total emissions and split of facility locations between urban and non-urban locations. For CO_2 emissions, GREET takes a carbon-balance approach. That is, the carbon in CO_2 emissions is equal to the carbon contained in the fuel burned minus the carbon contained in combustion emissions of VOC, CO, and CH_4. For details on calculation methodologies, see Wang (1999a and 1999b).

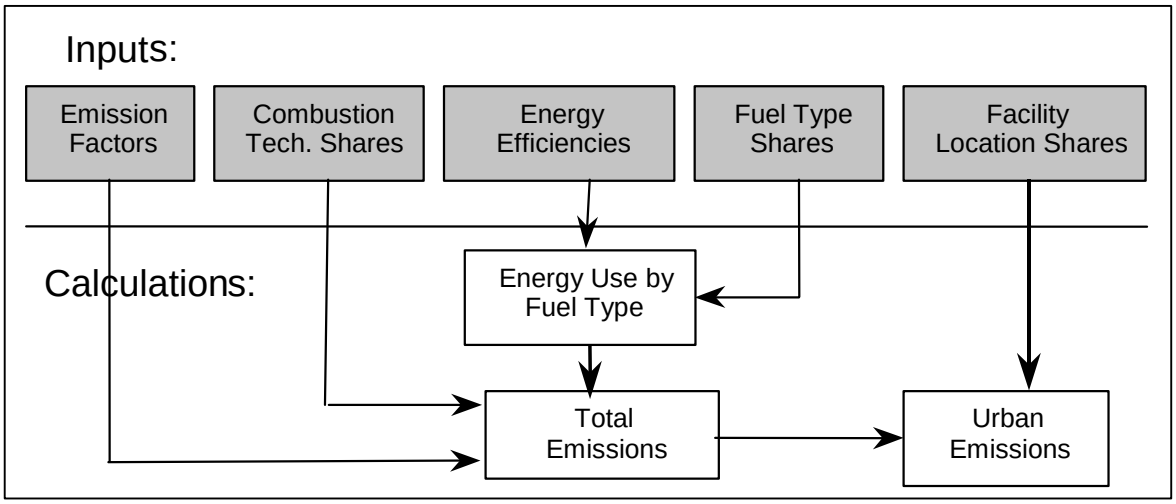

Figure 2 Calculation Logic for Well-to-Tank Energy Use and Emissions of Transportation Fuels

For this study, we used a new version of Argonne's GREET model. Through a separate ANL effort, the GREET model was expanded to incorporate detailed information on transportation modes and their corresponding distances for different energy feedstocks and fuels. This version is in draft form and is not yet available to the general public. Details regarding the expansion of feedstock and fuel transportation in GREET are presented in a later section of this report.

Through the GAPC project, ANL began to formally address in the GREET model the uncertainties involved in key input parameters with subjective probability distribution functions. Previously, ANL addressed uncertainties with range estimates for key input assumptions. This time, ANL began to explore probability distribution functions for some of the key input parameters. In particular, based on published data for given fuel-cycle stages, ANL established subjective probability distribution functions for each stage. These distribution functions are incorporated into the GREET model. A commercial software, Crystal Ball™, is used in GREET to conduct Monte Carlo simulations. Instead of the point estimates included in previous GREET versions, the new version generates results with probability distributions. In order to use the new feature of Monte Carlo simulations in GREET, users need to have both Excel and Crystal Ball software. However, if Crystal Ball software is not available, users can still conduct point estimates with the new GREET version.

3 Fuels and Fuel Production Pathways Included in This Study

3.1 Gasoline, Diesel, and Naphtha from Petroleum

The petroleum-based pathways examined in this study include three fuels: gasoline, diesel, and naphtha. We further establish cases for gasoline and diesel to represent different fuel requirements. Currently available gasoline includes federal conventional gasoline (CG), federal Complex Model Phase 2 reformulated gasoline (FRFG2), and California Phase 2 reformulated gasoline (CARFG2). These gasoline options have an average sulfur content ranging from 30 parts per million (ppm) to over 500 ppm. Evaluation of future gasoline (to dominate gasoline market around 2010) includes California Phase 3 reformulated gasoline (CARFG3) and the gasoline requirements in the U.S. Environmental Protection Agency's (EPA's) Tier 2 vehicle emission standards. These gasoline options may have an average sulfur content of 10 ppm to 30 ppm and may contain methyl tertiary butyl ether (MTBE), ethanol (EtOH), or no oxygenates. Current diesel includes federal conventional diesel (FCD) and California low-sulfur diesel (CALSD) with a sulfur content ranging from 150 ppm to 350 ppm. Future diesel includes EPA's recently adopted federal low-sulfur diesel (FLSD) with a maximum sulfur content of 15 ppm. Virgin naphtha produced in petroleum refineries has a sulfur content of about 370 ppm. We assumed that it would be subject to desulfurization to reduce its sulfur content to about 1 ppm for FCV applications.

3.1.1 Gasoline Requirements

3.1.1.1 California Reformulated Gasoline

In 1992, California began to require use of the so-called California Phase 1 reformulated gasoline (CARFG1). CARFG1 had the following composition requirements: a maximum aromatics content of 32% (by volume), a maximum sulfur content of 150 ppm, a maximum olefins content of 10% (by volume), and maximum 90% distillation temperature (T90) of 330^{o}F (California Air Resources Board [CARB] 1991).

In 1996, California began to require the use of CARFG2. Table 1 presents the composition requirements of CARFG2. However, under the CARFG2 requirement, gasoline producers are allowed to certify gasoline either by meeting the specified composition requirements or by meeting an emission reduction requirement with an alternative gasoline formula. The emissions performance of a given alternative reformulated gasoline (RFG) formula was simulated by using CARB's Predictive Model.

In the spring of 1999, because of the concern about underground water contamination by MTBE, California Governor Grey Davis issued an executive order banning the use of MTBE in California's gasoline beginning in 2003. In December 1999, CARB adopted CARFG3; use of CARFG3 will be required beginning in 2003 (Table 1). Under the CARFG3 requirements, gasoline producers will be allowed to certify gasoline with a specified composition requirement or by meeting emission reductions requirements with an alternative composition formula. As Table 1 shows, one significant difference between CARFG2 and CARFG3 lies in the reduction of sulfur content from 30 ppm to 15 ppm.

Table 1 Composition Requirements of CARFG2 and CARFG3[a]

Requirement	Flat Limits		Averaging Limits		Cap Limits	
	CARFG2	CARFG3	CARFG2	CARFG3	CARFG2	CARFG3
RVP[b] (psi, summer only)	7.00	7.00	NA[c]	NA	7.00	6.40–7.20
Sulfur content (wt. ppm)	40	20	30	15	80	60 (30 after 2004)
Benzene content (vol. %)	1.0	0.8	0.8	0.7	1.2	1.1
Aromatics content (vol. %)	25.0	25.0	22.0	22.0	30.0	35.0
Olefins content (vol. %)	6.0	6.0	4.0	4.0	10.0	10.0
T50 (°F)	210	213	200	203	220	220
T90 (°F)	300	305	290	295	330	330
Oxygen content (wt. %)	1.8–2.2	1.8–2.2	NA	NA	1.8–3.5 (winter areas); 0–3.5	1.8–3.7 (winter areas); 0–3.7
Ban of MTBE	No	Yes	No	Yes	No	Yes

[a] From CARB 2000.
[b] RVP = Reid vapor pressure.
[c] NA = Not available.

3.1.1.2 Federal Reformulated Gasoline

The 1990 Clean Air Act Amendments (CAAA) require use of RFG in the nation's worst ozone nonattainment areas. The requirement for so-called federal Simple Model Phase 1 reformulated gasoline (FRFG1) took effect in January 1995, and Complex Model FRFG2 in June 2000. Gasoline producers could certify FRFG1 with a specified composition requirement or by making Complex Model Phase 1 RFG. FRFG1 composition requirements were a maximum benzene content of 1% (by volume), a per-gallon maximum aromatics content of 25% (by volume), and a minimum oxygen content of 2% (by weight). Under the emissions reduction requirements, producers were required to reduce VOC emissions in FRFG1 by 16% (northern regions) to 35% (southern regions) and air toxic emissions by about 15% relative to CG (EPA 1994). Note that the reduction for VOC emissions is the combined reduction of exhaust and evaporative emissions. FRFG2 is certified by meeting emission performance standards: a per-gallon VOC emissions reduction of 27.5% in southern regions and 25.9% in northern regions, an air toxic emissions reduction of 20%, and a NO_x emissions reduction of 5.5%, all relative to CG. EPA's Complex Model is allowed for use in determining emissions of a given gasoline formula.

Although Complex Model FRFG2 was introduced into the market in 2000, some new requirements for gasoline will be in place in the next few years. In February 2000, EPA adopted the final rule of Tier 2 vehicle emission standards (EPA 2000a). Besides emission standards, the rule establishes a gasoline sulfur content requirement. While FRFG1 and FRFG2 have been required for use in ozone nonattainment areas only, the Tier 2 gasoline requirement will be applied to both CG and RFG nationwide, except in California, where CARFG3 will be in effect. We call this new requirement the Tier 2 FRFG requirement. Phase-in of the requirement will begin in 2004, and it will be fully implemented in 2006. The only new requirement for the FRFG is an average sulfur content of 30 ppm. This sulfur level is already accomplished in CARFG2. Also, BP began to introduce a 30-ppm sulfur premium gasoline in Chicago, Detroit, and some other cities in the spring of 2000.

Table 2 Typical Properties of CG and FRFG

Characteristic	CG[a]	FRFG2[b]	Tier 2 FRFG[c]
RVP (psi, summer)	8.9	6.7	6.7
Sulfur content (wt. ppm)	339	150	30 (max. 80)
Benzene content (vol. %)	1.53	0.68	0.68
Aromatics content (vol. %)	32.0	25	25
Olefins content (vol. %)	9.2	11	11
200°F distillation (%)	41	49	49
300°F distillation (%)	83	87	87
Oxygen content (wt. %)	0.4	2.26	2.26

[a] From National Research Council (NRC 2000).
[b] Based on input parameters to EPA's Complex Model for simulating emissions performances of FRFG2.
[c] From EPA (2000a).

3.1.2 Diesel Requirements

In October 1993, EPA began to require use of a diesel fuel with a lower sulfur content in on-road motor vehicles. The maximum sulfur content for on-road diesel fuels was set at 500 ppm. As a result, the current average of diesel sulfur content in the nation (except California) is about 350 ppm (EPA 2000b). We call this diesel fuel FCD. Before October 1993, the sulfur content of diesel fuel was about 3,000 ppm (EPA 2000b). Recently, EPA has adopted a rule to lower the maximum sulfur content for on-road diesel fuel to 15 ppm: this rule will be effective in June 2006. EPA estimates that the average sulfur content of diesel fuel under this requirement will be 7–10 ppm (EPA 2000b). We call the newly proposed diesel fuel FLSD.

In October 1993, California began to require use of a low-sulfur diesel. California refiners and importers are allowed to adjust the diesel fuel properties in proprietary formulations as long as these formulations meet CARB emission requirements as proven by emission tests. California's low-sulfur diesel has a maximum sulfur content of 500 ppm and a maximum aromatics content of 10%. As a result, the current average sulfur content in California's diesel is probably 120 ppm (ARCO Products Company 1999). We call this diesel fuel California conventional diesel (CACD). Meanwhile, in March 1999, ARCO announced that it would produce a clean diesel called emission control diesel (EC-D) for the California market (ARCO Products Company 1999). The specifications of EC-D are a sulfur content of less than 10 wt. ppm (maximum 15 wt. ppm), an aromatics content of less than 10% (by volume) (maximum 12% by volume), and a cetane number of 60 (minimum of 57). EC-D is already being sold in the California market.

3.1.3 Crude Naphtha

At petroleum refineries, virgin naphtha is produced primarily from an atmospheric distillation process (although some naphtha is produced from visbreaking and other refining processes). Virgin naphtha contains normal paraffins, iso-paraffins, and cycloparaffins of C5–C10. The boiling point of this naphtha is higher than that of straight-run gasoline but lower than that of kerosene. Thus, naphtha is separated during the distillation process after straight-run gasoline. Petroleum naphtha can be further separated into light naphtha and heavy naphtha according to boiling point ranges. The former has a boiling point of 50–200°F, while the latter has a boiling point of 200–400°F (McKetta 1992). Light naphtha may go through a hydrotreating process to

reduce its sulfur (S) content and then an isomerization process to produce high-octane gasoline blendstocks. Heavy naphtha also requires additional refining processes, such as catalytic reforming. As Table 3 shows, crude with different qualities may produce different yields and qualities of naphtha. Usually, lighter crude can produce more naphtha than heavy crude.

Because virgin naphtha has a lower octane number (about 60), it is not an attractive neat gasoline blendstock. On the other hand, because naphtha contains more hydrogen than some other petroleum hydrocarbons, it could be a good candidate for FCV reformer fuels, so we include crude naphtha in this analysis (see Table 4).

Table 3 Crude Quality and Product Yields from the Atmospheric Distillation Process[a]

	Crude Quality		Product Yield and Quality from the Atmospheric Distillation Process					
			Diesel		Gasoline		Naphtha	
Crude	API Gravity	S Content (ppm)	Yield (%)	S Content (ppm)	Yield (%)	S Content (ppm)	Yield (%)	S Content (ppm)
U.S. Crude								
Alaska-North Slope	27.5	11,000	NA[b]	NA	0	NA	NA	NA
S. Louisiana Light	31.0	20,000	0	NA	6.9	200	17.0	700
CA-Hondo Blend	20.8	42,900	0	NA	0	NA	NA	NA
West Texas Intermediate	40.8	3,400	0	NA	0	NA	NA	NA
Foreign Crude								
U.K.-Brent	38.9	3,500	20.8	2,110	9.4	NA	17.7	30
Russia-Siberian Light	35.3	5,800	21.7	3,160	7.8	NA	15.1	NA
Saudi Light	32.9	19,000	20.9	12,470	6.8	NA	13.4	NA
Algeria-Saharan	45.7	700	21.3	485	11.8	NA	19.4	NA
Nigeria-Bonny Light	33.8	1,400	30.9	1,665	6.0	NA	14.4	20
Indonesia-Minas	36.0	810	20.6	480	3.5	NA	9.0	17
Venezuela-Tia Juana Light	31.6	10,800	20.0	5,670	6.0	NA	12.4	NA
Mexico-Isthmus	31.8	12,500	20.4	9,080	7.7	NA	14.1	NA

[a] From *Oil and Gas Journal* (1999).
[b] NA = no data are available.

Table 4 Typical Properties of Crude and Fischer-Tropsch (FT) Naphtha

Specification	Crude Naphtha[a]	FT Naphtha[b]
Density (g/gal)	2,861	2,651
Lower heating value (Btu/gal)	118,760	111,780
Higher heating value (Btu/gal)	127,330	120,020
Carbon (wt. %)	85.3	84.2
Sulfur content (wt. ppm)	367[c]	0.2

[a] From Domalski and Jobe (1986).
[b] From Russell (2000).
[c] This is the sulfur content before desulfurization. Hydrotreating or other desulfurization measures will be needed to reduce crude naphtha sulfur content so that it can be used as a fuel-cell fuel. In our analysis, we assume that the sulfur content of crude naphtha will be reduced to about 1 ppm.

Figure 3 presents the pathways from crude to gasoline, diesel, and naphtha. In particular, Argonne's analysis for petroleum-based fuels includes these activities: crude recovery; crude transportation; petroleum refining; and transportation, storage, and distribution of fuel products. Because virgin naphtha is produced from the atmospheric distillation process at refineries, production of virgin naphtha should be more energy efficient than production of gasoline and diesel, both of which go through more refining processes. Because the boiling point of naphtha is higher than that of liquefied petroleum gas (LPG), we expect that the efficiency for naphtha production is lower than that for LPG production. Transportation, storage, and distribution of naphtha could be similar to those of gasoline.

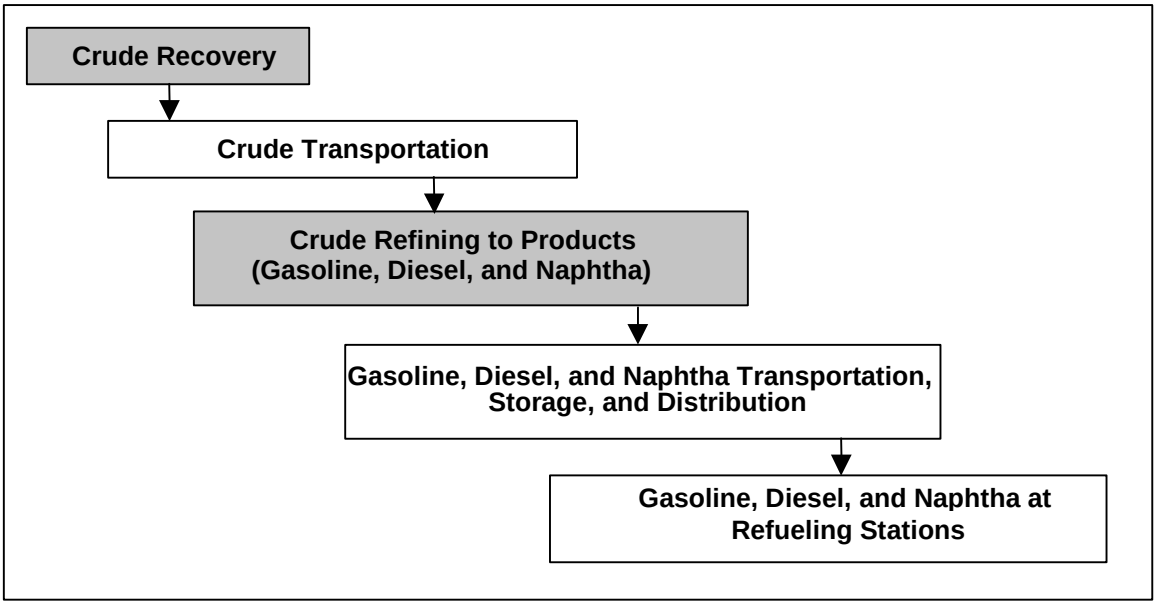

Figure 3 Well-to-Tank Stages for Three Petroleum-Based Fuels

3.1.4 Quality of Crude Oil

The quality of crude oil affects refinery product slates and energy use in refineries. Among the parameters measuring the quality of crude oil, two important ones are American Petroleum Institute (API) gravity and sulfur content. API gravity is one indicator of the amount of gasoline and other light fractions from crude distillation. Because of tightened sulfur requirements for gasoline and diesel, high-sulfur crude and its refined products will need to go through intensive desulfurization. Table 5 lists API gravities and sulfur contents of crude oils produced in different U.S. regions and in other countries that export crude oil to the United States. As the table shows, among the three U.S. crude production regions presented (the Gulf area, Alaska, and California), California crude contains more sulfur than does crude from the Gulf area and Alaska. Also, crude from California and Alaska is heavier than that from the Gulf area. This implies that petroleum refineries processing California and Alaska crude feeds need to employ more intensive refining processes than those with Gulf crude inputs.

Table 5 Quality of Crude Oil Used in U.S. Refineries

Country	API Gravity[a]		Sulfur Content (wt. %)[a]		Sources of U.S. Crude (1000 bbl/yr)[b]
	Range	Median	Range	Median	
United States					2,281,980
Gulf Area	31.0–40.8	35.9	0.34–2.00	1.17	638,880
Alaska	22.4–27.5	25.0	1.11–1.82	1.47	428,851
California	19.4–35.2	27.3	0.21–4.29	2.25	283,628
Saudi Arabia	27.4–38.7	33.1	1.19–2.80	2.00	517,072
Venezuela	10.1–31.8	21.0	1.10–5.50	3.30	499,580
Mexico	22.2–39.8	31.0	0.80–3.30	2.10	477,171
Canada	20.7–40.7	30.7	0.37–3.15	1.76	378,598
Nigeria	25.2–40.9	33.1	0.09–0.29	0.19	258,640
Angola	31.7–33.7	32.7	0.17–0.23	0.20	177,958
Colombia	30.8–36.4	33.6	0.25–0.47	0.36	130,364
Iraq	24.7–35.1	29.9	1.97–3.50	2.74	114,513
Kuwait	18.6–31.4	25.0	2.52–4.55	3.54	109,142
Norway	29.3–43.4	36.4	0.14–0.44	0.29	80,820
Gabon	31.8–39.5	35.7	0.05–0.11	0.08	75,543
The U.K.	33.6–41.7	37.7	0.05–1.01	0.53	66,002

[a] From *Oil and Gas Journal* (1999).
[b] From Energy Information Administration (1999).

Of the crudes imported to the United States, the crude from Kuwait, Venezuela, Iraq, and Saudi Arabia have a sulfur content of above 2% (sour crude). On the other hand, crudes from Gabon, Nigeria, Angola, Norway, and Colombia have a sulfur content of below 0.4% (sweet crude). As for API gravity, crudes from the U.K., Norway, Gabon, Colombia, Nigeria, Saudi Arabia, Mexico, and Canada have an API gravity above 30 (light crude). Crudes from Venezuela, Kuwait, and Iraq have an API gravity of below 30 (heavy crude). These crudes, with different sulfur contents and API gravity values, certainly have different impacts on refining energy intensities of U.S. refineries, and consequently, on petroleum refinery energy use and emissions.

The default energy efficiencies of U.S. petroleum refineries in the GREET model are based on studies for U.S. average refineries, which reflect the average quality of the crudes that U.S. refineries process. When marginal crude is used for a fuel-cycle analysis, it can have some impacts on energy use and emissions of petroleum refining. In this analysis, we implicitly assume the average quality of the crudes used in U.S. refineries.

3.1.5 Energy Efficiency Assumptions for Production of Gasoline, Diesel, and Naphtha

3.1.5.1 Specifications of Fuel Options

For the three petroleum-based fuels, we include the following fuel options, depending on sulfur content and use of oxygenates (for gasoline) and sulfur content only (for diesel and naphtha). For gasoline, we include five options: CG, FRFG2, low-sulfur (LS) RFG with MTBE, LS RFG with ethanol, and LS RFG with no oxygenate (see Table 6). In GREET, we simulated each of the five options separately. In Appendix A, we present results for two aggregate options — current

Table 6 Five Gasoline Options Included in This Study

Item	Current Gasoline		Future Gasoline		
	CG[a]	FRFG2 with MTBE[b]	LS RFG with MTBE[c]	LS RFG with EtOH[d]	LS RFG with no Oxygenate[e]
RVP (psi, for summer)	8.9	6.7	6.7	6.7[f]	6.7
Sulfur content (wt. ppm)	340	150	5-30	5-30	5-30
Benzene content (vol. %)	1.53	0.68	0.68	0.68	0.68
Aromatics content (vol. %)	32	25	25	25	25
Oxygen content (wt. %)	0.4	2.26	2.26	3.5	0
Oxygenate type	MTBE	MTBE	MTBE	EtOH	None

[a] CG is sold nationwide now except in the worst ozone nonattainment areas, where RFG is required. Nationwide, about 70% of gasoline sold now is CG.
[b] FRFG2 is currently required in the worst ozone nonattainment areas nationwide except in California.
[c] The RFG has significantly reduced sulfur content and uses MTBE to meet oxygen requirements.
[d] The RFG has significantly reduced sulfur content and uses ethanol to meet oxygen requirements.
[e] The RFG has significantly reduced sulfur content and uses no oxygenate.
[f] In order to meet the low RVP requirement, gasoline blendstock needs to have much lower RVP.

gasoline and future LS gasoline — and results for each of the five individual options. Current gasoline includes CG and FRFG2, and future gasoline includes LS RFG with MTBE, ethanol, and no oxygenate.

For on-road diesel fuels, we include two options: a current diesel and a future diesel. The current on-road diesel has a sulfur content of 120–350 ppm and includes the current federal diesel (350-ppm sulfur) and current California diesel (120-ppm sulfur). The future diesel reflects the new on-road diesel requirement adopted by EPA recently and will have sulfur content below 15 ppm.

Although virgin crude naphtha from petroleum refineries' distillation without desulfurization has a sulfur content of about 370 ppm, the sulfur content of naphtha will have to be reduced to an extremely low level in order for it to be used in FCVs. We assumed that the sulfur content of crude naphtha for fuel-cell application will be about 1 ppm. Thus, hydrotreating or some other desulfurization measures will be needed in refineries to reduce naphtha's sulfur content from the current level of about 370 ppm to 1 ppm.

3.1.5.2 Energy Efficiencies of Key Stages

Petroleum Recovery

The petroleum recovery stage includes activities from removing oil from underground to oil treatment in oil fields. In oil fields, gas is usually produced in association with oil production. In some locations, the associated gas has no value. In this case, the gas is often flared or vented. In calculating the energy efficiency of petroleum recovery, the energy (in Btu) in the flared and/or vented gas is not accounted for because it is not an intended energy source. However, in calculating emissions associated with petroleum recovery, flaring and/or venting of gas is taken into account.

Past published data in the United States showed an energy efficiency of 97% to 99% for petroleum recovery (Wang 1999a). In some parts of the world, the efficiency could be as low as 96%. An efficiency range of 96% to 99% was assumed in this study.

Petroleum Refining

Of the upstream and downstream activities from crude oil to gasoline and diesel fuels, crude refining is subject to the highest energy use, and consequently produces the largest amount of emissions. Thus, assumptions for the energy efficiency associated with refining crude into gasoline and diesel fuels are key factors in determining the upstream energy use and emissions of gasoline and diesel fuels.

Petroleum refinery operators have data on inputs of crude, other feedstocks, and process fuels (usually natural gas and electricity) and outputs of different petroleum products for their refineries. With input and output data for a given refinery, researchers can calculate the overall energy efficiency of the refinery. However, such data are usually not available to those outside of the individual companies. Thus, this approach may not be feasible for outside researchers.

Alternatively, a linear programming (LP) model may be run to simulate operations of a specified refinery (or a notional refinery) with certain crude quality and certain slate and quality of petroleum products. Results from refinery LP simulations can then be used to calculate the overall energy efficiency of the specified refinery. Admittedly, the energy efficiency of the notional refinery is different from that of individual refineries in operation, because the refinery configuration, advancement of refining technologies, crude quality, product slate, and gasoline quality (among many other factors) assumed in the notional refinery could be different those of actual refineries. Nonetheless, such LP simulations could provide information that is representative of petroleum refining. Ideally, LP simulations could be conducted for different sets of parameters regarding refinery input and output items to generate refining energy efficiencies for different refinery configurations. However, resource limitations have prevented almost all fuel-cycle studies, including Argonne's studies, from running LP models. Instead, these studies have relied on energy efficiencies generated from other detailed studies on petroleum refining modeling.

To complicate the matter further, the overall energy efficiency of a given refinery needs to be assigned to individual petroleum products so that a fuel-cycle analysis can be conducted for a given petroleum product (such as gasoline or diesel fuels). In other words, the total energy use in a refinery needs to be allocated to its different refinery products. The energy allocation can be done in the following steps. First, the energy use during each of the major refining processes (e.g., distillation, cracking, alkylation, isomeration, desulfurization) is estimated. Second, the estimated process-specific energy use is allocated into a product (or products), depending on the purpose of the process. Finally, the product-allocated energy use for all refinery processes is added together for a given product (e.g., gasoline) to represent the energy use for producing the product. Often, data at this level of detail are too scarce to take this approach.

Probably one of the most comprehensive refinery modeling studies that has been completed in the last ten years is the study conducted by the National Petroleum Council for production of various RFGs (NPC 1993). The NPC has recently completed a new study on the U.S. petroleum

refinery industry (NPC 2000). Energy efficiencies of producing various RFG types from the 1993 NPC study were summarized in Stork and Singh (1995). With data presented in Stork and Singh, we calculated an energy efficiency of 86.6–87.6% for CG, 86.3% for summer FRFG2 with MTBE, 88.2% for winter FRFG2 with MTBE, and 88.1% for winter RFG2 with ethanol (EtOH). It appears that efficiencies estimated with data from Stork and Singh are higher that those from other studies.

Three recently completed studies are available from MathPro, Inc. The first MathPro study was conducted for the Alliance of Automobile Manufacturers to simulate production of gasoline with 5-ppm sulfur in PADDs 1 to 3 (MathPro 1999a). The second study was conducted for the Engine Manufacturers Association to evaluate costs of diesel fuels with different sulfur contents (MathPro 1999b). The third study was conducted for California Energy Commission to evaluate the impacts of producing California's newly adopted CARFG3 (MathPro 1999c).

The three MathPro studies simulated notional refineries for producing gasoline and diesel with different specifications. The studies present the amounts of various input feeds and the amounts of various output products with many individual LP simulation cases. By using the higher heating values for input feeds and output products that are provided in the MathPro studies, we calculated the overall energy efficiencies of refinery configurations that are simulated in the MathPro studies. The difference between lower and higher heating value for a given fuel lies in whether the heat associated with condensation of water vapor generated during combustion is taken into account. In transportation fuel-cycle analysis, some studies have used lower heating values, some use higher heating values, and others use the combination of lower and higher heating values. Use of higher heating values is based on the belief that energy contained in combustion vapor could be recovered for use. Use of lower heating values is based on the fact that energy in combustion vapor from vehicles is impractical to recover. The GREET model is based on lower heating values.

Our estimated overall efficiencies for different refinery configurations are summarized in Table 7. The low and high efficiencies in Table 7 represent the range of the results for different refinery configurations to produce gasoline with the same specifications. Note that Table 7 shows that the high-end efficiency for producing RFG with MTBE or ethanol could be higher than that for producing CG, based on MathPro simulations. One reason could be the octane enhancement effect of adding MTBE and ethanol to gasoline, which makes production of gasoline blendstock (GBS) of RFG efficient.

Table 7 Overall Energy Efficiencies of Petroleum Refineries Extracted from MathPro Studies

	Refinery Overall Energy Efficiency (%)		
Refinery	Low	High	Source
Producing federal CG with 340 ppm S	88.4	88.4	MathPro (1999b)
Producing 150 ppm S FRFG2 with MTBE	87.7	87.9	MathPro (1999b)
Producing 5–30 ppm S RFG with MTBE	87.7	89.5	MathPro (1999a, 1999c)
Producing 5–30 ppm S RFG with EtOH	87.4	88.9	MathPro (1999a, 1999c)
Producing 5–30 ppm S RFG without oxygenate	87.6	87.8	MathPro (1999c)

The overall refinery efficiencies, as presented in Table 7, need to be converted into product-specific refinery efficiencies. We took the following steps for the conversion. As a rule of thumb in the petroleum industry, we allocated 60–65% of total refining process fuel use to gasoline production, 18–22% to diesel production, and the remaining 13–22% to other petroleum products. In 1999, of the total production volume of all petroleum products from U.S. refineries, motor gasoline accounts for 46.7%vol., diesel fuels for 20%vol., and other products for the remaining 33.3%vol. (EIA 2000). With the assumed allocations of total refinery fuel use and the product splits, we calculated a relative energy intensity of 1.28–1.39 for gasoline production, 0.90–1.10 for diesel production, and 0.39–0.66 for other products together, all relative to the energy intensity for production of all petroleum products combined.

With the above information, we estimated the energy efficiency of producing gasoline or diesel fuels. Table 8 presents our estimated energy efficiencies associated with producing various types of gasoline and diesel fuels.

From MathPro (1999a), we estimated that the amount of refining process fuels used (natural gas and electricity) is increased by 1.6% from 330-ppm diesel to 10-ppm diesel, and by 2.4% from 330-ppm diesel to 2-ppm diesel. By allocating all the increase to LS diesel production, we estimated the energy efficiencies for 10-ppm sulfur diesel and 5-ppm sulfur diesel (see Table 8).

Table 8 also shows that there might be an energy penalty for production of CARFG3 containing no oxygenates, relative to production of FRFG and CARFG containing oxygenates. We believe that the decreased efficiency for CARFG3 with no oxygenate is attributable to increased energy requirement for replacement octane (MathPro simulation results showed increased amounts of inputs of isobutene, isomerate, and CARBOB [California reformulated blendstock for oxygenate blending]) and decreased CARFG3 output, as shown in MathPro's simulations. Note that MathPro's simulations for national RFG and diesel production were conducted for PADDs I, II, and III, while the simulations for California RFG production were conducted for California (about 90% of PADD V). For comparison purpose, Unnasch estimated refinery efficiencies of 83.6% for CG production and 88.6% for CD production in California (Unnasch 2000).

Table 8 Energy Efficiencies of Producing Gasoline and Diesel Fuels

	Results from MathPro Simulations (%)		Values Adopted in This Study (%)	
Fuel	Low Efficiency[a]	High Efficiency[a]	Low Efficiency[a]	High Efficiency[a]
340 ppm S CG	84.5	85.5	85	86
150 ppm S RFG with MTBE	83.7 (84.7)	84.9 (85.9)	84 (85)	86 (87)
5–30 ppm S RFG with MTBE	83.6 (84.6)	86.9 (87.9)	83 (84)	86 (87)
5–30 ppm S RFG with EtOH	83.3 (84.4)	86.2 (87.2)	83 (84)	86 (87)
5–30 ppm S RFG3 without oxygenate	83.5	84.8	83	86
120–350 ppm S diesel	87.0	89.2	88	90
5–30 ppm S diesel	86.8	89.0	85	89
5–30 ppm S crude naphtha	89.0	93.0	89	93

[a] Numbers in parentheses are efficiencies for production of gasoline blendstocks for RFG. The increased efficiencies for gasoline blendstock production reflect the octane enhancement effect of adding oxygenates into RFG.

Table 8 shows that with the decrease in diesel fuel's sulfur content from 330 ppm to 10 ppm and then to 5 ppm, the energy penalty is minimal, based on MathPro's simulation results. Shell and BP suggest that MathPro's LP simulations may underestimate energy penalty of gasoline and diesel desulfurization. Based on its own experience, Shell believes a 1% point penalty for sulfur reduction from 350 ppm to 50 ppm, and another 1% point penalty from 50 ppm to 5 ppm, for both gasoline and diesel. We adjusted the efficiencies derived from MathPro's simulations with Shell's suggestion. In particular, we assumed the same efficiencies for the high-efficiency case between current gasoline and future gasoline and but lower efficiencies for future diesel than for current diesel. For gasoline, we reduced the efficiency for the low-efficiency case by 1% point from CG to 150-ppm S RFG and by another 1% point from 150-ppm S RFG to 5-30 ppm S RFG. For diesel fuels, we reduced the efficiency for the low-efficiency case by 2% points from current diesel to future diesel.

Historically, naphtha has been a gasoline upgrading process blendstock, not a major final product from petroleum refineries. Because of this, we have not seen any studies to evaluting energy efficiencies of producing naphtha in petroleum refineries. As stated in a previous section, virgin pipestill naphtha is produced from the atmospheric distillation process in refineries. The process is relatively energy efficient. However, as Tables 3 and 4 show, naphtha from the distillation process contains a high level of sulfur. FCVs will certainly require much lower sulfur content in naphtha.

LPG, straight-run gasoline, naphtha, and middle distillates rank from low to high in terms of their boiling points. We do not have energy efficiencies for naphtha production, but we do have energy efficiencies for production of LPG, gasoline, and diesel. However, gasoline energy efficiencies presented in existing studies are not for straight-run gasoline from the atmospheric distillation process. To approximate efficiencies for naphtha production, we used the efficiencies for LPG and diesel production. Based on how these three fuels are produced in refineries, we assumed that the efficiency for naphtha production is below that for LPG production but above that for diesel production.

Wang (1999a), showed LPG refining efficiencies of 90–94.6%, with a mean value of 93.5%. As the above table presents, refining efficiency for current diesel is 87–89% (with a mean value of 88%). Based on these data, we assumed refining efficiencies of 91–93% (with a mean value of 92%) for producing naphtha with a sulfur level of about 370 ppm. As stated above, there may be an energy efficiency penalty of 2 percentage points to reduce diesel sulfur level from 350 ppm to 1 ppm. Based on this, we assumed a 2% point reduction in refining efficiencies for the low-efficiency case of crude naphtha with sulfur level reduced from 370 ppm to 1 ppm. Thus, we assumed refining efficiencies of 89–93% (with a mean value of 91%) for producing 1-ppm S naphtha from crude.

Table 8 presents efficiencies of producing RFG that contains gasoline blendstocks (GBSs) and oxygenates (MTBE or ethanol). In GREET, energy efficiencies of RFG are further separated for gasoline blendstocks and oxygenates in order to conduct detailed simulations. For this purpose, we need energy efficiencies of producing gasoline blendstocks that are to be used for blending with oxygenates for different RFG types. Because of the octane enhancement effect of adding oxygenates to RFG, production of gasoline blendstocks for RFG could be more efficient than production of RFG without oxygenates. We allow some energy benefits of oxygenates' octane

enhancements in our analysis. The efficiencies with oxygenates' octane enhancement effect, as presented in parentheses of Table 8, are used in our simulations.

MTBE, ethanol, or no oxygenate is assumed for use in RFG (see Table 6). MTBE is allowed for use in RFG to meet its oxygen requirement until 2003 after which either ethanol could be used to meet oxygen requirements, or there may not be an oxygen requirement at all. Energy use and emissions of producing MTBE and ethanol are simulated separately in the GREET model. GREET assumes that MTBE is produced from methanol, which is, in turn, produced from natural gas. Ethanol is currently produced from corn. For details of energy use and emission simulations of MTBE and ethanol production, see Wang (1999a).

3.2 Fuels Produced from Natural Gas

This study includes these fuels that are produced from natural gas: compressed natural gas (CNG), methanol, Fischer-Tropsch diesel (FTD), gaseous hydrogen ($G.H_2$) produced in central plants, $G.H_2$ produced in refueling stations, liquid hydrogen ($L.H_2$) in central plants, $L.H_2$ in refueling stations, and naphtha via the Fischer-Tropsch process (FT naphtha).

All the fuels included here can be produced in North America. However, since abundant and inexpensive gas is available outside of North America, we include pathways of producing these fuels from non-North-American (NNA) gas as well. Furthermore, since there is a large amount of gas that is being flared each year in some parts of the world, for NNA gas-based pathways, we include both commercial gas and flared gas for production of the fuels included in this study. Details of production pathways are presented in sections below.

3.2.1 Natural-Gas-Based Fuel Pathways

Three sources of NG feed are included in this analysis: North American natural gas (NA NG, including natural gas from the U.S., Canada, and Mexico), non-North-American natural gas (NNA NG), and non-North-American flared gas (NNA FG). As Table 9 shows, NA NG accounts for only 5.8% of total world gas reserves. Because of the large amount of inexpensive NNA NG, it is conceivable that the U.S. transportation sector may tap into NNA NG in the future.

Table 9 Natural Gas Reserves[a]

Location	Natural Gas Reserve	
	10^{12} cubic feet (ft^3)	10^9 oil-equivalent barrels
North America	297.2	51.2
United States	167.2	28.8
Central and South America	221.9	38.3
Western Europe	166.5	28.7
Eastern Europe and Former USSR	1952.0	336.6
Middle East	1723.4	297.1
Africa	351.9	60.7
Far East and Oceania	378.5	65.3
World Total	5091.2	877.8
OPEC	2213.0	381.6

[a] From Wang and Huang (1999).

Worldwide, about 3.8 trillion ft^3 of gas (equivalent to about 655 million barrels of oil) is flared each year (EIA 1998). This is about 5% of the total NG produced each year. Some researchers suspect that the actual amount of gas flared is far greater than reported. As some countries started to impose economic penalties for gas flaring in an effort to reduce CO_2 emissions, energy companies began to look for other alternatives to dispose or use associated gas from oil fields. One option is to build production and transportation facilities near oil fields to produce liquid fuels from flared gas. We include NNA FG for fuel production in our analysis.

Among the fuels included in this study, while liquid fuels (i.e., methanol, $L.H_2$, FTD, and FT naphtha) can be produced outside of North America from either NG or FG and then transported to the U.S., gaseous fuels (CNG, $G.H_2$, and $L.H_2$ produced in refueling stations) must be produced in the U.S in order to avoid expensive cross-ocean transportation of gaseous fuels. For these cases, we assumed that liquefied natural gas (LNG) is produced from NNA NG and FG first. LNG is then transported to U.S. ports and gasified there. Finally, gasified NG is transmitted via pipelines to refueling stations where gaseous fuels are produced in the way similar to their production from NA NG. Figures 4–10 present production pathways for each of the fuels included in this study. The stages that are highlighted in shade in these figures are to be subject to probability distribution functions for their energy efficiencies (see a later section).

The fuel production pathways presented in the seven figures represent possible pathways. The economics of some of the pathways will certainly rule them out from further consideration. However, economics is not part of the scope of this study, so we present technologically possible pathways.

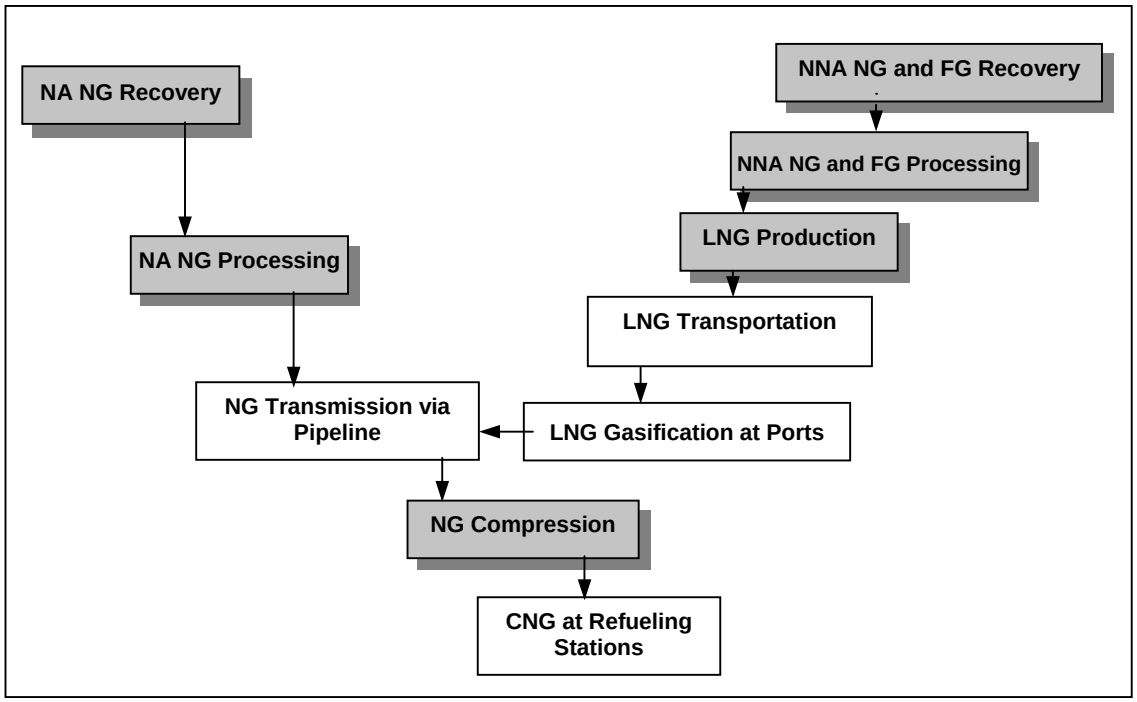

Figure 4 Pathways of CNG Production

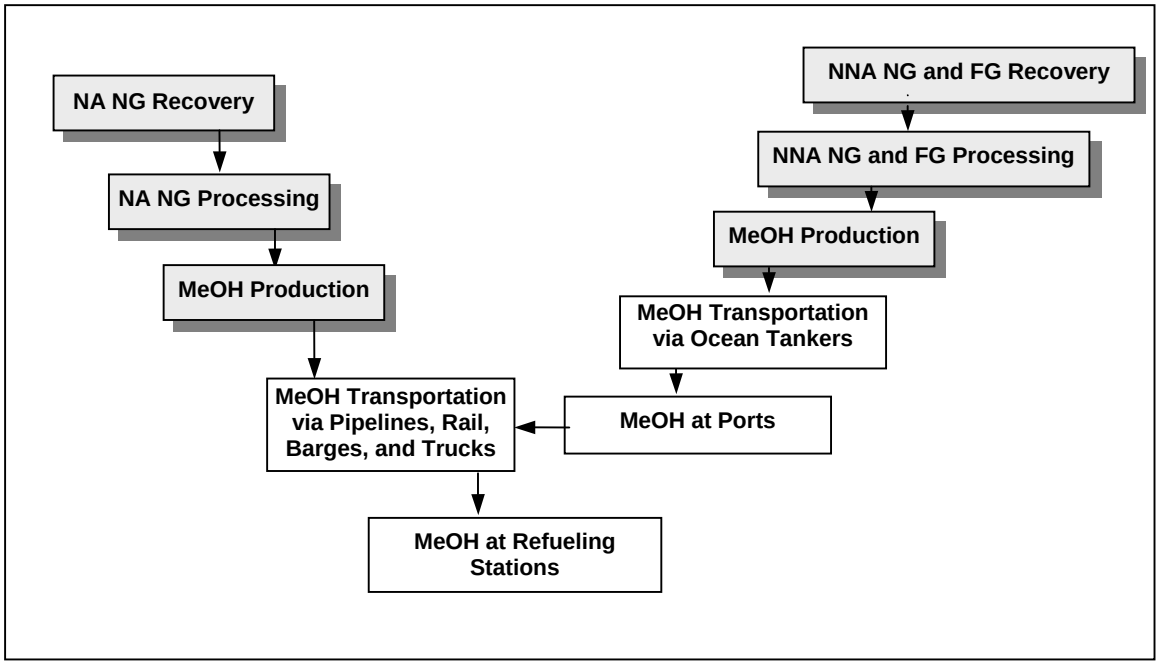

Figure 5 Pathways of Methanol Production

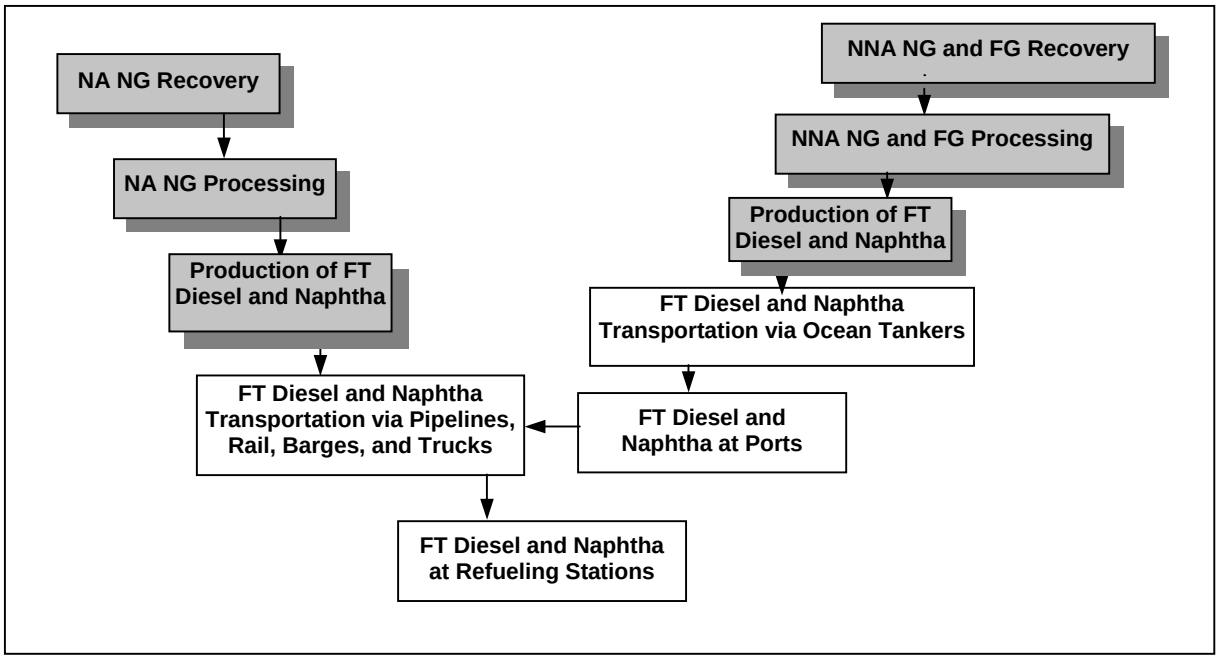

Figure 6 Pathways of Fischer-Tropsch Diesel and Naphtha Production

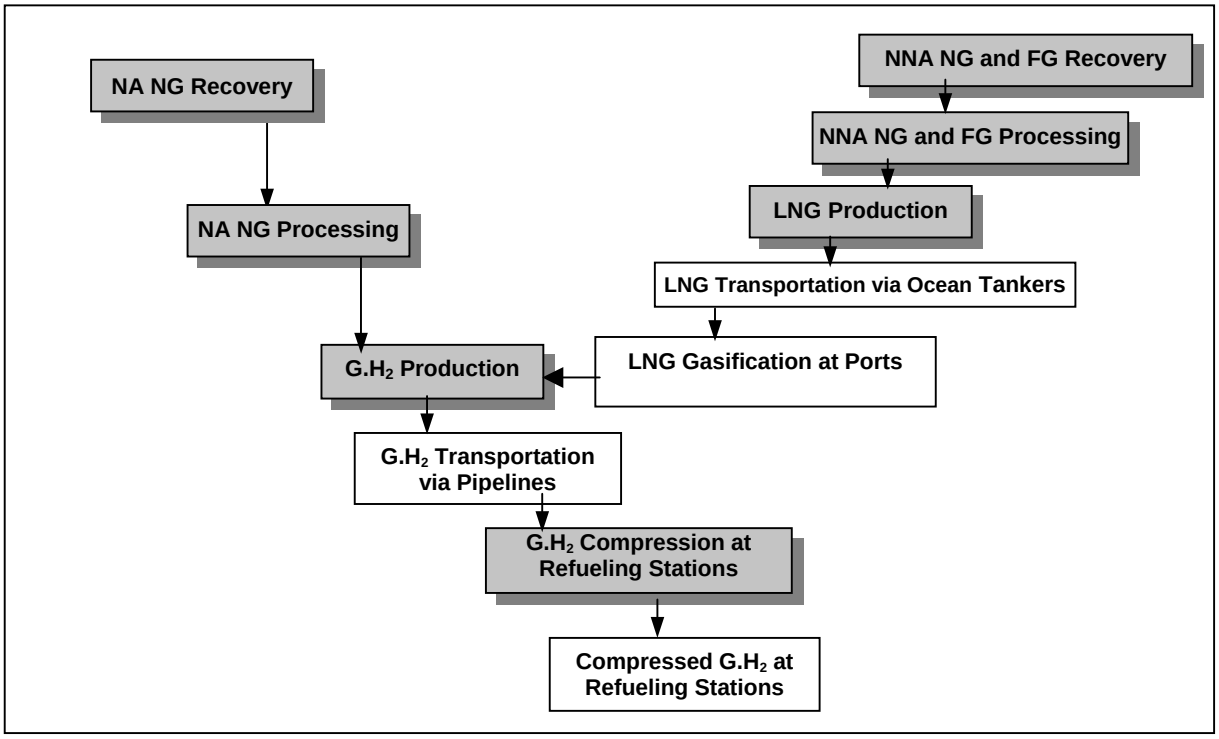

Figure 7 Pathways of Gaseous Hydrogen Production in Central Plants

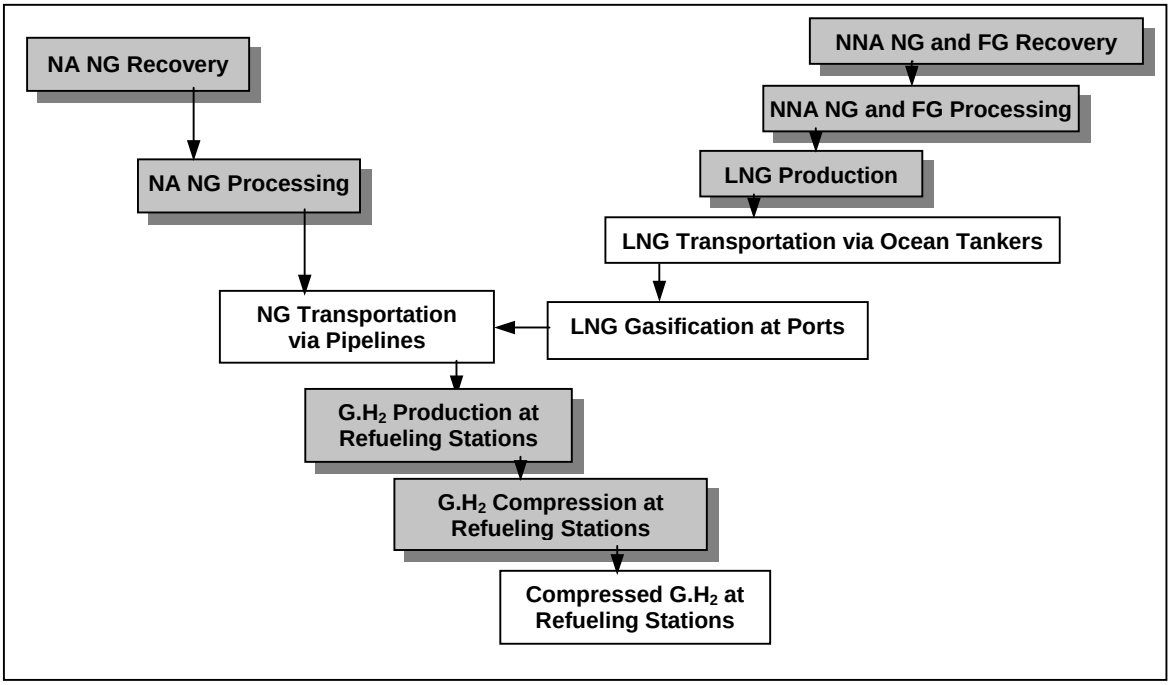

Figure 8 Pathways of Gaseous Hydrogen Production at Refueling Stations

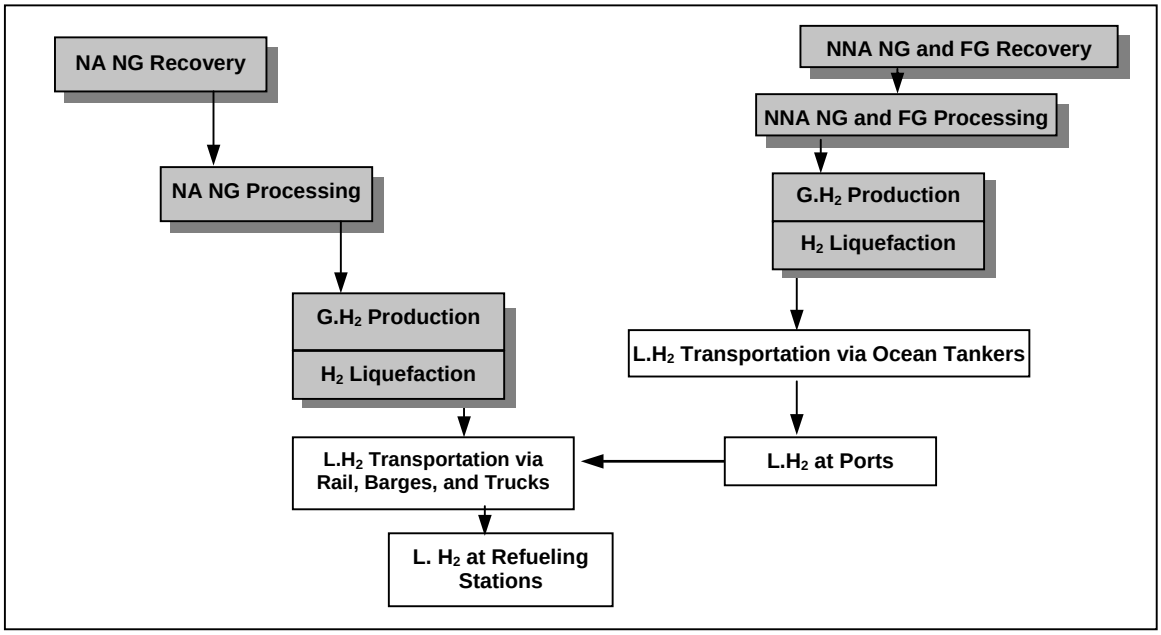

Figure 9 Pathways of Liquid Hydrogen Production in Central Plants

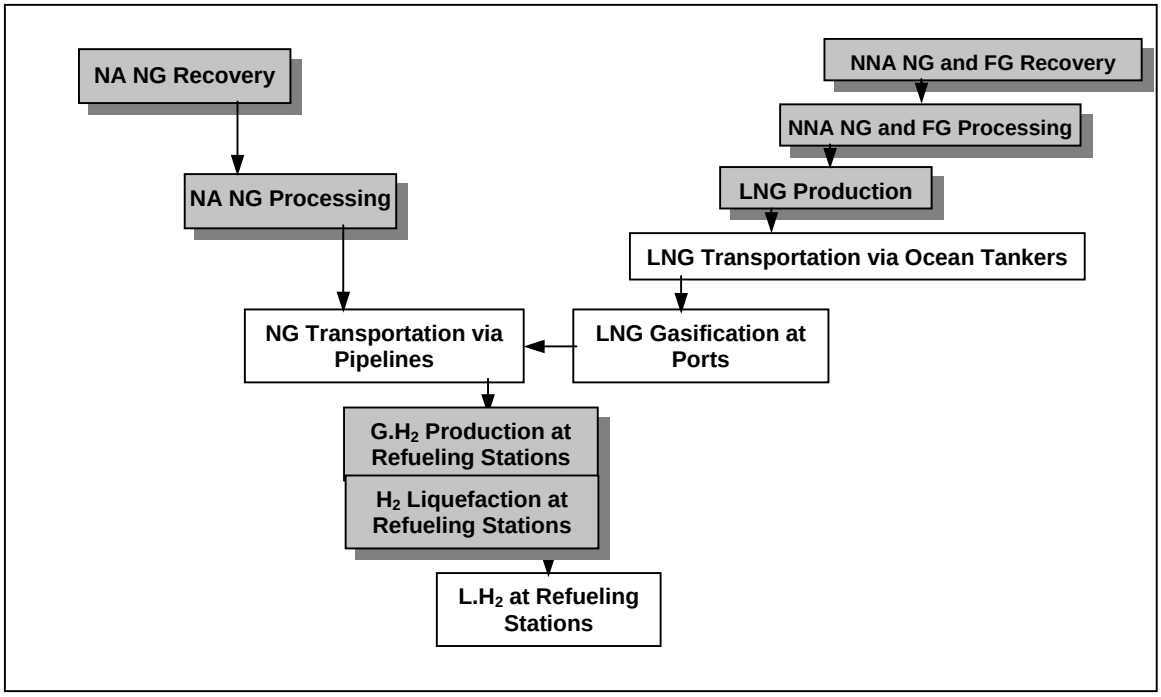

Figure 10 Pathways of Liquid Hydrogen Production at Refueling Stations

Figure 4 presents three pathways of producing CNG for motor vehicle applications: CNG from NA NG, NNA NG, and NNA FG. We assumed that CNG is stored onbaroad vehicles at a pressure of about 3,600 pounds per square inch (psi). In order to achieve this onboard pressure, natural gas in storage tanks at CNG refueling stations probably needs to be maintained at around 4,000 psi. We assumed that both electric and NG compressors will be used to compress NG. For the two NNA pathways, NG is liquefied and LNG is transported to the U.S. via ocean tankers. LNG is then gasified in LNG terminals. Because of production of LNG involved in these two pathways, these pathways suffer additional efficiency losses.

Figure 5 shows the three pathways for methanol production from NA NG, NNA NG, and NNA FG. At present, it is reported that worldwide there is at least 33% excess methanol production capacity. Most of the excess capacity is located where NG feed cost is high. If MTBE is eventually phased out in U.S. gasoline, there will be more excess capacity that can produce methanol for other applications such as powering FCVs. In our analysis, we take into account the potential use of the excess methanol production capacity for FCV applications. Among all the stages involved in the methanol pathways, methanol production suffers the largest efficiency losses.

Interest in Fischer-Tropsch diesel (FTD) that is produced from NG has been heightened in recent years mainly because of demand for cleaner diesel fuels for diesel engines to reduce emissions of NO_x and particulate matter. FT plants usually produce three groups of hydrocarbons: FT naphtha (C5–C9), FT middle distillates (C10–C20), and FT wax (>C20). In some FT plant designs, wax is further cracked into middle distillates. FT middle distillates (commonly called FT diesel) are a premium diesel engine fuel with virtually zero sulfur content and high cetane number but poor cold flow properties. FT naphtha, with virtually no sulfur, could be a reformer feedstock for fuel-cell vehicles. Typical properties of FT naphtha are presented in Table 4. Figure 6 presents the pathways from NG to FTD and FT naphtha. For each fuel, there are three production pathways (from NA NG, NNA NG, and NNA FG). The largest efficiency loss during these pathways occurs in FT plants. Wang and Huang (1999) discussed FT plant designs, production efficiencies, and other co-products in detail. In our analysis, we allocated energy use between FTD and FT naphtha according to the share of energy content in produced FTD and FT naphtha in FT plants. As the figure shows, FT naphtha is to be transported to refueling stations from FT plants. Although pipelines and tankers, which are used now to transport gasoline, could be used to transport FT naphtha, potential contamination of zero-sulfur FT naphtha by residual gasoline in transportation facilities needs to be avoided. FTD can be transported to refueling stations with the existing diesel transportation and distribution infrastructure.

Figure 7 shows the three pathways for producing the $G.H_2$ in central plants from NA NG, NNA NG, and NNA FG. To avoid expensive transportation of $G.H_2$ across oceans for NNA NG and NNA FG to $G.H_2$, we assumed that NNA NG and FG are liquified first. LNG is then transported via ocean tankers to U.S. LNG terminals where LNG is gasified. Gasified NG is transported to central H_2 plants via pipelines. Depending on economics, centralized H_2 plants can be built near LNG terminals or city gates. In the former case, NG transportation is avoided. In the latter case, long-distance transportation of $G.H_2$ is avoided.

For the three central $G.H_2$ pathways, the $G.H_2$ production stage suffers the largest efficiency losses among all of the activities associated with these pathways. $G.H_2$ is assumed to be stored

on FCVs at about 5,000 psi. To achieve this, $G.H_2$ may need to be compressed to 6000 psi at refueling stations. We assumed that electric compressors are used to compress H_2 at H_2 refueling stations. Compression of $G.H_2$ incurs a substantial efficiency penalty. For the two NNA pathways, production of LNG suffers additional large efficiency losses.

While H_2 production in central plants can have high-energy efficiencies and take the advantage of economy of scale in costs, centralized H_2 production requires pipelines for H_2 transportation, which can be very expensive to build. On the other hand, H_2 production at refueling stations avoids expensive H_2 pipelines. Figure 8 shows $G.H_2$ production pathways at refueling stations (sometimes called decentralized or distributed H_2 production). In this case, NG is transported to refueling stations where small-scale reformers will be used to produce $G.H_2$. But refueling station H_2 production suffers from low efficiency and high cost.

$L.H_2$ may be produced so that H_2 can be stored cryogenically on FCVs. Figures 9 and 10 show $L.H_2$ production pathways in central plants and at refueling stations. With these pathways, produced $G.H_2$ needs to be liquefied, which is very energy inefficient. Note that for production of $L.H_2$ from NNA NG and FG in central plants, $L.H_2$ is assumed to be produced offshore and then transported to the U.S. via ocean tankers. Although there is no $L.H_2$ ocean tanker now, the technological and economical feasibility has been studied in Japan. On the other hand, production of $L.H_2$ at refueling stations with NNA NG and FG requires production of LNG and transportation of it to U.S. LNG terminals.

As stated above, use of NNA NG and NNA FG for production of CNG, $G.H_2$, and $L.H_2$ production at refueling stations requires production of LNG outside of North America and transportation of LNG to North America, causing considerable energy losses. We estimate and include energy use and emissions of LNG production and transportation for these fuel options.

In general, production of liquid fuels (methanol, FTD, FT naphtha, and $L.H_2$) in North America can be more efficient than production outside of North America, since North American gas is more expensive than NNA gas, providing incentives for efficient plants. For this reason and for the reason that the transportation distance is very different between NA pathways and NNA pathways, the GREET model separates production pathways between NA gas and NNA gas so that individual reserachers can simulate these pathways separately.

3.2.2 Key NG Upstream Stages

3.2.2.1 Natural Gas Recovery and Processing

In gas fields, natural gas is lifted from underground and transmitted to processing plants via small distribution pipelines. At processing plants, natural gas liquids and impurities are removed from gas to produce pipeline-quality gas. The gas recovery stage includes lifting gas from underground and transportation of gas to processing plant gates. During this stage, gas may leak during lifting and transmission. Because gas is the intended energy source, the leaked gas should be taken into account in estimating gas recovery efficiency. On the other hand, the gas processing stage includes all the activities in gas processing plants to making gas available at the beginning of gas distribution pipelines. On the basis of published data and comments from the three energy companies, we assumed the same energy efficiencies for gas recovery and processing.

This study includes three NG supply sources for U.S. fuel production: NA NG, NNA NG, and NNA FG. Because of high gas demand, NA NG has high market value. Because of this, one might expect that efforts would be made to reduce gas leaks during gas recovery and processing, resulting in high energy efficienices. However, there are no data to differentiate energy efficiencies among NA NG, NNA NG, and NNA FG. Consequently, we assumed the same efficiencies for the three NG supply sources.

3.2.2.2 Fuel Production

Compression of Natural Gas

CNG vehicles can store NG onboard vehicles at a pressure of 3000–3600 psi. We assumed 3600 psi of NG pressure for NG stored onboard. To achieve this storage pressure, NG needs to be compressed to about 4000 psi and stored at that pressure in CNG refueling stations. We used the following formula to calculate the energy efficiency of NG compression.

$$W_{\min} = N \times \frac{k}{k-1} \times M \times R \times T \times Z \times \left(\left(\frac{P_2}{P_1} \right)^{\frac{k-1}{Nk}} - 1 \right) \quad (1)$$

$$\textit{Compression Efficiency} = \frac{FD}{\frac{W_{\min}}{CE \times EE} + FD} \quad (2)$$

where

$W_{\min}$ = minimum work requred for gas compression (W),
N = number of compression stages (4 for NG and 3 for G.H_2),
k = ratio of specific heats (1.32 for NG and 1.41 for H_2),
M = mass flow (kg/s),
R = univeral gas constant (J/kg K, 518 for NG and 4,124 for H_2),
T = temperature (K),
Z = compressibility factor (0.95 for NG and 1.2 for H_2),
P_2 = final pressure (bar),
P_1 = initial pressure (bar),
Compression efficiency = overall efficiency for compression,
FD = fuel delivered (kW),
CE = work efficiency of compressors (70% assumed here),
EE = engine efficiency (30–50% for NG-powered reciprocating engines and 90–92% for electric motors).

As the above formula shows, compression efficiency here is defined as the heating value of the compressed gas divided by the sum of energy used during NG compression and the heating value of the compressed gas. Several key factors determine the compression efficiency. They are initial pressure of NG, final pressure of NG, and the type of compressors. We assumed an initial pressure of 15 psi and a final pressure of 4000 psi for NG. We calculated compression

efficiencies for NG and electric compressors separately. For NG compressors, we assumed an energy efficiency range of 35% to 50% for reciprocating engines fueled with NG and an energy efficiency range of 90% to 93% for electric motors. Although it appears that electric compressors are much more efficient than gas compressors, there is a large efficiency loss during electricity generation. For example, conventional fossil fuel power plants have energy efficiencies of 32% to 38%. When electric power plant efficiencies are taken into account, the overall efficiency of gas compressors can be higher than that of electric compressors. The GREET model takes into account electric power plant efficiencies in estimating overall energy requirements of gas compression.

Using the above assumptions, we estimated the following compression efficiencies for CNG: 93% (with a range of 92% to 94%) for gas compressors and 97% (with a range of 96% to 98%) for electric compressors.

Natural Gas Liquefaction

As described in some previous sections, we assumed NG liquefaction for some of the fuel production pathways in order to bring NNA NG and FG to the U.S. for producing transportation fuels. In fact, at the current gas price in the U.S., some have maintained that LNG could be competitive against NA gas for use in the U.S. (*Oil and Gas Journal* 2000).

In LNG plants, substances such as water, CO_2, sulfur, and heavier hydrocarbons that freeze during NG liquefaction must be removed before liquefaction. Some of the substances are removed in NG processing plants. But usually pipeline-quality NG still has some remaining impurities that need to be removed before liquefaction. If LNG plants are built next to NG processing plants, or if two are integrated together, efficiencies of NG processing and NG liquefaction may be difficult to separate. In a fuel-cycle analysis, it is important that energy losses are not left out or double-counted.

The purified NG is cooled to about -260°F (at atmospheric pressure), the temperature at which NG becomes liquid. This is accomplished by heat exchange between NG feed and vaporization of refrigerants. NG can also be liquefied using an expansion cycle in which the gas (under high pressure) is expanded rapidly, thereby cooling it to its boiling point. Produced LNG is stored as a cryogenic liquid in insulated storage vessels at pressures of 50–150 psi. LNG stored this way can be transported by ocean tankers, trucks, rail, or barges.

The largest amount of energy in LNG plants is consumed in powering the refrigeration compressors. Energy required by the compressors can be provided by steam boilers, steam turbines, gas turbines, or electric motors. In old LNG plants, steam boilers or steam turbines, with low thermal efficiencies, were used. New plants are equipped with more efficient gas turbines, especially combined-cycle gas turbines (either providing shaft power directly or generating electricity for use in electric motors) (Kikkawa and Nozawa 1999; Vink and Nagelvoort 1998). We assumed that new centralized LNG plants employ combined-cycle turbines that provide shaft power directly to the compressors. Based on data in published studies, we assumed an energy efficiency range of 87–93% for NG liquefaction.

As the temperature in LNG tanks rises over time, some LNG evaporates and becomes NG. Pressure within an LNG tank can build up; this buildup is called a "boil-off effect" and the gas generated is called "boil-off gas." The boil-off effect can cause major losses of LNG during transportation and storage. Boil-off gas in LNG plants, ocean tankers, and bulk terminals is usually collected as a fuel for combustion. We accounted for the collected boil-off gas in our simulation.

Methanol Production

Methanol is produced through synthesis of a gaseous mixture of H_2, CO, and CO_2 (called syngas) into methanol via the steam-methane reforming (SMR) technology. This process requires a large amount of steam, and consequently consumes a large amount of energy. Syngas is then converted into methanol via the following reactions: $CO_2 + 2H_2 \rightarrow CH_3OH$ and $CO_2 + 3H_2 \rightarrow CH_3OH + H_2O$. Both reactions are exothermic, and efficient plants are designed to use the waste heat from the two reactions. However, most of the waste heat in a methanol plant is recovered when hot syngas from SR or ATR is cooled to lower the temperatures of the methanol synthesis reactor. This waste heat can be used to preheat reformer feed, generate steam for export, generate electricity for export, or purify product.

Another technology for methanol production is autothermal reforming (ATR). With ATR, the heat requirement for steam reforming is provided by combustion of a portion of the gas feed with pure oxygen inside a reforming reactor. One recent technology development for producing syngas to achieve the desired molar ratio is to integrate a partial oxidation (POX) process using pure oxygen with the SMR process. The integrated design, sometimes referred to as "two-step reforming," requires production of O_2 in methanol plants. The two-step reforming design is suitable for mega-size (3,000–5,000 ton/day capacity) methanol plants (Berggren 1997; Gronemann 1998; Islam and Brown 1997).

Wang and Huang (1999) summarized energy efficiencies of methanol plants with different designs. Recently, a study by $(S\&T)^2$ Consultants (2000) prepared for Methanex adopted the following energy efficiencies: 63% for existing SMR methanol plants and 73–75% for POX plants. The Methanex-commissioned study used an energy efficiency of 71% for year 2000 methanol plants and 73% for year 2010 methanol plants. Note that all efficiencies in that study are based on higher heating values, while all efficiencies used in Argonne's study are based on lower heating values.

As stated in an above section, at present, there is about 33% excess methanol production capacity. Furthermore, of the total amount of methanol used worldwide, about 26% is used for MTBE production. Several states in the U.S. already decided to ban use of MTBE in gasoline because of groundwater contamination by MTBE. There seems to be a trend that MTBE use in gasoline will decline significantly in the near future. We assume that MTBE use will be reduced by 50% worldwide in the next 10–15 years. This will result in additional methanol excess capacity. With these assumptions, we estimate that excess methanol capacity could reach 11 million metric tons a year (assuming no significant increase in methanol consumptions by other uses). This could fuel about 5 million methanol FCVs a year. Assuming 15 million methanol FCVs on road around 2015, we estimate that 1/3 of methanol for FCVs could be provided by idled existing methanol plants and 2/3 by new methanol plants. With an efficiency

of 63% for existing plants and 70% for new plants (based on lower heating values), we estimate an average efficiency of 67.5% for methanol production for FCV applications. This is for the plant design without steam generation.

As stated above, methanol plants are capable of producing steam for export or for electricity generation. We included three types of methanol plant designs: without steam generation, with steam generation for export, and with electricity generation for export. For the plant design with steam generation, we assumed an energy efficiency of 64% (without considering energy in co-generated steam) together with 78,130 Btu of steam per mmBtu of methanol produced. For the plants with electricity generation, we assumed the co-generated steam in methanol plants is used in steam boilers to generate electricity. Since the co-generated steam is low-quality steam (i.e., low-pressure steam), we assumed a low electricity generation efficiency of 30% with the low-quality steam.

In estimating energy and emission credits of the generated steam in methanol plants (and in FT diesel plants and hydrogen plants to be presented in sections below), we assumed that the co-generated steam will displace steam generation by conventional steam boilers fueled with natural gas, which have an energy efficiency of about 80% (Btu contained in steam divided by Btu contained in burned natural gas). In estimating energy and emission credits of the generated electricity in methanol plants (and in FT diesel plants and hydrogen plants to be presented in sections below), we assumed that the generated electricity would displace electricity generation by natural gas-fueled combined-cycle turbines.

Fischer-Tropsch Diesel and Naphtha Production

Production of FT diesel and naphtha consists of three steps: (1) production of syngas, (2) synthesis of middle distillates, and (3) upgrading of products. At the syngas production stage, NG feed is converted into syngas (a mixture of CO and H_2). Although SMR, POX, ATR technologies can all be used to generate syngas, POX and ATR reformers are preferred technologies for syngas production in FTD plants.

The next stage in FTD plants is the Fischer-Tropsch synthesis. The reaction, with the help of catalysts, produces a variety of hydrocarbon liquids including middle distillates and naphtha. The product mix from the process depends on the catalyst used and the operating temperature of the reactor. For example, an operating temperature of 180–250^{o}C helps produce predominately middle distillates and wax; an operating temperature of 330–350^{o}C helps produce gasoline and olefins.

Because the Fischer-Tropsch reaction is exothermic, some excess amount of steam is generated from the process. The generated steam can be exported to nearby facilities or used to generate electricity for export.

We included three types of FTD plant designs: with no steam generation, with steam generation, and with electricity generation. Both diesel fuels and naphtha can be produced from FTD plants. We assumed that they go through same processes in FTD plants and allocated energy and emissions according to their energy output shares.

The largest efficiency loss during FT pathways occurs in FT plants. Wang and Huang (1999) discussed FT plant designs, production efficiencies, and other co-products in details. In our analysis, we allocated energy use between FTD and FT naphtha according to the share of energy content in produced FTD and FT naphtha in FT plants. Based on published data and inputs from the three energy companies, we made the following assumptions. For the FTD plant design with no steam generation, we assumed energy efficiencies of 61% to 65%. For the design with steam generation, we assume energy efficiencies of 53% to 57% (without considering Btu in the generated steam) together with 189,000 to 210,500 Btu of steam per mmBtu of fuel products produced. For the design with electricity co-generation, we assumed the co-generated steam would be used in steam boilers to generate electricity for export.

It is important to notice that when comparing FTD with refinery diesel, the methodology used in this study and in many other transportation fuel-cycle studies does not give FTD any credit for the following: (1) an FT plant does not produce any less desirable co-products such as those from petroleum refineries (e.g., heavy residual oil and coke); and (2) FTD produced at a large scale could begin to allow diesel cars fueled with FTD to displace gasoline passenger cars in countries such as the United States, where, in some areas, tight emission regulations have recently restricted the penetration of diesel cars into the passenger car market.

Carbon efficiency of FT plants is defined as carbon in all products divided by carbon in NG feed. It is used to calculate net CO_2 emissions from FT plants. It is reported that the carbon efficiency of FTD plants can be 75% to 85% (see Table 3.3 of Wang and Huang [1999]). We used carbon efficiencies of 75% to 85%.

Gaseous Hydrogen Production in Central Plants

The majority of existing large-scale H_2 plants use SMR technology. Steam is added to NG feed, and the mixture of NG and steam is preheated before entering the reformer, where CH_4 is converted into the syngas (H_2, CO, and CO_2) in the presence of catalysts. The produced hot syngas, at a temperature of 900–930^{o}C, exits the SMR reformer and is cooled before entering the shift converter, where shift catalysts convert CO and steam to CO_2 and additional H_2. The gas from the shift converter is further cooled to ambient temperature before entering a pressure swing adsorption (PSA) unit, where high-purity H_2 is produced; the remaining gas mixture, the so-called tail gas, is used in the SMR reformer as supplemental fuel for the burners. Besides conventional SMR technology, other technologies such as POX and ATR can be applied in H_2 plants.

A H_2 plant can generate a significant amount of steam. Some of the steam can be used for processes within the plant, while the remainder can be exported to nearby facilities or to generate electricity for export. In our analysis, we assumed three types of H_2 plants: with no steam co-generation, with steam co-generation, and with electricity co-generation.

Based on published data and comments from the three energy companies, we assumed the following efficiency assumptions for the three plant types. For the H_2 plant design with no steam co-generation, we assumed energy efficiencies of 68% to 75%. For the H_2 plant design with steam co-generation, we assumed energy efficiencies of 66% to 73% (without considering the energy contained in the co-generated steam) together with 120,000–170,000 Btu of steam per

mmBtu of H_2 produced. For the plant design with electricity export, we assumed that co-generated steam is used in steam boilers to generate electricity for export.

In H_2 plants, all the carbon in CH_4 eventually ends up as CO_2. The produced CO_2 could be sequestered into depleted oil and gas wells to limit CO_2 emissions from H_2 plants or to enhance oil or gas recovery in oil or gas fields. Some researchers maintain that injection of CO_2 into oil and gas wells helps increase oil and gas production, which could make CO_2 injection an economical way to increase oil and gas production (Williams and Wells 1997; Blok et al. 1997). However, without economic incentives or regulations, it is uncertain whether CO_2 from H_2 plants will be sequestered. In our analysis, we did not assume CO_2 sequestration in H_2 plants.

Liquid Hydrogen Production in Central Plants

For this L.H_2 production option, we assumed that G.H_2 is produced in central plants first and then liquefied at the same facility. Thus, G.H_2 production efficiencies assumed in the previous section are applied to this pathway. In addition, H_2 liquefaction efficiencies are applied to the pathway.

Power requirements for refrigeration compressors during liquefaction consume a large amount of energy. Although energy for the compressors can be provided by steam boilers, steam turbines, gas turbines, or electric motors, most studies assumed that electricity is to be used for H_2 liquefaction. Because the boiling point of L.H_2 is much lower that that of LNG (-253ºC vs. -163ºC), the amount of energy required for H_2 liquefaction is much higher than that required for NG liquefaction. In our study, we assumed liquefaction efficiencies of 65% to 77% for central H_2 plant liquefaction (see Wang and Huang 1999).

We assumed three types of L.H_2 plants: without steam co-generation, with steam co-generation, and with electricity co-generation. Since L.H_2 plants require a large amount of electricity for liquefaction, we assumed the co-generated electricity is used in the plants for liquefactions. On the other hand, for plants with steam co-generation, we assumed that the co-generated steam is exported. In practice, the low-quality, low-pressure steam generated in H_2 plants could be upgraded and used to drive compressors for the liquefaction process.

Because of cryogenic storage of L.H_2 during L.H_2 transportation and storage, L.H_2 is subject to the boil-off effect. Because of this, L.H_2 is subject to some losses. The extent of L.H2 loss during to the boil-off effect depends on the duration of L.H_2 in a storage vessel. The duration of L.H_2 in L.H_2 tankers depends on transportation distance. For example, transportation of L.H_2 from NNA locations to U.S. ports may require about 13 days. Also, we assume an average storage time of 5 days on L.H_2 production plants, L.H_2 bulk terminals, and L.H_2 refueling stations each. We assume a boil-off rate of 0.3% per day for L.H_2 (see Wang and Huang 1999). The gaseous H_2 from boil-off of L.H_2 can be recovered as a process fuel. We assume a recovery rate of 50% for the generated gaseous H_2. Similarly, LNG is subject to the boil-off effect. Because the boil-off temperature for LNG is 98 ºC higher than that for L.H_2 (-161ºC vs. 259ºC), the boil-off rate for LNG is smaller than that for L.H_2. We assume a boil-off rate of 0.1% per day for LNG.

Gaseous Hydrogen Production in Refueling Stations

To avoid long-distance transportation and storage of $G.H_2$ and $L.H_2$, which can be very expensive, $G.H_2$ may be produced from NG in refueling stations with small-scale SMR systems. For this production option, we did not assume that steam is co-generated with H_2 in stations. Because operating conditions may not be optimized with small-scale SMRs, and operators may not be able to maintain a constant H_2 output, we expect that H_2 production efficiency at refueling stations is lower than that in central plants. We assumed energy efficiencies of 62–72%.

Gaseous Hydrogen Compression in Refueling Stations

$G.H_2$ may need to be stored onboard FCVs at pressures above 5,000 psi. So $G.H_2$ may need to be compressed to 6,000 psi or greater at refueling stations. For $G.H_2$ produced in central plants and transported to stations via pipelines, we assumed that electric compressors would be used to compress H_2 at the refueling stations. We assumed an initial pressure of 250 psi for $G.H_2$ coming out of H_2 pipelines at refueling stations. By using the formula presented in a previous section with specific parameters for H_2 compression, we estimated H_2 compression efficiencies of 90% to 95% for electric compressors (and 82.5% to 87.5% for corresponding NG compressors). In our analysis, compression efficiency is defined as the energy contained in the compressed H_2 divided by the sum of energy in electricity or NG used for compression and the energy in the compressed H_2. Energy loss during electricity generation is taken into account in a different part of the GREET model.

For $G.H_2$ produced at refueling stations, we assumed that both NG and electric compressors would be used to compress H_2. We assumed an initial pressure of 500 psi for $G.H_2$ produced at refueling stations. By using the formula that we presented previously, we estimated $G.H_2$ compression efficiencies of 91.5–96.5% for electric compressors and 83.5–88.5% for NG compressors.

To validate the compression formula presented in Section 3.2.2.2, we ran the ASPEN model at Argonne National Laboratory to generate $G.H_2$ compression efficiencies using similar assumptions. We calibrated our compression formula to make our estimated compression efficiencies close to the ASPEN-generated compression efficiencies.

Liquid Hydrogen Production in Refueling Stations

For this fuel production option, we assumed $G.H_2$ is produced at refueling stations first and H_2 is liquefied there. We assumed H_2 liquefaction efficiencies of 60–72%, which are lower than the liquefaction efficiencies in central plants.

3.3 Bio-Ethanol Production Options

Currently, the United States has an annual ethanol production capacity of 1.8 billion gallons, virtually all of which use corn as the feedstock. The transportation sector consumes about 1.5 billion gallons of ethanol a year, most of which is consumed in E10 (10% ethanol and 90% gasoline by volume). Meanwhile, the U.S. Department of Energy has been funding R&D efforts on cellulosic ethanol with emphasis on farming of trees and grasses and ethanol production from

cellulosic biomass. In this study, we included three ethanol production pathways: ethanol from corn, woody biomass (trees), and herbaceous biomass (grasses).

3.3.1 Bio-Ethanol Pathways

Figure 11 presents the three pathways of ethanol production from corn, woody biomass, and herbaceous biomass. These pathways begin with production of fertilizers and pesticides that are applied to corn and biomass farms. For corn-based ethanol, ethanol plants are the largest fossil energy-consuming source for the entire fuel cycle. Corn-based ethanol plants can be wet milling or dry milling. Wet milling plants employ more processes, require more capital investments to build, and are usually larger in size than dry milling plants. At present, a larger amount of ethanol is produced from wet milling plants than from dry milling plants in the U.S., even though recent additions of ethanol plants in the United States have virtually all been dry milling plants (primarily because smaller capital investment is required for dry milling plants and relatively large tax advantages are available for small ethanol plants in some states). We analyzed energy and emission impacts for both wet and dry milling plants.

Corn-based ethanol plants produce other products besides ethanol. These so-called co-products include distillers' grains and solubles (DGS) in dry milling plants, and corn gluten feed, corn gluten meal, corn oil, and other products in wet milling plants. Energy use and emissions need to be allocated between ethanol and its co-products. Several ways have been employed by researchers to allocate energy use and emissions (see Wang 1999a). We used the displacement

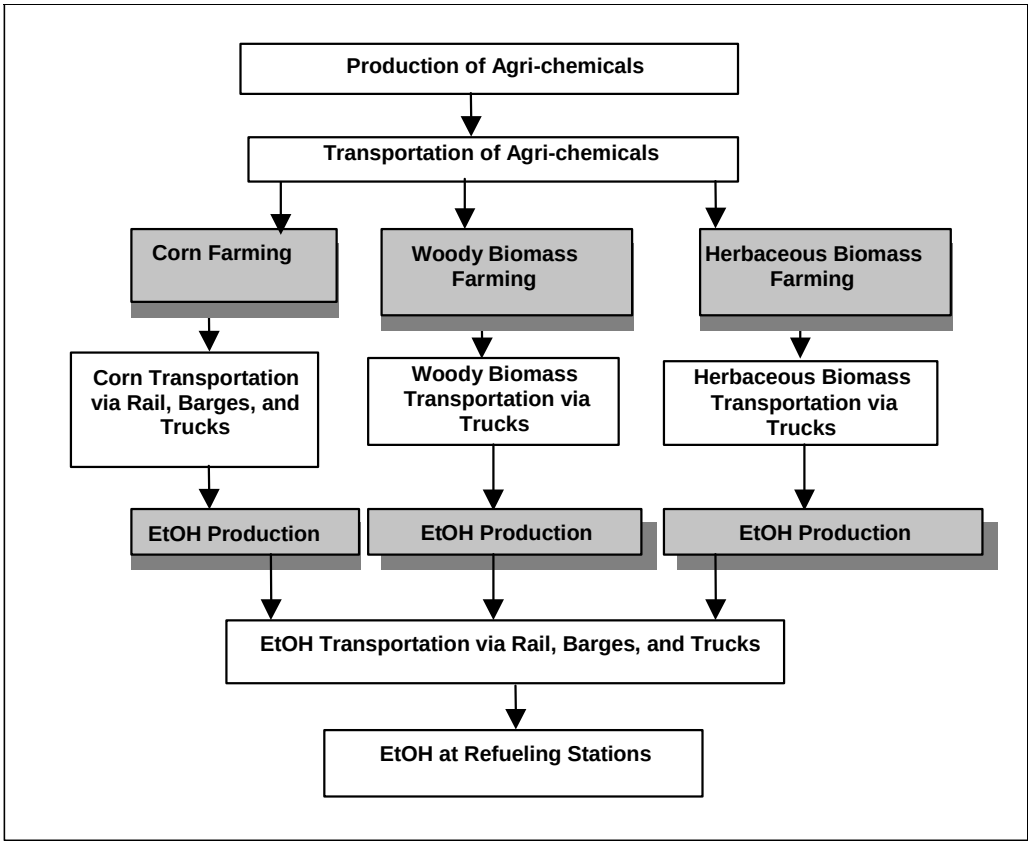

Figure 11 Pathways of Ethanol Production

method and market value method in this study. With the displacement method, first, the amount of co-products produced in an ethanol plant is estimated. Second, the products to be displaced by these co-products in marketplace are identified. Third, the displacement ratios between co-products and the displaced products are determined. Finally, energy use and emissions of producing the amount of displaced products are estimated. The estimated amount of energy and emissions, which represent energy and emission credits of ethanol co-products, are subtracted from total energy and emissions of ethanol pathways.

On the other hand, the market value method allocates energy and emissions among products on the basis of the market values of different products from corn ethanol plants. The method provides higher energy and emission credits than the displacement method does for corn ethanol. In our analysis, we used both the displacement and market value methods to cover the range of potential energy and emission credits of ethanol co-products.

In cellulosic ethanol plants, cellulose in biomass is converted into ethanol through enzymatic processes. The lignin portion of biomass can be burned in ethanol plants to provide needed steam. Co-generation systems can be employed to generate both steam and electricity from lignin. In this case, some amount of extra electricity can be generated in cellulosic ethanol plants. The co-generated electricity can be exported to the electric grid to displace electricity generation in some conventional electric power plants. We took electricity credit into account in calculating energy use and emissions of cellulosic ethanol production. In estimating energy and emission credits of cellulosic ethanol electricity, we used electricity generation with the U.S. average electric generation mix.

3.3.2 Parametric Assumptions

For corn-to-ethanol pathways, key input parameters determining ethanol's energy and GHG emissions impacts include: (1) energy use of corn farming (Btu per bushel of corn harvested), (2) nitrogen fertilizer use of corn farming (grams per bushel of corn harvested), (3) N_2O emissions from nitrification and denitrification of nitrogen fertilizer in cornfields (grams of nitrogen in N_2O per gram of nitrogen in nitrogen fertilizer applied to cornfields; N_2O is 310 times as potent as CO_2 in terms of potential global warming effects), (4) energy use in ethanol plants (Btu per gallon of ethanol produced), (5) ethanol yield per bushel of corn, and (6) ways of dealing with ethanol co-products. For the first five parameters, we established probability distribution funcitions. For co-product credits, since selection of allocation methods of dealing with co-product credits is more important than parametric values used for each allocation method, we used two methods to cover the potential range. The first method is the displacement method, which is the GREET-default method. The second method is the market value-based method. The market value-based method gives higher credits to co-products than the displacement method does.

For biomass-to-ethanol pathways, key input parameters include: (1) energy use for farming of trees and grasses, (2) fertilizer use for farming of trees and grasses, (3) N_2O emissions from nitrification and denitrification of nitrogen fertilizer in biomass farms, (4) ethanol yield per ton of biomass, and (5) electricity credit from cellulosic ethanol plants.

Table 10 lists parametric assumptions used in the GREET model.

Table 10 Parametric Assumptions for Ethanol Production Pathways[a]

Item	Pessimistic Assumption	Optimistic Assumption
Corn farming energy use (Btu/bushel of corn harvested)	18,990	17,090
Corn farming N fertilizer use (g/bushel of corn harvested)	440	396
N_2O emissions in cornfields (N in N_2O as % of N in N fertilizer)	1.5	1.5
Soil CO_2 emissions (g/bushel of corn harvested)	390	0
Energy use for tree farming (Btu/dry ton of trees harvested)	234,770	211,290
Energy use for grass farming (Btu/dry ton of grass harvested)	217,230	195,510
N fertilizer use for tree farming (g/dry ton of trees harvested)	709	638
N fertilizer use for grass farming (g/dry ton of grass harvested)	10,633	9,570
N_2O emissions in biomass farms (N in N_2O as % of N in N fertilizer)	1.3	1.3
Soil CO_2 sequestration in tree farms (g/dry ton of trees harvested)	0	-225,000
Soil CO_2 sequestration in grass farms (g/dry ton of grasses harvested)	0	-97,000
EtOH yield of dry milling plants (gal/bushel)	2.6	2.8
EtOH yield of wet milling plants (gal/bushel)	2.5	2.7
Energy use in dry milling plants (Btu/gal)	41,400	36,900
Energy use in wet milling plants (Btu/gal)	40,300	34,000
EtOH yield of woody biomass plants (gal/dry ton)	76	98
EtOH yield of herbaceous biomass plants (gal/dry ton)	80	103
Electricity credit in woody biomass plants (kWh/gal)	-1.730	-1.730
Electricity credit in herbaceous biomass plants (kWh/gal)	-0.865	-0.865

[a] From Wang (1999a).

3.4 Electricity Generation

Electricity can be used in battery-powered electric vehicles (EVs) and grid-connected hybrid electric vehicles (HEVs). Although use of electricity by these vehicles does not produce emissions, electricity generation does. In this study, we estimated energy use and emissions of electricity generation for these vehicle types. One of the key factors determining energy use and emissions of electricity generation is electric generation mix (the mix of the power plants fired with different fuels). Electric generation mix varies with regions. We included three generation mixes: the U.S., the California, and the Northeast U.S. electric generation mixes to cover a broad range of generation mixes. Some studies have concluded that NG-fired CC turbines will provide marginal electricity in the U.S. To approximate marginal electricity supply for EVs and HEVs, we included electricity generation with NG-fired CC turbines.

3.4.1 Electricity Generation Pathways

Figure 12 shows pathways for electricity generation. In GREET, four types of electric power plants are included for energy and emissions estimations: oil-fired, NG-fired, coal-fired, and nuclear power plants. Other power plants, such as hydroelectric power plants and windmill plants, have virtually zero operation emissions. Emissions from nuclear power plants are due to uranium recovery, enrichment, and transportation. As the figure shows, to estimate emsisions associated with electricity generation, GREET includes fuel production stages as well as

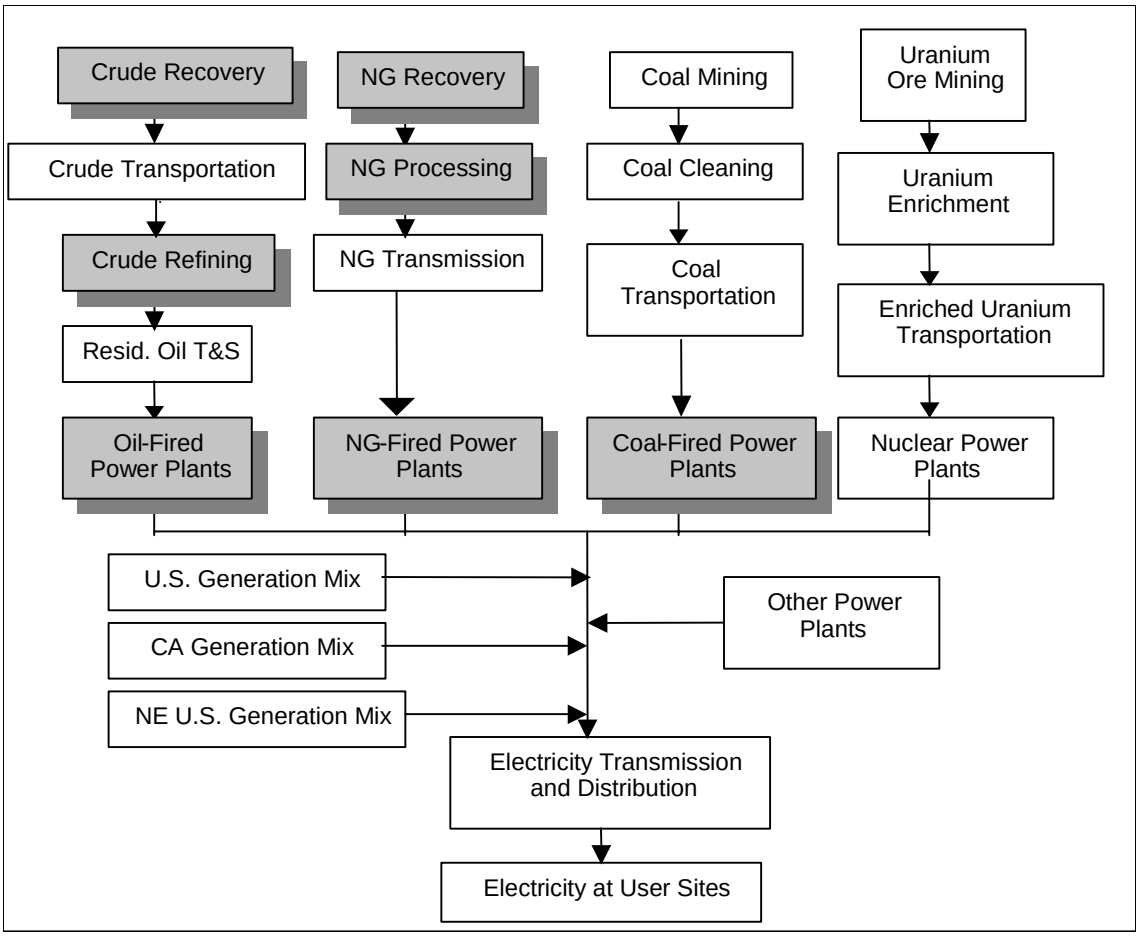

Figure 12 Pathways of Electricity Generation

electricity generation. In this study, the four types of power plants are eventually combined together with U.S., California, or Northeast U.S. electric generation mix to generate utility system energy use and emissions results.

3.4.2 Electricity Generation Efficiencies

The most important factor determining energy and emissions of electricity generation pathways is power plant energy conversion efficiencies. Based on published data, we assessed the following conversion efficiencies: 32–35% for steam boilers fired by oil, NG, and coal, 50–60% for NG-fired combined-cycle turbines, and 38–44% for advanced coal-fired power plants such as integrated gasification combined-cycle turbines.

There is an energy loss during transmission of electricity from power plants to user sites. The average electricity transmission loss is about 8% in the U.S. We included this loss in our calculation.

3.5 Hydrogen Production via Electrolysis at Refueling Stations

3.5.1 Pathway Definitions

Hydrogen can be produced from electricity via electrolysis of water in refueling stations. Since the electric transmission and distribution system is already extensive, electricity can readily be transmitted to refueling stations. Thus, this pathway helps avoid long-distance transportation and storage of H_2. In particular, if H_2 will eventually become a fuel-cell fuel, this pathway could help overcome inadequate H_2 distribution infrastructure in the early stage of FCV introduction and in areas outside of major metropolitan areas. Urban H_2 distribution infrastructure will be probably established first and will be more extensive than non-urban areas.

To generate H_2 with clean electricity, some have proposed production of H_2 from hydroelectric power and nuclear power. In Canada, CO_2-free H_2 is currently produced from hydroelectricity (though the quantity is limited). In this analysis, we evaluated H_2 production with electricity that is generated from hydroelectric power, nuclear power, the U.S. generation mix, the California generation mix, the Northeast U.S. generation mix, and electricity generation with NG-fired combined-cycle turbines. The last case represents the most efficient electricity generation with fossil fuels.

Figure 13 shows the pathways of producing H_2 from electricity via electrolysis of water. Although H_2 can be produced via electrolysis in central plants, the central plant production pathway requires long-distance transportation of gaseous or liquid H_2, which can be very expensive. To avoid this, we did not include central plant H_2 production from electricity.

In refueling stations, H_2 production via electrolysis requires a large amount of electricity. Electric distribution lines and local electric transmitters may need to be upgraded to deliver the large amount of electricity. The cost of upgrading electric distribution and transmission system is beyond the scope of this project. We included production of both $G.H_2$ and $L.H_2$ via electrolysis.

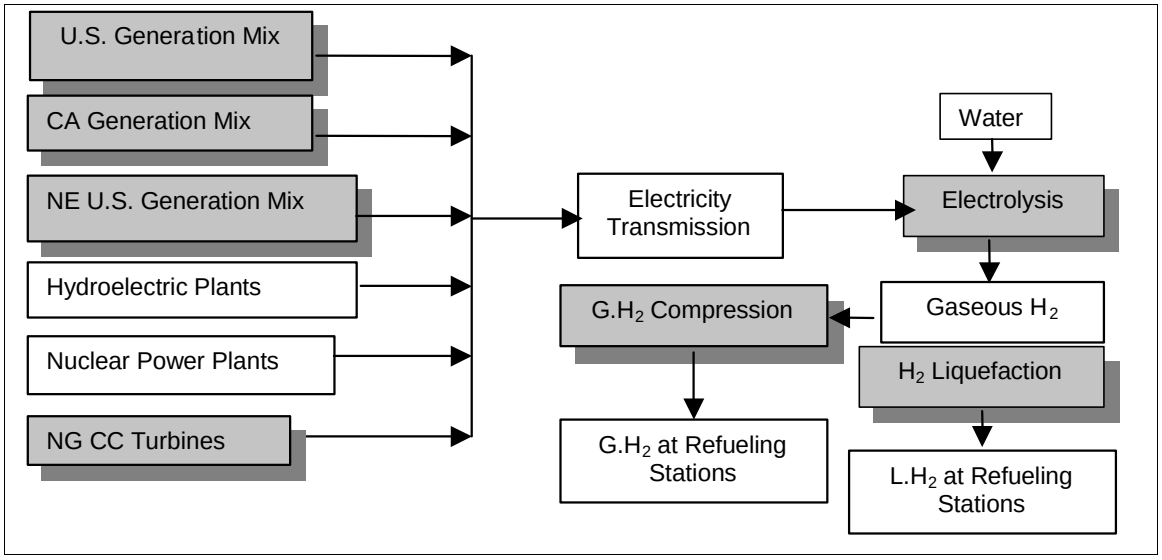

Figure 13 Pathways of Hydrogen Production via Electrolysis

We assumed that $G.H_2$ would be stored onboard vehicles at a pressure of about 5,000 psi. To achieve this onboard pressure, $G.H_2$ probably needs to be compressed to 6,000 psi at refueling stations. We assumed this pressure in order to estimate efficiencies for H_2 compression (with an initial pressure of 500 psi). Liquefaction of H_2 consumes a large amount of energy. We assumed the required energy would be electricity. $L.H_2$ will be cryogenically stored onboard vehicles.

In GREET, five types of electric power plants are included for energy and emissions estimations – oil-fired, NG-fired, coal-fired, nuclear power plants, and other power plants. Other power plants include such plants as hydroelectric power plants and windmill plants. They have virtually zero emissions. As Figure 13 shows, to estimate emsisions associated with electricity generation, GREET includes fuel production activities as well as electricity generation. In this analysis, we evaluated six pathways for electricity generation: the U.S. electric generation mix, the California electric generation mix, the Northeast U.S. electric generation mix, nuclear power plants, hydroelectric power plants, and NG-fired CC gas turbines. The first three pathways show the importance of the electric generation mix in determining energy and emissions effects of electricity-to-hydrogen pathways. The next two pathways show the effects of potentially clean sources for electricity generation (radiation effects of nuclear power plants and ecological effects of hydroelectric power plants are not considered in this analysis). The last pathway shows the effect of the most efficient fossil fuel power plants. As for nuclear power to H_2 production, DOE is funding some research efforts at Argonne National Laboratory for potential H_2 production from nuclear power.

3.5.2 Efficiencies of Electrolysis

For the pathways of producing $G.H_2$ and $L.H_2$ from electricity, energy efficiencies for electricity generation for coal-fired, NG-fired, oil-fired, and nucler power plants were presented in a section above. Energy efficiencies for $G.H_2$ compression and liquefaction were presented in a separate section above. We used those data for the electrolysis pathways here.

The additional step for electrolysis pathways is H_2 production via electrolysis. There are large efficiency losses during this stage. Table 11 summarizes electrolysis efficiencies of H_2 production presented in different studies. The table shows a wide range of 60% to 80% for electrolysis efficiencies. When the two outliers are taken out (60% and 80%), the energy efficiency range appears to be within the range of 67% to 76%.

Table 11 Electrolysis Energy Efficiencies for Hydrogen Production

Source	Energy Efficiency: Based on Lower Heating Value of H_2 (%)	Remarks
Thomas et al. (1997)	66.7–68.0	Home electrolyzers
	68.0–73.0	Station electrolyzers
Amstutz and Guzzella (1998)	76.0	
Berry et al. (1996)	68.0	
Ogden (1999)	70.0	Current technology
	80.0	Year 2020 technology
Adamson and Pearson (2000)	60.0	
Pembina Institute (2000)	68.0	
Unnasch and Browning (2000)	68.0	Near-term technology
	72.0	Long-term technology

4 Development of Probability Distribution Functions for Key Parameters

In this project, we began to formally address uncertainties in fuel-cycle analysis with the GREET model. Using the Crystal Ball software, we conducted Monte Carlo simulations for the pathways included in this study. To do so, we needed to develop probability distribution functions for key parameters, which can be developed with two approaches. One approach is to generate enough data from tests, surveys, or other methods so that objective distribution functions can be developed from the collected data. The other approach is to develop subjective distribution functions based on one's understanding of uncertainty levels and parametric ranges for given parameters.

In our analysis, we used our professional judgments to establish subjective distribution functions. We first developed ranking of the uncertainty level involved in a given input parameter. Then, based on the range of values for the parameter from published results and the developed uncertainty level, we determined the values for the input parameter at probability of 20% and 80%. Furthermore, we assumed that the input parameter (except as noted) follows the normal distribution curve in order to establish the probability distribution function for the parameter.

4.1 Assignment of Uncertainty Levels

Energy efficiencies of key upstream stages in a fuel-cycle pathway are determined by many factors. Because of this, efficiencies are subject to uncertainties. Key upstream stages mainly include fuel production, compression, and liquefaction. We developed a rating system to assign uncertainty levels to key parameters. With our rating system, we assigned more dots to the parameters with greater uncertainties. In determining the number of dots for input parameters, we considered the following factors that affect energy efficiencies of fuel production facilities: (1) status of technology development; (2) variability in existing operations/resources; (3) by-product uncertainties (steam, electricity, etc.); (4) uncertainty in business decision of promoting certain technologies, and (5) the regulatory uncertainty in developing and operating certain facilities. Needless to say, our uncertainty rating is qualitative and crude, and involves significant professional judgments.

4.1.1 Petroleum-Based Fuel Pathways

Because crude quality, crude production locations, petroleum refinery configurations, and many other factors are different for different cases of producing gasoline, diesel fuels, and naphtha, estimated energy efficiencies for upstream activities of petroleum-based fuels are subject to great uncertainties. Two key stages for petroleum pathways are petroleum recovery and petroleum refining. Table 12 presents our ranking of uncertainty levels in energy efficiencies for upstream activities of petroleum-based fuels. Energy efficiencies of crude recovery may be subject to moderate degree of uncertainties since crude quality and production locations for U.S. refinery crude can vary (Table 5). For petroleum refining, production of currently available fuels is subject to moderate uncertainties, but production of new gasoline and diesel fuel may be subject to great uncertainties. Our assignment of the degree of uncertainties in Table 12 reflects these situations.

Table 12 Uncertainty Levels for Energy Efficiencies of Petroleum Pathway Activities[a]

Pathway	Petroleum Recovery	Fuel Production
340 ppm sulfur CG	• •	• •
150 ppm sulfur RFG with MTBE	• •	• •
5–30 ppm sulfur RFG with MTBE	• •	• • •
5–30 ppm sulfur RFG with EtOH	• •	• • •
5–30 ppm sulfur RFG with no oxygenate	• •	• • •
120–350 ppm sulfur diesel	• •	• •
5–30 ppm sulfur diesel	• •	• • •
5–30 ppm sulfur naphtha	• •	• • •

[a] • – least uncertain; • • • • – most uncertain.

4.1.2 Natural-Gas-Based Fuels

Key well-to-tank stages for natural-gas-based pathways are highlighted in Figures 4 through 10. Energy efficiencies of these key stages are subject to great uncertainties. Table 13 presents our ranking of uncertainty levels in energy efficiencies for NG pathway upstream activities. Energy efficiencies of NG recovery may be subject to moderate degrees of uncertainties because production location can impact efficiencies. Liquefaction of NG may be subject to a moderate degree of uncertainty. Production of liquid fuels from NG and FG are subject to the greatest degree of uncertainty. Compression of NG and $G.H_2$ may be subject to a large degree of uncertainty. Our assignment of the degrees of uncertainty listed in Table 13 reflects these situations**.**

Table 13 Uncertainty Levels for Energy Efficiencies of Natural Gas Pathway Activities[a]

Pathway	NG Recovery	NG Processing	NG Liquefaction	Fuel Production	Fuel Liquefaction	Gaseous Fuel Compression
CNG	•	•	NA	NA	NA	• • •
$G.H_2$ in central plants	•	•	NA	• • • • •	NA	• • • •
$G.H_2$ in stations	•	•	NA	• • • • • •	NA	• • • •
$L.H_2$ in stations	•	•	NA	• • • • • •	• • • •	NA
Methanol	•	•	NA	• • • •	NA	NA
FTD	•	•	NA	• • • • •	NA	NA
Naphtha w/no sulfur	•	•	NA	• • • • •	NA	NA
CNG	•	•	• • •	NA	NA	• • •
$G.H_2$ in central plants	•	•	• • •	• • • • •	NA	• • • •
$G.H_2$ in stations	•	•	• • •	• • • • • •	NA	• • • •
$L.H_2$ in central plants	•	•	NA	• • • • •	• • • • •	NA
$L.H_2$ in stations	•	•	• • •	• • • • • •	• • • •	NA
Methanol	•	•	NA	• • • •	NA	NA
FTD	•	•	NA	• • • • •	NA	NA
Naphtha w/no sulfur	•	•	NA	• • • • •	NA	NA

[a] • – least uncertain; • • • • • • – most uncertain; NA – not applicable.

4.1.3 Bio-Ethanol Pathways

Table 14 presents our ranking of uncertainty levels in key upstream parameters for bio-ethanol pathways. Energy and fertilizer use for farming of corn and biomass may be subject to moderate degree of uncertainties since farming regions, climate, soil conditions, and many other factors can affect application rates for each unit of corn or biomass harvested. N_2O emissions from soil in cornfields may be subject to a greater degree of uncertainty than those in biomass farms because cornfield soil is more disturbed than biomass farm soil. Fossil energy use in cellulosic ethanol plants may be subject to less uncertainty than that in corn ethanol plants, since the former uses much less fossil fuels than the latter (steam is generated by burning of biomass lignin, whose uncertainty level is determined by ethanol yield per dry ton of cellulosic biomass). Ethanol yield per unit of corn or biomass can vary, depending on plant designs and technologies employed. Co-product credits can vary, depending on technologies employed in ethanol plants and market conditions for co-products (animal feeds for corn ethanol plants and electricity for cellulosic ethanol plants).

Table 14 Uncertainty Levels for Parameters of Ethanol Pathway Activities

Pathway	Energy Use of Feedstock Farming	Fertilizer Use of Feedstock Farming	N_2O Emissions from Farms	Soil CO_2 Seques-tration	Energy Use in Ethanol Plants	Ethanol Yield	Co-Product Credits
Corn to EtOH: dry mill	• • • •	• • • •	• • •	•	• • •	• •	NA[b]
Corn to EtOH: wet mill	• • • •	• • • •	• • •	•	• • •	• •	NA[b]
W. cellulosic EtOH	• •	• •	• •	• • • •	NA[a]	• • •	• • • •
H. Cellulosic EtOH	• •	• •	• •	• • • •	NA[a]	• • •	• • • •

[a] • – least uncertain; • • • • • • – most uncertain; NA – not applicable.

[b] The amount of fossil fuels used in cellulosic plants is very small. Virtually all the energy needed in these plants is provided by burning of lignin. The uncertainty of the amount lignin burned is addressed by ethanol yield per dry ton of cellulosic biomass.

[c] Though uncertainties are associated with the amount of co-products produced per gallon of ethanol and the displacement ratios between ethanol co-products and the displaced products, the most significant factor determining co-product energy and emission credits is whether the displacement method or the market value-based method is considered for estimating co-product credits (see Wang [1999a] for details of the two methods). We conducted analyses with the two methods rather than conducting probability-based analysis for the displacement method.

4.1.4 Electricity Generation

Of all the upstream stages involved in electricity generation, production of petroleum and natural gas is already covered in previous sections. Upstream stages for coal and uranium production and processing are usually efficient. We did not establish probability distribution functions for these stages. Electricity generation suffers the largest efficiency losses for the complete electricity cycle. In this section, we address uncertainties in electricity generation in fossil fuel power plants.

Table 15 presents our ranking of uncertainty levels in power plant conversion efficiencies. Energy conversion efficiencies of oil-fired plants may be subject to a moderate degree of uncertainties. On the other hand, efficiencies of NG- and coal-fired power plants may be subject to a large degree of uncertainties, since advanced technologies such as combined-cycle turbines, which may be employed in these two types of power plants, can increase efficiencies significantly, and deployment of these technologies is affected by many factors.

Table 15 Uncertainty Levels for Electricity Generation Efficiencies[a]

Power Plants	Conversion Efficiency
Oil-fired plants	• •
NG-fired plants	• • • •
Coal-fired plants	• • • •

[a] • – least uncertain; • • • • – most uncertain.

4.2 Electricity to Hydrogen via Electrolysis

As discussed in an above section, the pathway of electricity to H_2 via electrolysis includes production of primary energy (petroleum, natural gas, coal, etc.), electricity generation, electricity transmission, H_2 production, H_2 compression (in the case of G.H_2), and H_2 liquefaction (in the case of L.H_2). All these stages, except H_2 production via electrolysis, have been covered in other sections of this report. This section covers electrolysis efficiencies only.

As a previous section showed, our survey of studies on electrolysis efficiencies shows a wide range of electrolysis efficiencies. Because current electrolysis systems are less mature and small in scale, there is a large potential for improved efficiencies. We assigned six dots, the highest level of uncertainties, to electrolysis efficiencies.

4.3 Determination of Probability Distribution Functions

We determined probability distribution functions with the following steps. We presented the ranges of efficiencies for key stages that we obtained from open literature and communications with experts. In the above section, we assigned uncertainty levels to these stages with number of dots (the more dots, the more uncertain). For a given stage, we determined the range of efficiency for probability of 20% and 80% (P20 and P80) by considering the range we obtained and the number of dots we assigned for the uncertainty level of the stage. If a stage has more dots assigned, we increased our original range for the stage. If a stage has less dots assigned, we reduced our original range. For most stages, we assumed the normal distribution curve for probability distribution of efficiencies.

4.3.1 Petroleum-Based Fuel Pathways

We developed efficiencies for upstream activities of petroleum-based fuel pathways under probabilities of 20%, 50%, and 80% (P20, P50, and P80, respectively). Since we assumed the normal distribution curve for most parameters, the value for P50 is usually the average of the values for P20 and P80. Table 16 presents our estimated values.

Table 16 Energy Efficiencies for Petroleum Pathway Activities

Activity	Energy Efficiency (%)		
	P20	P50	P80
Petroleum recovery[a]	96.0	98.0	99.0
Petroleum refining: 340 ppm S CG	85.0	85.5	86.0
Petroleum refining: 150 ppm S RFG with MTBE: GBS[b]	85.0	86.0	87.0
Petroleum refining: 5–30 ppm S RFG with MTBE: GBS[b]	84.0	85.5	87.0
Petroleum refining: 5–30 ppm S RFG with EtOH: GBS[b]	84.0	85.5	87.0
Petroleum refining: 5–30 ppm S RFG with no oxygenate	83.0	84.5	86.0
Petroleum refining: 120–350 ppm S diesel	88.0	89.0	90.0
Petroleum refining: 5–30 ppm S diesel	85.0	87.0	89.0
Petroleum refining: 5 ppm naphtha	89.0	91.0	93.0

[a] A triangle distribution curve was assumed for petroleum recovery.
[b] GBS – gasoline blendstock.

Figure A1 of Appendix A shows the probability distribution functions for crude recovery and refining, as developed with the Crystal Ball software with the assumptions made in Table 16. As the figures show, we assumed the normal distribution curve for all the parameters except petroleum recovery efficiency.

4.3.2 Natural-Gas-Based Fuels

With the assigned uncertainty levels in Table 13 and energy efficiency ranges that we obtained from open literature and communication with experts, we established values under P20, P50, and P80 for efficiencies of natural-gas-based pathway activities. Table 17 presents the estimated values. (Note that compression of NG or G.H_2 has smaller efficiency ranges for each compressor type presented than the ranges implied in a previous section. This is because, in the previous section, we discussed compression efficiencies for both NG and electric compressors together. If one combines the compression efficiencies of both types listed in Table 17, the range of compression efficiencies is much larger than the range for each type.)

In FT plants, if naphtha is produced as a fuel-cell fuel, together with FT diesel as a diesel engine fuel, it is likely that both FT naphtha and diesel will be subject to similar intensive production and refining processes. This implies that production of one unit of energy in FT naphtha and FT diesel could require about the same amount of energy. Thus, we assumed same energy efficiencies between FT naphtha and FT diesel. In other words, we allocated energy use and emissions in FT plants between naphtha and diesel based on their energy output shares. On the energy basis, FT plants may produce 60–70% of its output products as diesel, 20–30% as naphtha, and remainings as other products such as waxes.

Figure A2 of Appendix A graphically shows probability distribution functions for the parameters presented in Table 17. These distribution charts are developed with the Crystal Ball software. We assumed triangle distribution functions for NG liquefaction, electric compressors for NG compression, and steam credits from methanol plants, H_2 liquefaction in central plants, NG compressors for G.H_2 compression, and electric compressors for G.H_2 compressors. These triangle distribution functions were assumed to ensure that Crystal Ball simulations did not yield unrealistic efficiency ranges (i.e., values exceeding 100%).

Table 17 Energy Efficiencies for Natural-Gas-Based Pathway Activities

Activity	P20	P50	P80
NG recovery: NA NG, NNA NG, NNA FG	96.0%	97.5%	99.0%
NG processing: NA NG, NNA NG, NNA FG	96.0%	97.5%	99.0%
LNG production from NG and FG[a]	87.0%	91.0%	93.0%
NG compression: NG compressor	92.0%	93.0%	94.0%
NG compression: electric compressor[a]	96.0%	97.0%	98.0%
MeOH production: with no steam production[a]	65.0%	67.5%	71.0%
MeOH production: with steam production[a]	62.0%	64.0%	66.0%
MeOH production, with steam production, steam credit (Btu/mmBtu)[a]	64,520	78,130	90,910
FT diesel and naphtha production: with no steam production	61.0%	63.0%	65.0%
FT diesel and naphtha production: with steam production	53.0%	55.0%	57.0%
FT diesel and naphtha production: with stream production, steam credit (Btu/mmBtu)	189,000	200,000	210,500
G.H_2 production in central plant: with no steam production	68.0%	71.5%	75.0%
G.H_2 production in central plant, with steam production	66.0%	69.5%	73.0%
G.H_2 production in central plant, with steam production, steam credit (Btu/mmBtu)	120,000	145,000	170,000
H_2 liquefaction in central plants[a]	65.0%	71.0%	77.0%
G.H_2 production in stations	62.0%	67.0%	72.0%
G.H_2 compression for central G.H_2: NG compressor[a]	82.5%	85.0%	87.5%
G.H_2 compression for central G.H_2: electric compressor[a]	90.0%	92.5%	95.0%
G.H_2 compression for station G.H_2: NG compressor[a]	83.5%	86.0%	88.5%
G.H_2 compression for station G.H_2: electric compressor[a]	91.5%	94.0%	96.5%
H_2 liquefaction in stations	60.0%	66.0%	72.0%

[a] Triangle distribution functions were assumed for these parameters.

4.3.3 Bio-Ethanol Pathways

With the assigned uncertainty levels in Table 14 and parametric value ranges that we obtained from published literature, we developed values for P20, P50, and P80 for key bio-ethanol upstream parameters. Table 18 presents the estimated values.

Figure A3 of Appendix A graphically shows probability distribution functions for the bio-ethanol activities that we developed with the Crystal Ball software. To ensure that Crystal Ball simulations do not go beyond reasonable efficiency ranges, we assumed triangle distribution functions for the following parameters: corn farming energy use, N_2O emissions in corn farms, soil CO_2 emissions from corn farms, ethanol yield of dry milling ethanol plants, ethanol yield of wet milling ethanol plants, N_2O emissions in biomass farms, soil CO_2 sequestration in biomass farms, and electricity credits of cellulosic ethanol plants.

4.4 Electricity Generation

With the assigned uncertainty levels in Table 15 and the range of parametric values that we obtained from published literature, we developed values for P20, P50, and P80 for power plant conversion efficiencies (Table 19).

Table 18 Energy Efficiencies and Other Values for Bio-Ethanol Pathway Activities

Activity	P20	P50	P80
Corn-to-Ethanol Pathways			
Corn farming energy use (Btu/bushel of corn)[a]	12,600	26,150	39,700
N fertilizer use in corn farms (g/bushel of corn)	370	475	580
N_2O emissions in corn farms (N in N_2O as % of N in N fertilizer)[a]	1.0	1.5	2.0
Soil CO_2 emissions in corn farms (g/bushel of corn)[a]	0	195	390
Ethanol yield, dry mill plants (gal/bushel of corn)[a]	2.5	2.65	2.8
Ethanol yield, wet mill plants (gal/bushel of corn)[a]	2.4	2.55	2.7
Energy use in dry mill plants (Btu/gal of ethanol)	36,900	39,150	41,400
Energy use in wet mill plants (Btu/gal of ethanol)	34,000	37,150	40,300
Cellulosic Biomass-to-Ethanol Pathways			
Energy use for tree farming (Btu/ton of trees)	176,080	234,770	293,460
Energy use for grass farming (Btu/ton of grasses)	162,920	190,080	271,540
N fertilizer use for tree farming (g/ton of trees)	532	709	886
N fertilizer use for grass farming (g/ton of grasses)	7,980	10,630	13,290
N_2O emissions in biomass farms (N in N_2O as % of N in N fertilizer)[a]	0.8	1.15	1.5
Soil CO_2 sequestration in tree farms (g/ton of trees)[a]	-225,000	-112,500	0
Soil CO_2 sequestration in grass farms (g/ton of grasses)[a]	-97,000	-48,500	0
Ethanol yield, woody biomass plants (gal/ton of trees)	76	87	98
Ethanol yield, herbaceous biomass plants (gal/ton of grasses)	80	92	103
Electricity credit of woody biomass plants (kWh/gal of ethanol)[a]	-1.73	-1.15	-0.56
Electricity credit of herbaceous biomass plants (kWh/gal of ethanol)[a]	-0.865	-0.57	-0.28

[a] Triangle distribution functions are assumed for these parameters.

Table 19 Energy Conversion Efficiencies for Electric Power Plants

	Efficiency (%)		
Power Plant Type	P20	P50	P80
Oil-fired power plants: steam boiler	32.0	35.0	38.0
NG-fired power plants: steam boiler	32.0	35.0	38.0
NG-fired power plants: combined-cycle turbines[a]	50.0	55.0	60.0
Coal-fired power plants: steam boiler	33.0	35.5	38.0
Coal-fired power plants: advanced technologies	38.0	41.5	45.0

[a] A triangle distribution function is assumed for NG-fired CC gas turbines.

Figure A4 of Appendix A graphically shows probability distribution functions for electric power plant conversion efficiencies. We assumed normal distribution functions for conversion efficiencies except for that of NG-fired CC gas turbines, for which as assumed a triangle distribution function.

Table 20 presents the U.S., California, and Northeast U.S. electricity generation mix. About 54% of U.S. electricity is generated from coal. In California and Northeast U.S., over 30% of electricity is generated from natural gas. In addition, about 33% of California's electricity is generated from hydro, geothermal, organic waste, wind and other energy sources.

Table 20 The U.S., California, and Northeast U.S. Electricity Generation Mix

Generation Mix	Coal	Oil	Natural Gas	Nuclear	Others[a]
U.S. Mix[b]	53.8%	1.0%	14.9%	18.0%	12.3%
CA Mix[c]	21.3%	0.0%	32.9%	14.7%	31.3%
NE U.S. Mix[b]	28.2%	2.5%	31.6%	26.3%	11.4%

[a] Including hydro, geothermal, organic waste, solar, wind, and other electric power plants.
[b] From Wang (1999a).
[c] From Kelly (2000).

Table 20 presents the average generation mixes for the U.S., California, and Northeast, which we used to simulate electricity generation under the three generation mixes. To precisely simulate energy and emission effects of electricity use by EVs and HEVs, marginal electric generation mix — the mix for providing electricity for these vehicles — should be estimated and used for analyses. Some have maintained marginal electricity will be probability generated with NG-fired CC gas turbines. In our analysis, we included this technology to approximate the U.S. marginal electricity supply.

Some analyses conducted in California took a different approach in estimating energy and emissions effects of EVs and HEVs. These analyses excluded emissions of power plants located outside of California on the ground that emissions from those plants occur outside of the state. For power plants located within an air basin (such as the South Coast Air Basin), the analyses sometimes assumed zero emissions from the in-basin plants for EV electricity demand on belief that the emissions from increased electric generation from in-basin electric plants to meet EV and HEV electricity demand must be offset by other sources because the emission cap regulation, as adopted in some air basins, must be met. These steps are extremely in favor of EVs and HEVs, which we did not take in our analysis. Although this discussion is more relevant to emissions of criteria pollutants, which we did not include in this analysis, use of one approach over the other affects calculations of energy use and GHG emissions significantly.

4.5 Electricity to Hydrogen via Electrolysis

We developed values for P20, P50, and P80 for hydrogen electrolysis efficiencies (Table 21). Figure A5 of Appendix A graphically shows the probability distribution function for electrolysis efficiencies.

As we stated in an above section, we simulated electricity-to-hydrogen pathways with three electricity generation mixes — the U.S., the California, and the Northeast U.S. mixes — as well as electricity generation in nuclear power plants, hydroelectric power plants, and NG-fired combined-cycle turbine plants. The six options cover wide ranges of potential energy and emission impacts of hydrogen production via electrolysis.

Table 21 Hydrogen Electrolysis Efficiencies

	Efficiency (%)		
Activity	P20	P50	P80
Electrolysis	67.0	71.5	76.0

5 Transportation of Feedstocks and Fuels

Through a separate Argonne project, we have expanded the simulations of transportation of energy feedstocks and fuels. In previous GREET versions, transportation of feedstocks and fuels was simulated with aggregate energy efficiencies for transportation of various feedstocks and fuels. In the new GREET version, for a given feedstock or fuel, its transportation is simulated with transportation mode split, transportation distance for each mode, and energy intensity of each mode. Development of transportation simulations is documented in He and Wang (2000). Eventually, we could establish probability distribution functions for transportation distance and energy intensity of each transportation mode. Because of time and funding constraints, we did not establish such distribution functions this time.

5.1 Methodology

We employed the following approach to estimate energy use and emissions for transportation of feedstocks and fuels. First, we determined the types and shares of transportation modes (i.e., ocean tankers, pipelines, barges, rail, and trucks) to be used for transporting a given feedstock or fuel. Second, we identified the types and shares of process fuels (residual oil, diesel fuels, natural gas, electricity, etc.) to be used for powering a given transportation mode. Third, we calculated the energy intensity and emissions associated with a given transportation mode fueled with a given process fuel. Finally, we added together the energy use and emissions of all transportation to be used for transporting the given feedstock or fuel. Figure 14 shows the way in which the new GREET version simulates transportation of feedstocks and fuels.

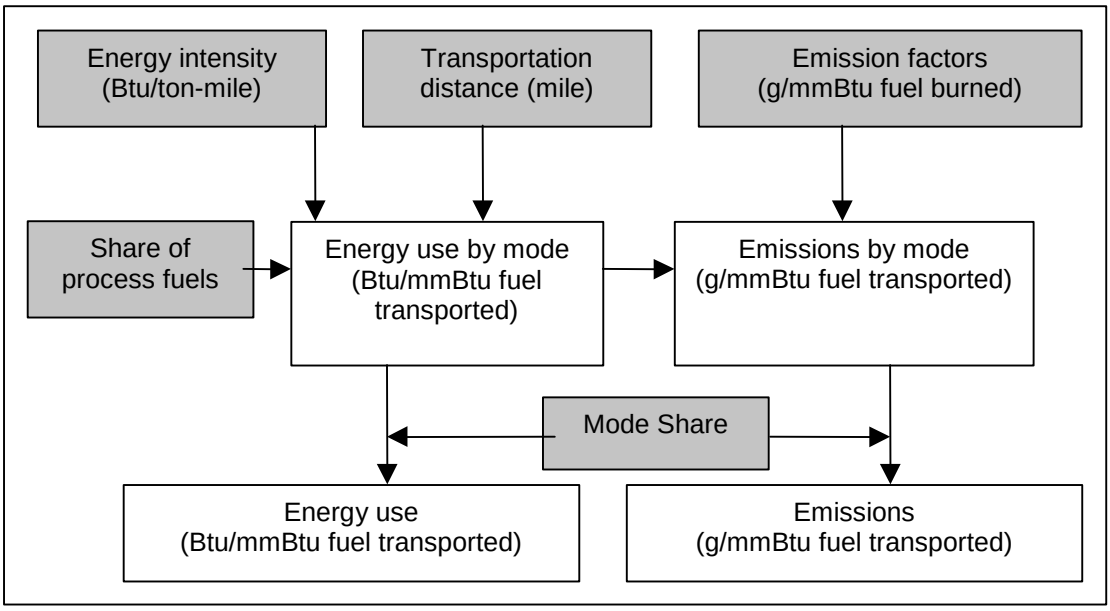

Figure 14 Calculation Logic of Energy Use and Emissions Associated with Feedstock and Fuel Transportation

5.2 Assumptions

5.2.1 Crude Oil

Figure 15 shows our specifications of transportation of crude from wells to U.S. refineries. In 1998, 58% of crude oil consumed in the United States was imported (EIA 1999). We assumed that ocean tankers are used to ship imported crude oil from Alaska and countries outside of North America, and pipelines are used for shipping crude from Canada and Mexico. Four transportation modes may be used for in-land transportation: pipelines, barge, and rail. The U.S. Department of Transportation (U.S. DOT 1996) estimated that, in 1993, 52.6% of crude oil was shipped by pipeline, 47.3% by water carriers, and 0.1% by rail. These mode splits were incorporated into the new GREET version to represent U.S. average mode splits. A GREET user can specify a different set of mode splits according to the specific case in simulation.

We calculated the average distance associated with ocean tanker transportation according to port-to-port distances (from www.distance.com) and the amount of imported oil transported from different countries to the United States. Crude oil from Southeast Asia (across the Pacific Ocean) was assumed to reach Los Angeles; crude from Europe, the Middle East, and Africa was assumed to reach Houston and New York across the Atlantic Ocean. For in-land transportation, the travel distance for each mode was obtained from the Commodity Flow Survey (U.S. DOT and U.S. Department of Commerce [DOC], 1997). Round trips were considered for ocean tankers, barges, and tanker trucks because no other goods could be hauled for the back haul.

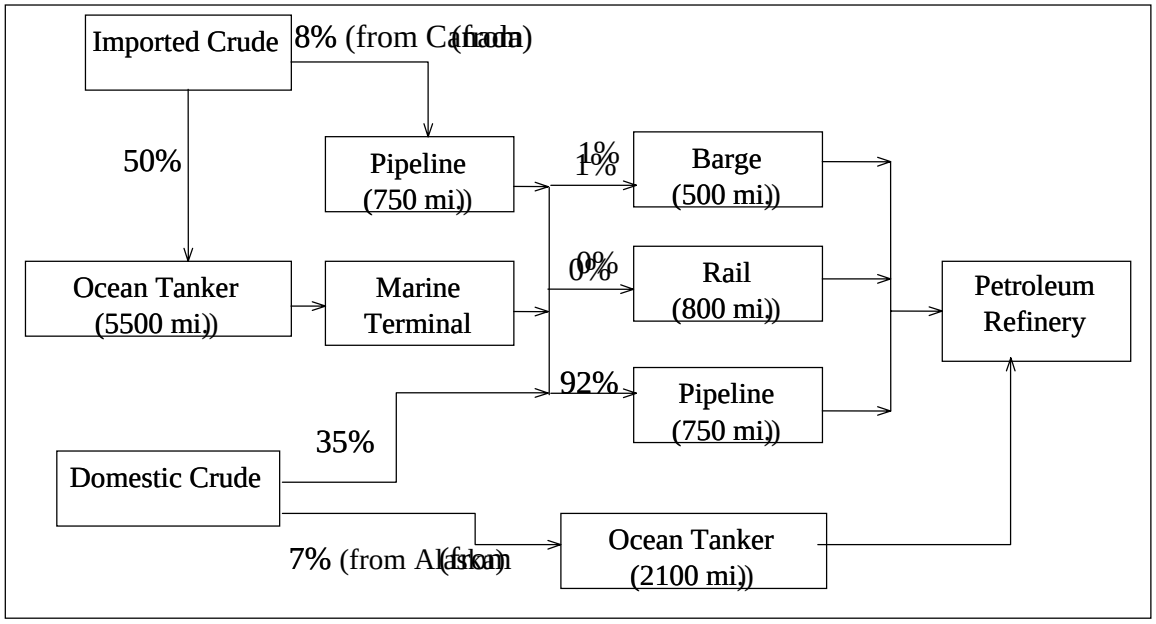

Figure 15 Crude Transportation from Oil Fields to U.S. Petroleum Refineries

5.2.2 Gasoline and Diesel

Although both domestic and imported gasoline and diesel supply the U.S. market, imported gasoline and diesel are small, relative to domestic production. EIA (1999) estimated that in 1998, less than 5% of U.S. motor gasoline and diesel fuels was imported. Except for Canadian gasoline and diesel, we assumed imported gasoline and diesel to be shipped by ocean tankers. For in-land transportation, we assumed that 59% of gasoline and diesel is moved from refineries/marine terminals to bulk terminals by pipeline, 32.7% by water carriers, and the rest by railroads (U.S. DOT 1996). We assumed that delivery trucks move gasoline and diesel from bulk terminals to service stations. The average transportation distance of ocean tankers was calculated according to the amount of imported petroleum products and the port-to-port distance from a country of origin to major U.S. ports. The distances for in-land transportation modes were based on the Commodity Flow Survey (U.S. DOT and U.S. DOC 1997). Figures 16 and 17 present our specifications of gasoline and diesel transportation.

5.2.3 Methanol

The United States produces almost one-quarter of the world's methanol. In 1995, methanol production capacity from 17 U.S. plants in 8 states totaled 2,205 million gallons. These plants meet three quarters of the U.S. methanol demand. The remaining demand is met by import, of which Canada supplies over one half. In 1995, 90% of methanol consumed in the United States was produced in North America; 8% in Trinidad, Venezuela, and Chile; and the remaining 2% in and the rest by pipeline. Trucks were assumed for transportation from bulk terminals to refueling stations. Figure 18 shows our specifications for methanol transportation. As the figure shows, we used question marks for the shares of pipeline, rail, and ocean tanker for imported methanol. This is because that we simulated three cases: methanol from NA NG, NNA NG, and NNA FG. Each

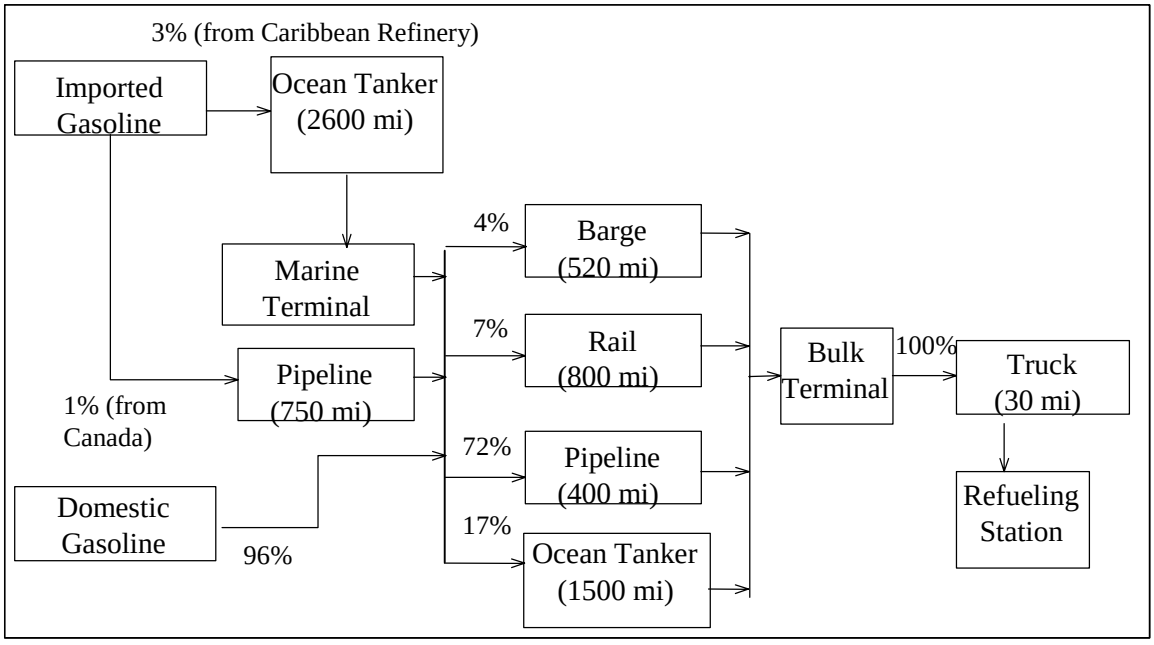

Figure 16 Gasoline Transportation from Petroleum Refineries to Refueling Stations

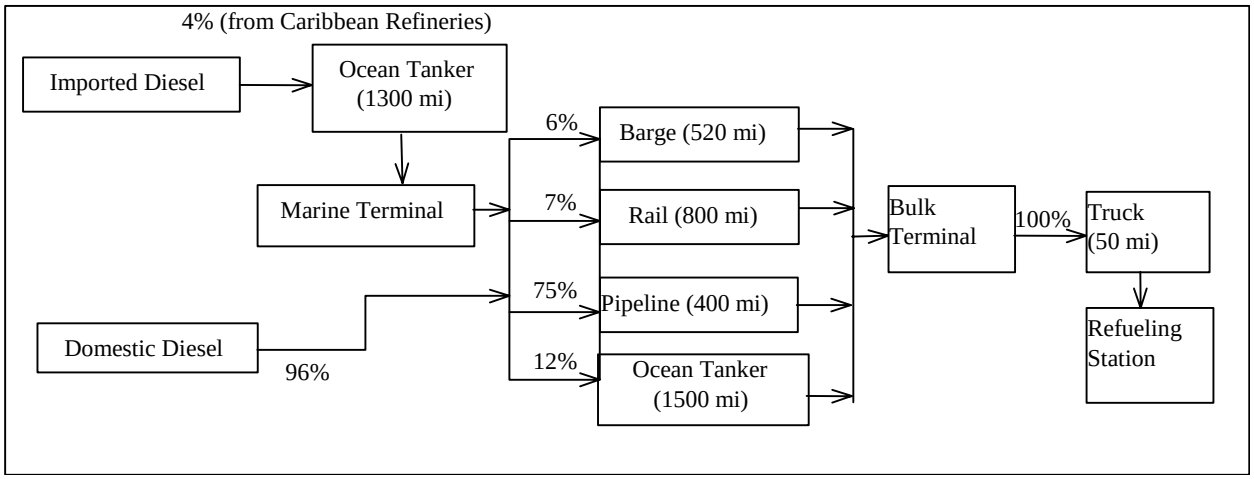

Figure 17 Diesel Fuel Transportation from Petroleum Refineries to Refueling Stations

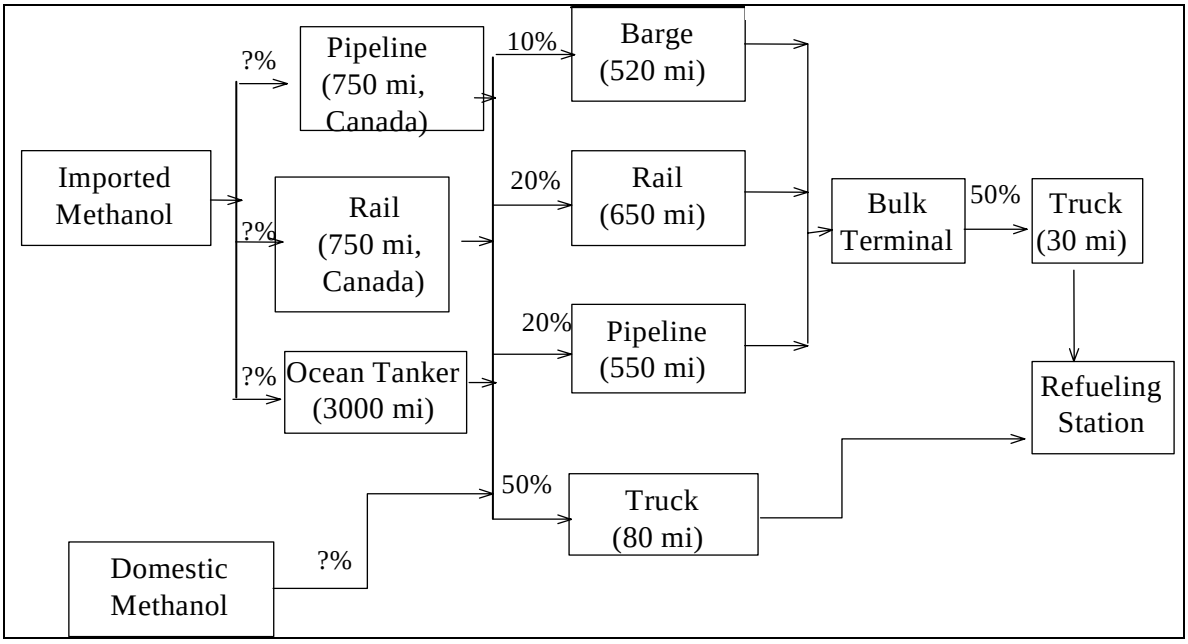

Figure 18 Methanol Transportation from Methanol Plants to Refueling Stations

Europe, Southeast Asia, and the Middle East (American Methanol Institute [AMI] 1996). On the basis of this information, we estimated that the average marine travel distance for methanol is about 2,000 miles. For in-land transportation, we assumed that half of methanol is moved by truck from methanol plants or marine terminals to bulk terminals, 10% by barge, 20% by rail, case has different shares. Furthermore, for ocean tanker transportation distance of methanol from NNA NG and NNA FG, we assumed a distance of 5,900 miles (which were based on our assumptions of 1/3 offshore methanol will come from the Persian Gulf area with a transportation distance of 10,000 miles, 1/3 from North and West Africa with a transportation distance of 5,200 miles, and 1/3 from South America with a transportation distance of 2,300 miles).

5.2.4 Liquefied Natural Gas

In this study, LNG itself is not a motor vehicle fuel for evaluation. Instead, it is an intermediate fuel that we assumed in order to bring NNA NG and FG to the U.S. for production of other motor fuels (CNG, G.H_2, and production of L.H_2 at refueling stations). That is, LNG is produced offshore and transported to U.S. LNG terminals where LNG is gasified and transported via pipelines to fuel production sites.

1998, the amount of LNG imported by the United States reached 85 billion cubic feet (relative to more than 20 trillion cubic feet of natural gas consumption in the U.S.). Algeria supplied 80%, and Australia and the United Arab Emirates supplied the remaining 20% (EIA 1998). We assumed an average LNG transportation distance of 5,900 miles from offshore production sites to U.S. LNG terminals (see discussion in the methanol section).

5.2.5 Fischer-Tropsch Diesel and Naphtha

FT diesel and naphtha may be transported with existing diesel and gasoline transportation infrastructure. FT diesel and naphtha from offshore production can be transported to the U.S. via ocean tankers. FT diesel and naphtha produced in the U.S. and Canada can be transported to refueling stations via pipelines, rail, barges, and trucks. FT diesel and naphtha produced in Alaska can be transported to the continental U.S. via ocean tankers. Figure 19 shows our specifications of transportation of FT diesel and naphtha. As the figure shows, we used question marks for the shares of pipeline, ocean tanker, and domestic production for FT diesel and naphtha. This is because we simulated three cases: FT diesel and naphtha from NA NG, NNA NG, and NNA FG. Each case has different mode shares. Furthermore, for ocean tanker transportation distance of FT diesel and naphtha from NNA NG and NNA FG, we assumed a distance of 5,900 miles (see discussion in the methanol section).

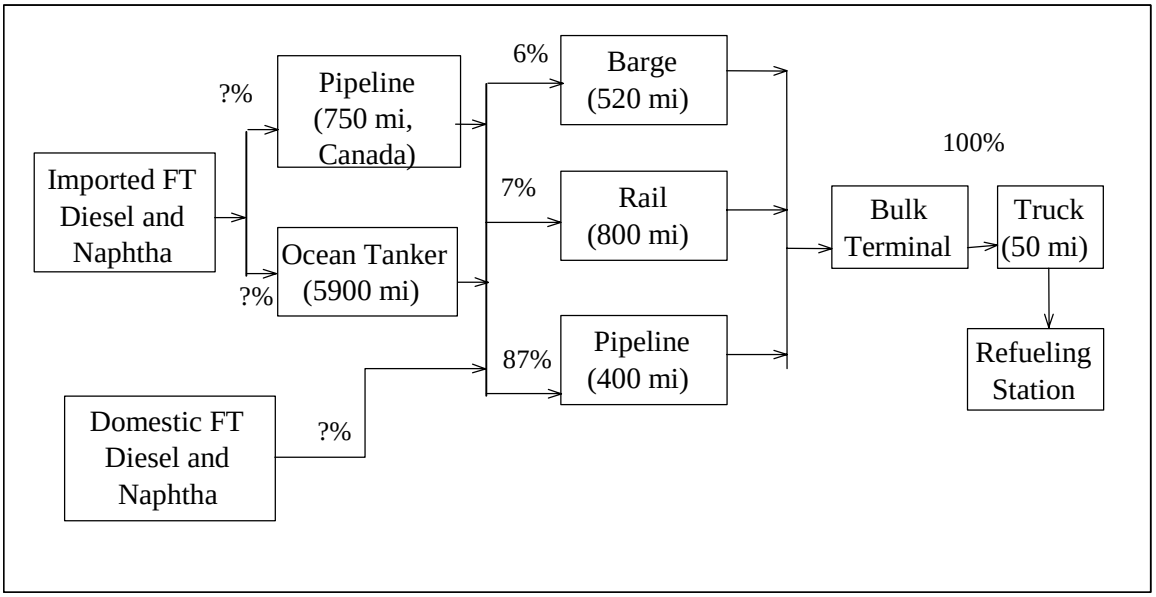

Figure 19 Transportation of Fischer-Tropsch Diesel and Naphtha from Plants to Refueling Stations

5.2.6 Liquid Hydrogen

$L.H_2$ for U.S. use could be produced in North America or in other offshore countries. Because the transportation system for large volumes of LH_2 is not in place yet, we assumed transportation distances and mode shares for $L.H_2$ based on our understanding of LNG transportation. Figure 20 shows our specifications of $L.H_2$ transportation. For NNA $L.H_2$, an ocean tanker transportation distance of 5,900 miles is assumed (see discussion in the methanol section).

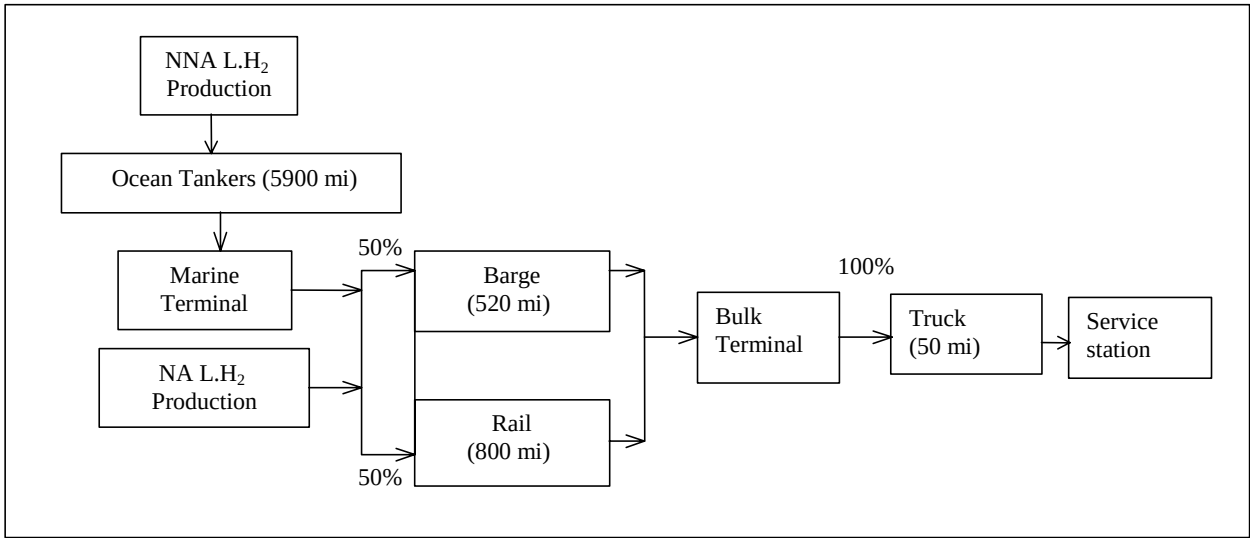

Figure 20 Transportation of Liquid Hydrogen from Central Plants to Refueling Stations

5.2.7 Ethanol

We assumed that fuel ethanol is produced in the United States and moved through the same transportation modes as gasoline. However, no pipeline is currently used for ethanol transportation. We further assumed that ethanol is transported from ethanol plants to bulk terminals by barge (40%), rail (40%), and truck (20%) and that only trucks are used for transportation from bulk terminals to refueling stations. Figure 21 presents our specifications of ethanol transportation.

5.2.8 Natural Gas and Gaseous Hydrogen

For NG and $G.H_2$ produced in central plants, pipelines were assumed to be the only transportation mode. For natural gas, we assumed a pipeline transportation distance of 750 miles, which was based on the U.S. average transportation distance for natural gas. For $G.H_2$ production in central plants, we assumed a pipeline transportation distance of 750 miles from plants to refueling stations. For $G.H_2$ production at refueling stations, we assumed zero transportation distance.

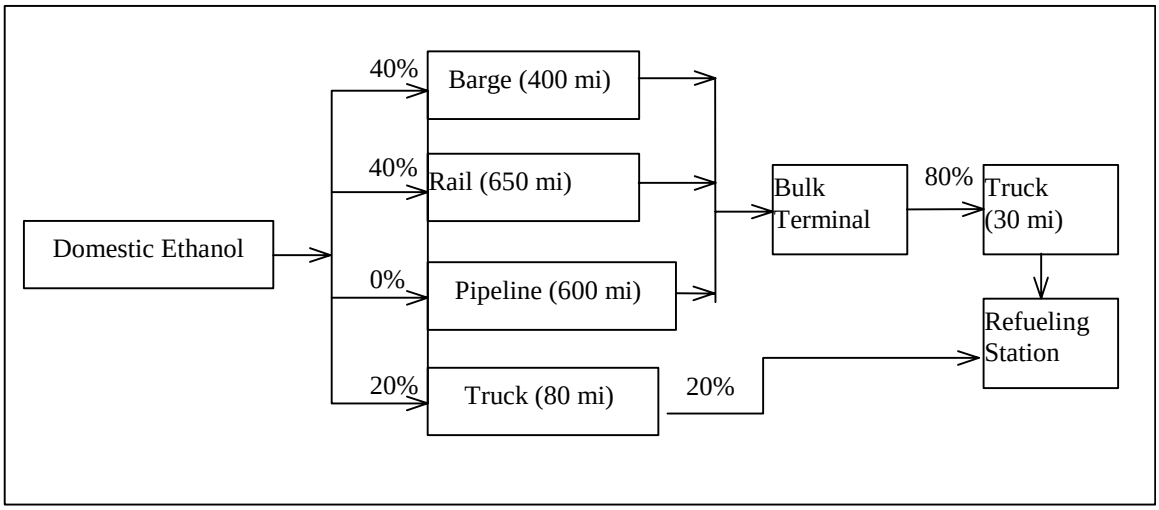

Figure 21 Transportation of Ethanol from Plants to Refueling Stations

5.2.9 Electricity Transmission

When electricity is transmitted from electric power plants to user sites, some electricity is lost. The U.S. average electricity loss during transmission and distribution is about 8%. The GREET model takes this loss into account.

Besides the feedstocks and fuels presented above, the GREET model also simulates some other feedstocks such as coal and uranium for electricity generation, agricultural chemicals (fertilizers, pesticides, and herbicides) for agricultural farming, and corn and biomass for ethanol production. Assumptions regarding transportation of these feedstocks are presented in He and Wang (2000).

5.2.10 Input Energy Efficiencies for Feedstock and Fuel Transportation

Many previous studies, including previous GREET studies, inputted energy efficiencies for transportation of feedstocks and fuels into fuel-cycle energy and emission calculations. With detailed assumptions regarding transportation modes, distance, and energy intensities, this study simulated energy use and emissions of transportation activities in a more transparent way than previous studies did. To put the results from detailed simulations of feedstock and fuel transportation conducted in this study into comparison with other previous studies, we imputed energy efficiencies of feedstock and fuel transportation with the GREET-calculated energy use for feedstock and fuel transportation with the detailed assumptions listed in above sections.

Table 22 presents our imputed energy efficiencies for transportation of various feedstocks and fuels. For most of the feedstocks and fuels, transportation energy efficiencies are above 99%. Transportation of NNA-produced fuels has lower energy efficiencies because of longer distances involved. Transportation of methanol has low energy efficiencies since a large of portion of methanol is assumed to be transported via trucks within the U.S. (see Figure 18). Pipeline transportation of $G.H_2$ has low efficiencies since a large quantity of $G.H_2$ needs to be compressed and moved due to the low volumetric energy content $G.H_2$ at the atmospheric pressure.

Transportation of $L.H_2$ from NNA locations has low efficiencies because of the low volumetric energy content of $L.H_2$ and the boil-off loss of $L.H_2$ during transportation. Ethanol's low transportation efficiency is due to use of trucks to transport a large quantity of it (Figure 21).

Table 22 Energy Efficiencies for Transportation of Feedstocks and Fuels Calculated from GREET Outputs

Feedstock/Fuel	Energy Efficiency (%)
Crude oil from oil fields to U.S. refineries	99.0
Gasoline from U.S. refineries to refueling stations	99.4
CA gasoline from CA refineries to refueling stations	99.7
Diesel from U.S. refineries to refueling stations	99.2
Petroleum naphtha from U.S. refineries to refueling stations	99.0
NG from NA fields to refueling stations	99.3
LNG from NNA plants to U.S. LNG terminals	98.5
Methanol from NA plants to refueling stations	98.0
Methanol from NNA plants to refueling stations	96.8
FT naphtha and diesel from NA plants to refueling stations	99.2
FT naphtha and diesel from NNA plants to refueling stations	98.2
Central $G.H_2$ from NA plants to refueling stations	96.3
$L.H_2$ from NA plants to refueling stations	98.9
$L.H_2$ from NNA plants to refueling stations	95.8
Ethanol from U.S. plants to refueling stations	98.5

6 Results: Well-To-Tank Energy Use and Emissions

With the assumptions presented in above sections and other default assumptions already in GREET, we estimated energy use and emissions of producing and delivering one million Btu of each fuel to vehicle tanks. Table 23 shows all the fuel pathways options analyzed in this study. We analyzed 75 fuel pathways options. For the main text of this report, we graphically present the results for 30 pathway options. Results of all pathway options are presented in Appendix B of this report. The 30 selected fuel pathway options are highlighted in bold in Table 23.

As the table shows, in determining pathway options for methanol, FT diesel, FT naphtha, central plant G.H_2, and central plant L.H_2, we assumed that plants to be built in North America could be designed to co-produce steam or electricity, since these plants can be built next to other chemical plants where co-generated steam can be exported. If these plants are to built outside of North America, we assumed that they may be designed to co-generate electricity. Plants outside of North America may not be built next to other chemical plants. Thus, export of co-generated steam may not be feasible. If NNA FG is the feed for plants, the plants will probably be built in remote areas. Export of either steam or electricity may not be feasible. We did not assume co-generation of steam or electricity for FG-based plants.

For electricity generation, we included the U.S., the California, and the northeast U.S. generation mixes in order to show the importance of electric generation mixes. In addition, we included NG-fired CC turbines, which are very efficient and are considered probably to supply U.S. marginal electricity. Also for H_2 production via electrolysis, we included electricity generation from nuclear power and hydroelectric power in order to show the effect of air-pollution-clean electricity generation on H_2 production.

Four pathway options were analyzed for corn-based options, depending on milling technology (dry or wet) and the way of dealing with ethanol co-products (the displacement method or the market value method). Besides E100 (pure ethanol) for FCV applications, we included E85 (85% ethanol and 15% gasoline) for ICE applications. There is about 5% of gasoline in ethanol serving as denaturant for ICE application. Thus, in our analysis, E85 actually has 80% ethanol and 20% gasoline.

In selecting the 30 pathway options for presentation in this section, we dropped all the FG-based pathways, since the amount of FG available worldwide could be limited (though their efficiency and emission benefits are huge, see Appendix B). Also, we dropped all the NG-based pathways with co-generation of steam or electricity. Plant designs with co-generation of steam or electricity achieve additional efficiency and emission benefits (again, see Appendix B). We combined CG and the 150-ppm S RFG together to represent current gasoline. We combined the three RFGs with 5-30 ppm S together to represent future gasoline. We combined the four corn-ethanol pathways. The results for the combined pathways are presented in Appendix B.

Table 23 Fuel Pathway Options Analyzed in This Study[a]

Feedstock	Fuel
Petroleum	**(1) Conventional gasoline (CG)[b]** (2) 150 ppm S RFG with MTBE (current federal RFG)[b] (3) 5-30 ppm S RFG with MTBE[c] (4) 5-30 ppm S RFG with EtOH[c] **(5) 5-30 ppm S RFG without oxygenate[c]** **(6) Conventional diesel (CD)** **(7) Low-sulfur (LS) diesel** **(8) Crude naphtha**
Natural gas to compressed natural gas (CNG)	**(9) CNG from North American (NA) natural gas (NG)** **(10) CNG from non-North American (NNA) NG** (11) CNG from NNA flared gas (FG)
Natural gas to methanol	**(12) Methanol from NA NG without steam or electricity co-generation** (13) Methanol from NA NG with steam co-generation (14) Methanol from NA NG with electricity co-generation **(15) Methanol from NNA NG without steam or electricity co-generation** (16) Methanol from NNA NG with electricity co-generation (17) Methanol from NNA FG without steam or electricity co-generation
Natural gas to Fischer-Tropsch diesel	**(18) FT diesel from NA NG without steam or electricity co-generation** (19) FT diesel from NA NG with steam co-generation (20) FT diesel from NA NG with electricity co-generation **(21) FT diesel from NNA NG without steam or electricity co-generation** (22) FT diesel from NNA NG with electricity co-generation (23) FT diesel from NNA FG without steam or electricity co-generation
Natural gas to Fischer-Tropsch naphtha	**(24) FT naphtha from NA NG without steam or electricity co-generation** (25) FT naphtha from NA NG with steam co-generation (26) FT naphtha from NA NG with electricity co-generation **(27) FT naphtha from NNA NG without steam or electricity co-generation** (28) FT naphtha from NNA NG with electricity co-generation (29) FT naphtha from NNA FG without steam or electricity co-generation
Natural gas to G.H_2 in central plants	**(30) G.H_2 from NA NG without steam or electricity co-generation** (31) G.H_2 from NA NG with steam co-generation (32) G.H_2 from NA NG with electricity co-generation **(33) G.H_2 from NNA NG without steam or electricity co-generation** (34) G.H_2 from NNA NG with electricity co-generation (35) G.H_2 from NNA FG without steam or electricity co-generation
Natural gas to L.H_2 in central plants	**(36) L.H_2 from NA NG without steam or electricity co-generation** (37) L.H_2 from NA NG with steam co-generation (38) L.H_2 from NA NG with electricity co-generation **(39) L.H_2 from NNA NG without steam or electricity co-generation** (40) L.H_2 from NNA NG with electricity co-generation (41) L.H_2 from NNA FG without steam or electricity co-generation

Table 23 Fuel Pathway Options Analyzed in This Study (Cont.)

Feedstock	Fuel
Natural gas to $G.H_2$ in refueling stations	**(42) $G.H_2$ from NA NG without steam or electricity co-generation** **(43) $G.H_2$ from NNA NG without steam or electricity co-generation** (44) $G.H_2$ from NNA FG without steam or electricity co-generation
Natural gas to $L.H_2$ in refueling stations	**(45) $L.H_2$ from NA NG without steam or electricity co-generation** **(46) $L.H_2$ from NNA NG without steam or electricity co-generation** (47) $L.H_2$ from NNA FG without steam or electricity co-generation
(48) U.S. mix (49) CA mix (50) NE U.S. mix **(51) NA NG CC turbines**	Electricity
$G.H_2$ via electrolysis in refueling stations	**(52) Electricity with U.S. generation mix** (53) Electricity with CA generation mix (54) Electricity with Northeast U.S. generation mix **(55) Electricity with NA NG-fired combined-cycle turbines** (56) Electricity with nuclear power (57) Electricity with hydroelectric power
$L.H_2$ via electrolysis in refueling stations	**(58) Electricity with U.S. generation mix** (59) Electricity with CA generation mix (60) Electricity with Northeast U.S. generation mix **(61) Electricity with NA NG-fired combined-cycle turbines** (62) Electricity with nuclear power (63) Electricity with hydroelectric power
(64) Dry mill, displacement[d] (65) Dry mill, market value[d] (66) Wet mill, displacement[d] **(67) Wet mill, market value[c]** **(68) Woody cellulose** **(69) Herbaceous cellulose**	Ethanol (E100, pure ethanol)
(70) Dry mill, displacement[d] (71) Dry mill, market value[d] (72) Wet mill, displacement[d] (73) Wet mill, market value[d] (74) Woody cellulose (75) Herbaceous cellulose	E85 (85% ethanol and 15% gasoline by volume. Ethanol contains 5% gasoline as denaturant. Gasoline is assumed to be RFG without oxygenate)

[a] Results for the options highlighted in bold are presented in this section. All options are presented in Appendix B.
[b] Conventional gas and 150-ppm sulfur RFG are combined together to represent current gasoline.
[c] These three RFG options are combined together to represent future gasoline.
[d] These four corn-based ethanol options are combined together to represent corn-based ethanol.

In the following sections, we graphically present the results for the 30 selected pathways. With Crystal Ball simulations, we were able to estimate energy use and emissions with probability distribution. Appendix B presents energy and emission results at probability of 0% to 100% for each 10% interval. The charts in the following sections show the range results from P20 (20% probability) to P80 (80% probability).

6.1 Total Energy Use

Total energy use from wells to tanks includes use of all energy sources (non-renewables and renewables). To calculate total energy use, the GREET model traces energy use back to energy

content of the primary energy feedstocks for most of transportation fuels. For example, GREET considers energy contained in crude oil in oil fields to calculate energy use for gasoline. However, there are exceptions for fuels based on biomass, solar energy, hydroelectric power, and nuclear power. For ethanol, one could estimate the amount of solar energy used for a unit of energy in ethanol produced. In this case, the energy efficiency of the photosynthesis process during plant growth would be taken into account. However, since solar energy is never a constraint for plant growth, tracing back to solar energy for ethanol does not have much meaning. We traced back the energy use for ethanol production to the energy in grown plants in our calculations.

For solar H_2 production via solar photovoltaic panels, one could trace the energy use for H_2 production all the way back to solar energy received by photovoltaic panels. In this case, the efficiency of photovoltaic panels would be taken into account. However, since solar energy is so abundant, we traced energy use for H_2 production back only to the energy contained in electricity generated by photovoltaic panels.

One could trace energy use for hydroelectric power generation back to energy contained in water behind dams. However, we traced energy back only to energy contained in the electricity generated in hydroelectric power plants.

For nuclear power, one could trace energy use for nuclear power generation all the way back to energy contained in uranium. However, we traced energy back only to energy contained in the electricity generated in nuclear power plants.

As Figure 22 shows, petroleum-based fuels have the lowest total energy use for each unit of energy delivered to vehicle tanks. NG-based fuels generally have high total energy use (except for CNG). The fuels with the highest energy use are: L.H_2 (production in both central plants and refueling stations), G.H_2 and L.H_2 production via electrolysis, and electricity generation. L.H_2 suffers large efficiency losses during H_2 liquefaction. H_2 production via electrolysis suffers two large efficiency losses – electricity generation and H_2 production.

Use of NNA NG for NG-based fuel production results in slightly higher total energy use than use of NA NG does. This is because transportation of liquid fuels produced outside of North America consumes an additional amount of energy. In the case of CNG, G.H_2, and station L.H_2, NG liquefaction, which has additional energy efficiency losses, is involved in order to bring NNA NG to the U.S.

There is a large reduction in total energy use from the U.S. electric generation mix to NG-fired CC turbines for electricity generation and consequently for H_2 production via electrolysis with the latter. This is because while the average conversion efficiency of existing U.S. fossil fuel plants is 32-35%, NG-fired CC turbine conversion efficiency is over 50%. Thus, use of electricity generated with CC turbines results in reduced total energy use.

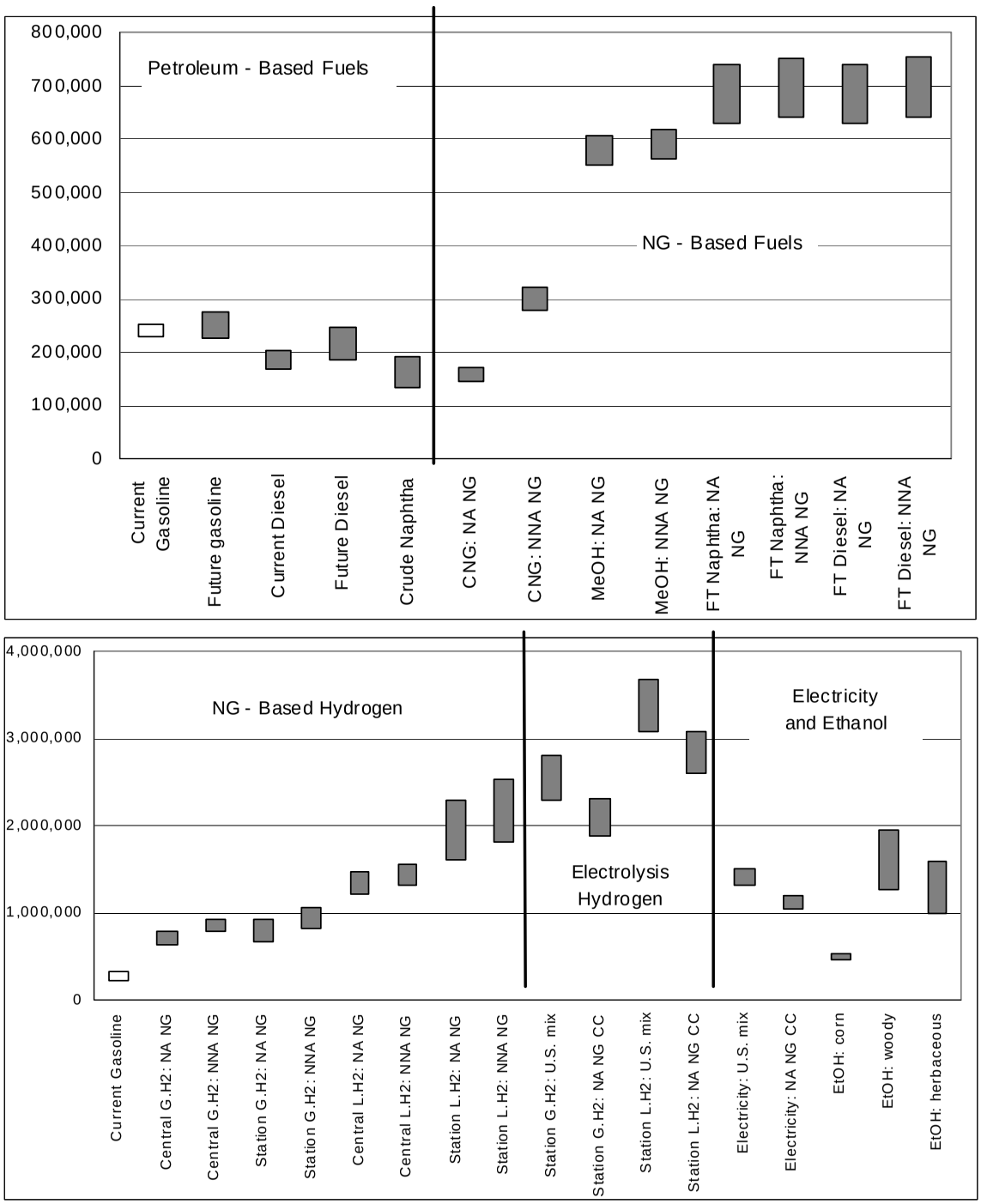

Figure 22 Well-to-Tank Total Energy Use (Btu/mmBtu of fuel delivered to vehicle tanks)

6.2 Well-to-Tank Energy Efficiencies

Energy efficiencies are calculated here with total energy use, as presented in Figure 22. In particular, the following formula was used to calculate energy efficiency:

Efficiency = 1,000,000/(1,000,000 + total energy use) ,

where

1,000,000 = 1 mmBtu of a given fuel available in vehicle tanks and

total energy use = WTT total energy use to produce and deliver 1 mmBtu to vehicle tanks (in Btu per mmBtu of fuel available in vehicle tanks, as presented in the above section).

Figure 23 shows energy efficiencies of the 30 fuel pathways. While gasoline, diesel, crude naphtha, and CNG have efficiencies near or above 80%, energy efficiencies of station L.H_2, G.H_2 and L.H_2 via electrolysis, and electricity generation with the U.S. mix are below 40%. This means that vehicles using these fuels must achieve doubled vehicle efficiencies in order for these vehicles to achieve well-to-wheel efficiencies comparable to gasoline vehicle overall efficiencies.

As the above efficiency formula shows, the efficiency calculated this way takes into account both energy used for producing a fuel and its energy content. The efficiency treats different energy sources the same. For example, energy use for and energy contained in petroleum- and natural gas-based fuels are primarily petroleum and natural gas, both of which are with finite amounts on the earth. On the other hand, energy use for and energy contained in cellulosic ethanol are primarily energy in biomass, which is eventually from solar energy and is renewable. If resources for converting renewable energy sources into ethanol are not a constraint, use of renewable energy sources should have a much less concern than use of non-renewable energy sources. The efficiency based on total energy use is less meaningful for renewable energy-based fuels than for non-renewable energy-based fuels. A better indicator for renewable energy-based fuels could be a ratio between the energy produced in renewable fuels and the non-renewable energy used for the production. Such ratio provides some indication of the enhancement effect of renewable fuel production on prolonging use of finite amounts of non-renewable resources. The results on fossil energy use by each fuel presented in the next section are intended to serve this purpose.

6.3 Fossil Energy Use

Figure 24 presents well-to-tank fossil fuel use for the 30 pathway options. Fossil fuels include petroleum, NG, and coal – the three major non-renewable energy sources. Except for ethanol pathway options, fossil fuel use patterns are similar to those of total energy use. A large amount of lignin is burned in cellulosic ethanol plants. While the energy in lignin is accounted in calculating total energy use, it is not accounted in calculating fossil fuel use. Consequently, fossil fuel use by the two cellulosic ethanol pathways is much lower than total energy use by the two pathways.

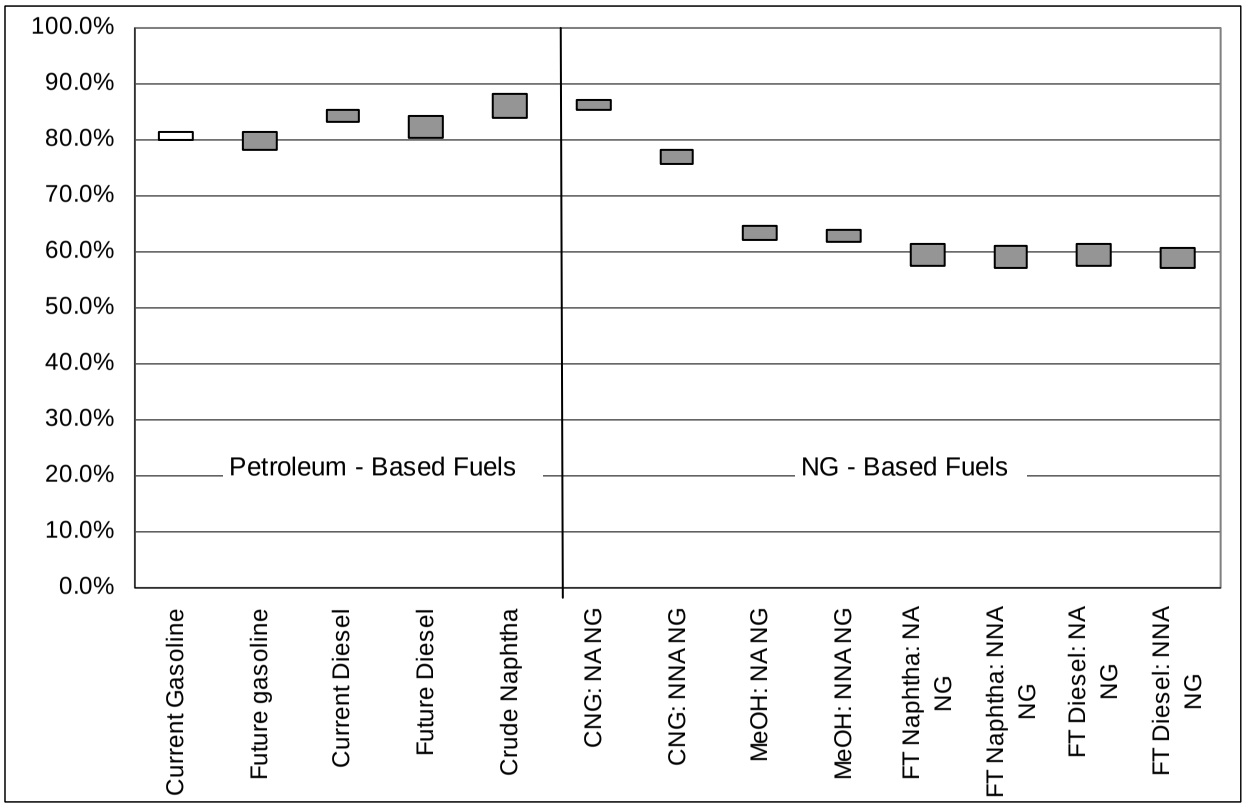

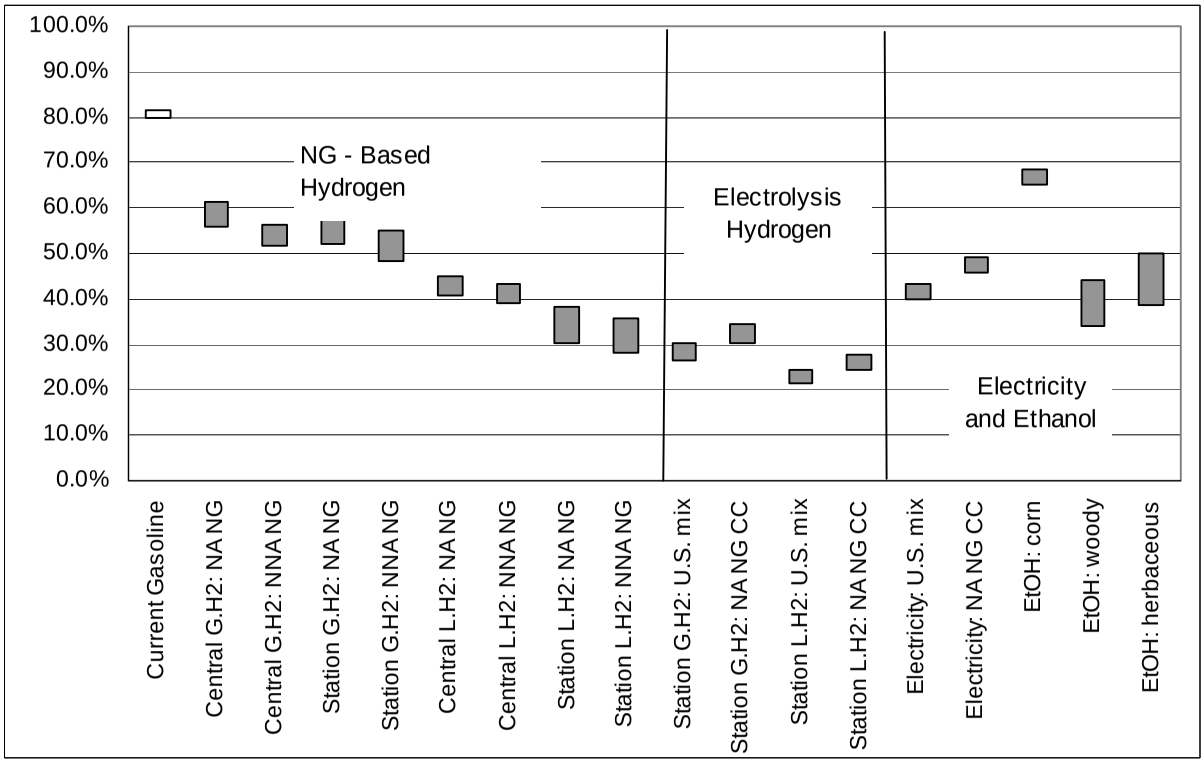

Figure 23 Well-to-Tank Energy Efficiencies

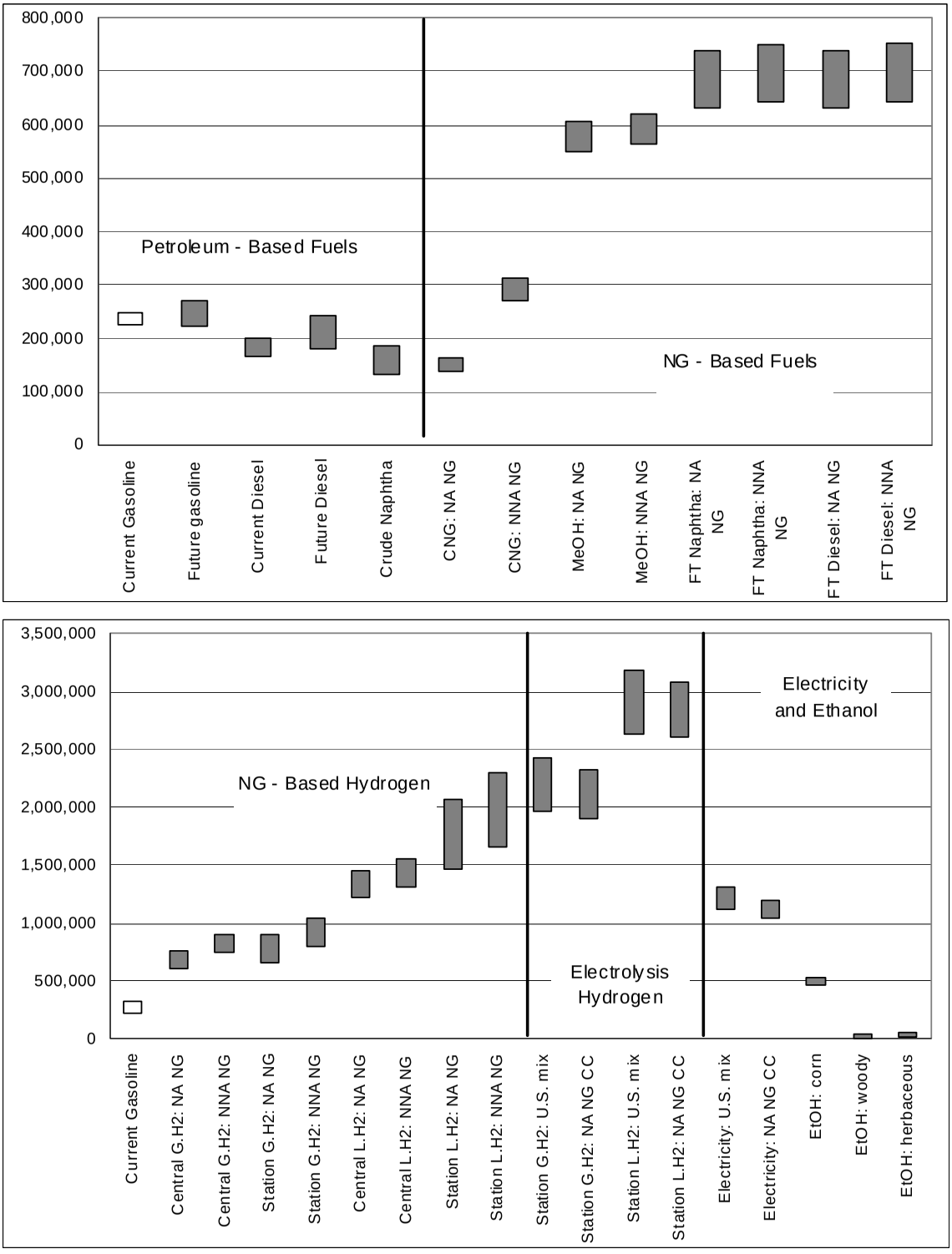

Figure 24 Well-to-Tank Fossil Energy Use (Btu/mmBtu of fuel delivered to vehicle tanks)

With electricity generation and H_2 production via electrolysis, fossil fuel use between the U.S. generation mix and NG-fired CC turbines is very similar. This is because while the U.S. generation mix has an overall conversion efficiency lower than that of CC turbines, under the U.S. average mix, there are some non-fossil fuel power plants (such as nuclear and hydroelectric power plants), which are not accounted in calculating fossil fuel use.

6.4 Petroleum Use

We estimated petroleum use for each pathway to provide information on potential petroleum displacement by a given pathway, relative to conventional gasoline.

Figure 25 shows that all the petroleum-based fuel pathways have expectedly high petroleum use. Methanol pathways have relatively high petroleum use because trucks and rails were assumed to transport a large quantity of methanol. The high petroleum use for central G.H_2 relative to station G.H_2 is due to our assumption that central G.H_2 is compressed in refueling stations with electric compressors, but station G.H_2 is compressed in refueling stations by both electric and NG compressors. Electricity pathways consume some amount of petroleum.

With electricity generation and H_2 production via electrolysis, there is a large reduction in petroleum use from the U.S. average generation mix to NG-fired CC turbines. This is because with the U.S. generation mix, a small amount of electricity is generated with residual oil. Also, mining and transportation of coal consume a significant amount of oil. The three ethanol pathways consume the amount of oil similar to that by the petroleum gasoline pathways. This is caused by the large amount of petroleum diesel that is consumed during farming and transportation of corn and cellulosic biomass. Also note that herbaceous cellulosic ethanol has petroleum use less than that by corn ethanol and woody cellulosic ethanol. This is because corn ethanol consumes a relatively large amount of diesel and because of transportation of woody biomass, which has high moisture content, consumes more energy than transportation herbaceous biomass.

6.5 Greenhouse Gas Emissions

GHG emissions here include emissions of CO_2, CH_4, and N_2O, the three major GHGs specified in the Kyoto protocol. In our analysis, these three gases were combined together with their global warming potentials (1 for CO_2, 21 for CH_4, and 310 for N_2O) to derive CO_2-equivalent GHG emissions. Figure 26 shows well-to-tank GHG emissions.

Petroleum-based fuels and CNG from NA NG have low GHG emissions. CNG from NNA NG has relatively high GHG emissions because of CH_4 emissions from boil-off effect and LNG leakage during LNG transportation from offshore to U.S. LNG terminals. Methanol and FT fuels have high GHG emissions because of CO_2 emissions during fuel production.

All H_2 pathways have very high GHG emissions because all the carbon in feedstocks for H_2 production ends up as CO_2 emissions. As stated in a previous section, we did not assume carbon sequestration during H_2 production. Note that L.H_2 production, electrolysis H_2, and electricity generation have the highest GHG emissions. There is a large reduction in GHG emissions from

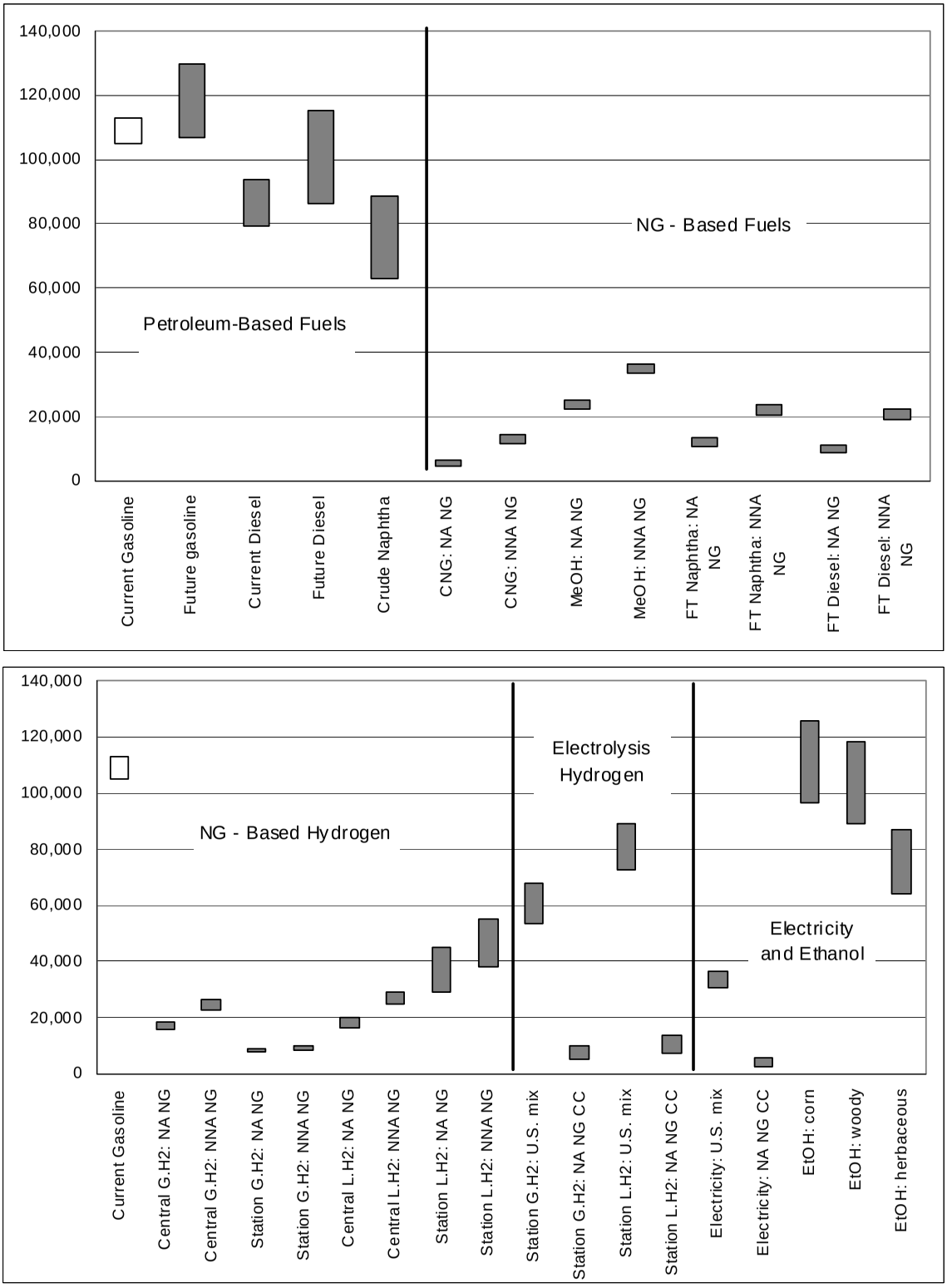

Figure 25 Well-to-Tank Petroleum Use (Btu/mmBtu of fuel delivered to vehicle tanks)

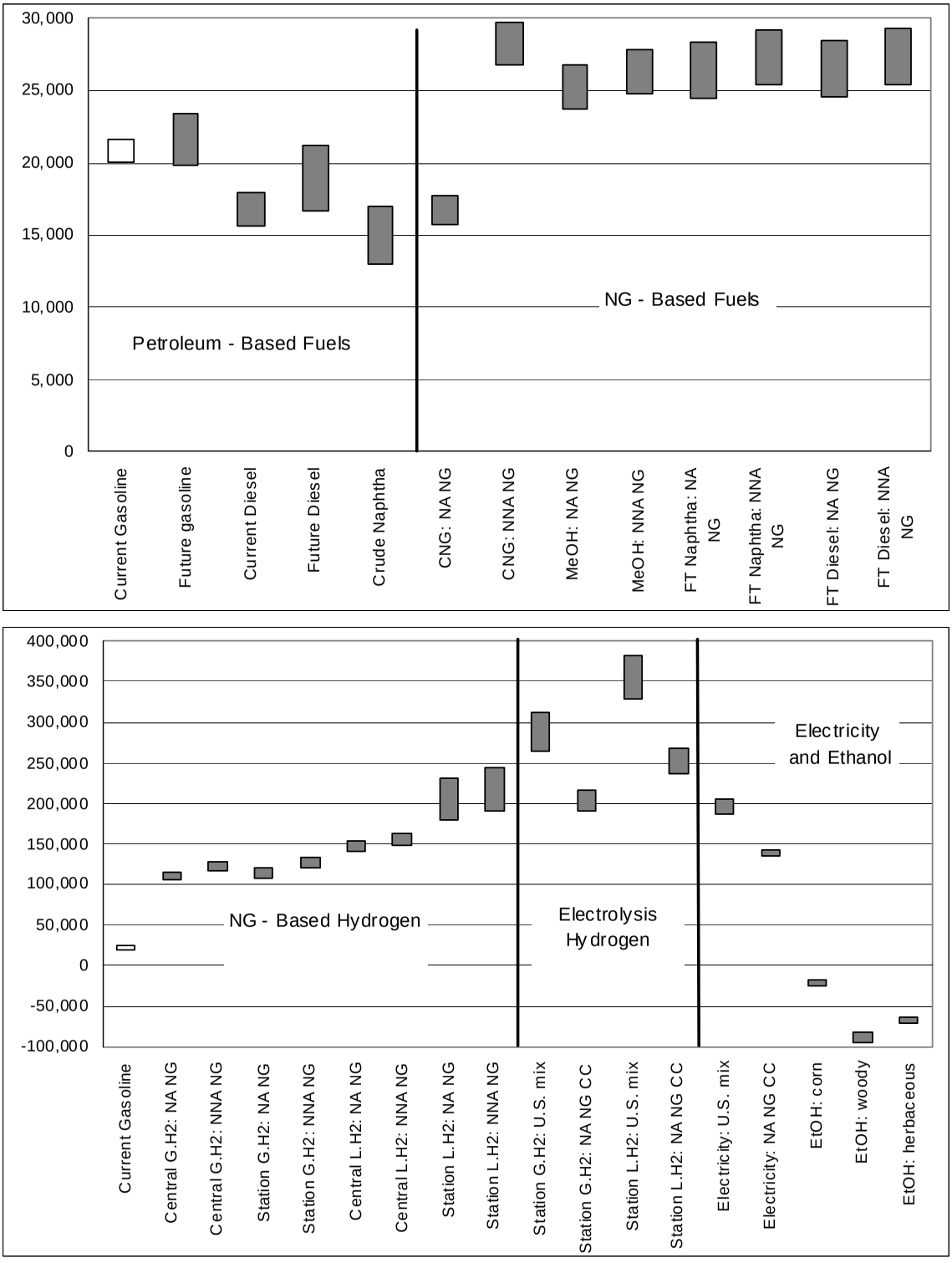

Figure 26 Well-to-Tank GHG Emissions (g/mmBtu of fuel delivered to vehicle tanks)

the U.S. average electric generation mix to NG-fired CC turbines. This is primarily caused by high GHG emissions from coal- and oil-fired electric power plants, relative to those from NG-fired CC turbine plants.

The three ethanol pathways have negative GHG emissions. This is because of carbon sequestration during growth of corn plants, trees, and grass. The carbon sequestrated during biomass growth will emit to the air during combustion of ethanol on vehicles.

The very high GHG emissions for H_2 and electricity and negative GHG values for ethanol on the well-to-tank basis, as shown in Figure 26, demonstrates incomplete, sometimes misleading, conclusions for comparison of GHG emissions of fuel/vehicle technologies on the well-to-tank basis. This is because during the tank-to-wheels stage, all the hydrocarbon fuels will emit a large amount of carbon, while H_2 and electricity will have zero carbon emissions. For ethanol, while there is carbon sequestration during biomass growth (resulting in negative WTT GHG emissions), most of the carbon sequestrated during biomass growth will be emitted back to the air. At net, ethanol fuels may have close to zero GHG emissions, not a large negative GHG value. In this regard, the results presented in this report is partial results. Readers should read a separate report that is prepared by GM on well-to-wheels GHG emission results.

7 Conclusions

Our WTT analysis resulted in the conclusions stated below. It is important to remember that WTT results are incomplete in evaluating fuel/propulsion systems. The systems must be evaluated on a WTW basis; this analysis is presented in Part 3 of Volume 2.

- *Total Energy Use.* For the same amount of energy delivered to the vehicle tank for each of the fuels evaluated in our study, petroleum-based fuels and CNG are subject to the lowest WTT energy losses. Methanol, FT naphtha, FTD, and G.H_2 from NG and corn-based ethanol are subject to moderate WTT energy losses. Liquid H_2 from NG, electrolysis H_2 (gaseous and liquid), electricity generation, and cellulosic ethanol are subject to large WTT energy losses.

- *Fossil Energy Use.* Fossil energy use — including petroleum, NG, and coal — follows patterns similar to those for total energy use, except for cellulosic ethanol. Although WTT total energy use of cellulosic ethanol production is high, its fossil energy use is small because cellulosic ethanol plants would burn lignin, a non-fossil energy source, for needed heat.

- *Petroleum Use.* Production of all petroleum-based fuels requires a large amount of petroleum. Electrolysis H_2 (with the U.S. average electricity) and the three ethanol pathways consume an amount of petroleum about equal to that consumed by petroleum-based fuels. NG-based fuel pathways require only small amounts of petroleum.

- *Greenhouse Gas Emissions.* Production of petroleum-based fuels and NG-based methanol, FT naphtha, and FTD results in a smaller amount of WTT GHG emissions than production of H_2 (gaseous and liquid) and electricity generation. WTT GHG emission values of the three ethanol pathways are negative because of carbon sequestration during growth of corn plants, trees, and grass.

Overall, our WTT analysis reveals that petroleum-based fuels have lower WTT total energy use than do non-petroleum-based fuels. L.H_2 production (in both central plants and refueling stations) and production of G.H_2 and L.H_2 via electrolysis can be energy-inefficient and can generate a large amount of WTT GHG emissions. Cellulosic ethanol, on the other hand, because it is produced from renewable sources, offers significant reductions in GHG emissions. The other fuels options examined here have moderate WTT energy and GHG emissions effects.

8 Acknowledgments

This work was funded by the Global Alternative Propulsion Center of GM. Argonne would like to acknowledge guidance and input from the GM project managers, Dr. Tony Finizza, Dr. Jim Wallace, and Greg Ruselowski. We are grateful to Dr. James Simnick and Andrew Armstrong of BP, Gilbert Jersey and Dr. John Robbins of ExxonMobil, Norman Brinkman of GM Research and Development Center, and Jean Cadu of Shell for their input to and review of this report. We would also like to thank our colleagues Marianne Mintz, Dan Santini, and Chris Saricks for their input.

Finally, the study participants would like to thank Tien Nguyen, Dr. Phillip Patterson, and David Rodgers of the U.S. Department of Energy's Office of Transportation Technologies; without their support of previous versions of the GREET model, this study would not have been possible. We would also like to acknowledge the excellent editorial support provided by Mary Fitzpatrick of Argonne.

9 References

Adamson, K.A., and P. Pearson, 2000, "Hydrogen and Methanol: a Comparison of Safety, Economics, Efficiencies, and Emissions," *Journal of Power Sources* 86:548–555.

AMI, 1996, *Methanol: North America's Clean Fuel and Chemical Building Block,* American Methanol Institute (http://www.methanol.org/methanol/fact/methanol.html).

Amstutz, A., and L. Guzzella, 1998, "Fuel Cells for Transportation — an Assessment of Its Potential for CO_2 Reduction," *Proceedings of the Fourth International Conference on Greenhouse Gas Control Technologies,* Aug. 30–Sept. 2, Interlaken, Switzerland.

ARCO Products Company, 1999, "Emission Control Diesel," presentation material, Los Angeles, Calif., March.

Berggren, M.A., 1997, "Mega-Methanol — Methane Madness vs. Money Maker," presented at the 1997 World Methanol Conference, Tampa, Fla., Dec. 8–10.

Berry, J.R., A.L. Pasternak, G.D. Rambach, J.R. Smith, and T.N. Schock, 1996, "Hydrogen as a Future Transportation Fuel," *Energy* 21:289–303.

Blok, K., et al., 1997, "Hydrogen Production from Natural Gas, Sequestration of Recovered CO_2 in Depleted Gas Wells and Enhanced Natural Gas Recovery," *Energy* 22(2-3):161–168.

California Air Resources Board, 1991, *California Phase 2 Reformulated Gasoline Specifications, Volume 1, Proposed Regulations for California Phase 2 Reformulated Gasoline,* Sacramento, Calif., Jan. 28.

California Air Resources Board, 2000, *Updated Informative Digest of California Reformulated Gasoline,* Sacramento, Calif.

CARB: see California Air Resources Board.

Domalski, E.S., and T.L. Jobe, 1986, *Thermodynamics Data for Biomass Conversion and Waste Incineration,* SERI/SP-271-2839, prepared by National Institute of Standards and Technology, Washington, D.C., for Solar Energy Research Institute, Golden, Colo.

EIA: see Energy Information Administration.

Energy Information Administration, 1998, *International Energy Annual 1996,* DOE/EIA-0219(96), Washington, D.C., Dec.

Energy Information Administration, 1999, *Petroleum Supply Annual, 1998,* Washington, D.C.

Energy Information Administration, 2000, *Petroleum Supply Annual, 1999, Volume 1,* Washington, D.C., June.

EPA: see U.S. Environmental Protection Agency.

Gronemann, V., 1998, “Methanol Process Developments; Mega Methanol Synthesis,” presented at the 1998 IMPCA Latin American Methanol Conference, San Juan, Puerto Rico, May 4–6.

He, D., and M.Q. Wang, 2000, *Contribution of Feedstock and Fuel Transportation to Total Fuel-Cycle Energy Use and Emissions*, SAE paper 2000-01-2976, Society of Automotive Engineers.

Islam, M.N., and K.J. Brown, 1997, “Building Large Methanol Plants for Reliability and Economy,” presented at the 1997 World Methanol Conference, Tampa, Fla., Dec. 8–10.

Kelly, L., 2000, personal communication, California Energy Commission, Sacramento, Calif., Aug. 24.

Kikkawa, Y., and N. Nozawa, 1999, “Optimizing Liquefied Natural Gas Power Chain,” presented at the 1999 Spring Meeting of the American Institute of Chemical Engineers, Houston, Texas, March 14–18.

MathPro, 1999a, *Refining Economics of 5 PPM Sulfur Standards for Gasoline in PADDS 1-3*, prepared for the Alliance of Automobile Manufacturers, West Bethesda, Md., Oct. 18.

MathPro, 1999b, *Refining Economics of Diesel Fuel Sulfur Standards*, prepared for Engine Manufacturers Association, West Bethesda, Md., Oct. 5.

MathPro, 1999c, *Analysis of California Phase 3 RFG Standards*, submitted to California Energy Commission, West Bethesda, Md., Dec. 7.

McKetta, J.L., 1992, *Petroleum Processing Handbook*, Macel Dekker, Inc., New York, N.Y.

National Petroleum Council, 1993, *U.S. Petroleum Refining, Meeting Requirements for Cleaner Fuels and Refineries, Volume II — General Information Appendices*, Washington, D.C, Aug.

National Petroleum Council, 2000, *U.S. Petroleum Refining: Assuring the Adequacy and Affordability of Cleaner Fuels*, Washington, D.C., June.

National Research Council, 2000, *Ozone-Forming Potential of Reformulated Gasoline*, National Academy Press, Washington, D.C.

NPC: see National Petroleum Council.

Ogden, J.M., 1999, “Developing an Infrastructure for Hydrogen Vehicles: A Southern California Case Study,” *International Journal of Hydrogen Energy* 24:709–730.

Oil and Gas Journal, 1999, *Oil and Gas Journal Databook, 1999 Edition*, PennWell Publisher, Tulsa, Okla.

Oil and Gas Journal, 2000, “LNG Imports Needed to Meet Growing U.S. Gas Supply Deficit,” Oct. 2.

Pembina Institute, *Climate-Friendly Hydrogen Fuel: a Comparison of the Life-Cycle Greenhouse Gas Emissions for Selected Fuel Cell Vehicle Hydrogen Production Systems*, Drayton, Alberta, Canada, March.

Russell, B., 2000, personal communication, Syntroleum Corporation, Tulsa, Okla., Sept., 15.

$(S\&T)^2$ Consultants, Inc., 2000, *Assessment of Emissions of Greenhouse Gases from Fuel Cell Vehicles*, prepared for Methanex Corporation, Delta, British Columbia, Canada, June 5.

Stork, K., and M. Singh, 1995, *Impacts of the Renewable Oxygenate Standard for Reformulated Gasoline Ethanol Demand, Energy Use, and Greenhouse Gas Emissions*, ANL/ESD-28, Center for Transportation Research, Argonne National Laboratory, Argonne, Ill., April.

Thomas, C.E., B.D. James, I.F. Kuhn, F.L. Lomax, and G.N. Baum, 1997, *Direct-Hydrogen-Fueled Proton-Exchange-Membrane Fuel Cell System for Transportation Applications: Hydrogen Infrastructure Report*, DOE/CE/50389-504, prepared for the U.S. Department of Energy, Office of Transportation Technologies, Washington, D.C., July.

Unnasch, S., 2000, *Refinement of Selected Fuel-Cycle Emission Analyses*, draft final report, prepared by Arthur D. Little, Mountain View, Calif., for California Air Resources Board, Feb. 9.

Unnasch, S., and L. Browning, 2000, *Fuel-Cycle Energy Efficiency Analysis*, prepared for California Energy Commission, Sacramento, Calif., May.

U.S. DOT, 1996, *National Transportation Statistics 1996*, Bureau of Transportation Statistics, U.S. Department of Transportation, Washington, D.C.

U.S. DOT and U.S. DOC, *1997 Commodity Flow Survey*, Bureau of Transportation Statistics, U.S. Department of Transportation, and Economics and Statistics Administration, U.S. Department of Commerce, Washington, D.C.

U.S. Environmental Protection Agency, 1994, *Regulation of Fuels and Fuel Additives; Standards for Reformulated and Conventional Gasoline, Final Rule*, Federal Register, Vol. 59, Feb. 16.

U.S. Environmental Protection Agency, 2000a, *Control of Air Pollution from New Motor Vehicles: Tier 2 Motor Vehicle Emissions Standards and Gasoline Sulfur Control Requirements, Final Rule*, Federal Register, Vol. 65, No. 28, Feb. 10.

U.S. Environmental Protection Agency, 2000b, *Control of Air Pollution from New Motor Vehicles: Heavy-Duty Engine and Vehicle Standards and Highway Diesel Fuel Sulfur Control Requirements, Final Rule*, Dec. 21.

Vink, K.J., and R.K. Nagelvoort, 1998, "Comparison of Baseload Liquefaction Processes," presented at the 12th International Conference and Exhibition on Liquefied Natural Gas, May.

Wang, M.Q., 1999a, *GREET 1.5 — Transportation Fuel-Cycle Model, Volume 1: Methodology, Development, Use, and Results*, ANL/ESD-39, Vol. 1, Center for Transportation Research, Argonne National Laboratory, Argonne, Ill., Aug.

Wang, M.Q., 1999b, *GREET 1.5 — Transportation Fuel-Cycle Model, Volume 2: Appendices of Data and Results*, ANL/ESD-39, Vol. 2, Center for Transportation Research, Argonne National Laboratory, Argonne, Ill., Aug.

Wang, M.Q., and H.S. Huang, 1999, *A Full Fuel-Cycle Analysis of Energy and Emissions Impacts of Transportation Fuels Produced from Natural Gas*, ANL/ESD-40, Center for Transportation Research, Argonne National Laboratory, Argonne, Ill., Dec.

Williams, R., and B. Wells, 1997, "Solar-Assisted Hydrogen Production from Natural Gas with Low CO_2 Emissions," presented at the International Conference on Technologies for Activities Implemented Jointly of the IEA Greenhouse Gas R&D Programme, Vancouver, British Columbia, Canada.